Thesis for the degree of Doctor of Technology
Sundsvall 2013

High Frequency (MHz) Planar Transformers for Next Generation Switch Mode Power Supplies

Radhika Ambatipudi

Supervisors
Associate Professor Kent Bertilsson
Professor Bengt Oelmann

Department of Electronics Design
Mid Sweden University, SE-851 70 Sundsvall, Sweden

ISSN 1652-893X
Mid Sweden University Doctoral Thesis 159

ISBN 978-91-87557-02-6

Mittuniversitetet
MID SWEDEN UNIVERSITY

Akademisk avhandling som med tillstånd av Mittuniversitetet i Sundsvall framläggs till offentlig granskning för avläggande av teknologie doktorsexamen i elektronik fredagen den 4th oktober 2013, klockan 10:30 i sal O102, Mittuniversitetet Sundsvall. Seminariet kommer att hållas på engelska.

High Frequency (MHz) Planar Transformers for Next Generation Switch Mode Power Supplies

Radhika Ambatipudi

Department of Electronics Design,
Mid Sweden University, SE-851 70 Sundsvall
Sweden

Telephone: +46 (0)60 148982

Printed by Kopieringen Mittuniversitetet, Sundsvall, Sweden, 2013

Dedicated at the lotus feet of

Bhagavan Sree Sathya Sai Baba,
Sree Swami Sivananda &
Ammagaru

"LOVE ALL, SERVE ALL"

ABSTRACT

Increasing the power density of power electronic converters while reducing or maintaining the same cost, offers a higher potential to meet the current trend in relation to various power electronic applications. High power density converters can be achieved by increasing the switching frequency, due to which the bulkiest parts, such as transformer, inductors and the capacitor's size in the converter circuit can be drastically reduced. In this regard, highly integrated planar magnetics are considered as an effective approach compared to the conventional wire wound transformers in modern switch mode power supplies (SMPS). However, as the operating frequency of the transformers increase from several hundred kHz to MHz, numerous problems arise such as skin and proximity effects due to the induced eddy currents in the windings, leakage inductance and unbalanced magnetic flux distribution. In addition to this, the core losses which are functional dependent on frequency gets elevated as the operating frequency increases. Therefore, this thesis provides an insight towards the problems related to the high frequency magnetics and proposes a solution with regards to different aspects in relation to designing high power density, energy efficient transformers.

The first part of the thesis concentrates on the investigation of high power density and highly energy efficient coreless printed circuit board (PCB) step-down transformers useful for stringent height DC-DC converter applications, where the core losses are being completely eliminated. These transformers also maintain the advantages offered by existing core based transformers such as, high coupling coefficient, sufficient input impedance, high energy efficiency and wide frequency bandwidth with the assistance of a resonant technique. In this regard, several coreless PCB step down transformers of different turn's ratio for power transfer applications have been designed and evaluated. The designed multilayered coreless PCB transformers for telecom and PoE applications of 8, 15 and 30W show that the volume reduction of approximately 40 - 90% is possible when compared to its existing core based counterparts while maintaining the energy efficiency of the transformers in the range of 90 - 97%. The estimation of EMI emissions from the designed transformers for the given power transfer application proves that the amount of radiated EMI from a multilayered transformer is less than that of the two layered transformer because of the decreased radius for the same amount of inductance.

The design guidelines for the multilayered coreless PCB step-down transformer for the given power transfer application has been proposed. The designed transformer of 10mm radius has been characterized up to the power level of 50W and possesses a record power density of 107W/cm^3 with a peak energy efficiency of 96%. In addition to this, the design guidelines of the signal transformer for driving the high side MOSFET in double ended converter topologies have been proposed. The measured power consumption of the high side gate drive circuit

together with the designed signal transformer is 0.37W. Both these signal and power transformers have been successfully implemented in a resonant converter topology in the switching frequency range of 2.4 – 2.75MHz for the maximum load power of 34.5W resulting in the peak energy efficiency of converter as 86.5%.

This thesis also investigates the indirect effect of the dielectric laminate on the magnetic field intensity and current density distribution in the planar power transformers with the assistance of finite element analysis (FEA). The significance of the high frequency dielectric laminate compared to FR-4 laminate in terms of energy efficiency of planar power transformers in MHz frequency region is also explored.

The investigations were also conducted on different winding strategies such as conventional solid winding and the parallel winding strategies, which play an important role in the design and development of a high frequency transformer and suggested a better choice in the case of transformers operating in the MHz frequency region.

In the second part of the thesis, a novel planar power transformer with hybrid core structure has been designed and evaluated in the MHz frequency region. The design guidelines of the energy efficient high frequency planar power transformer for the given power transfer application have been proposed. The designed core based planar transformer has been characterized up to the power level of 50W and possess a power density of 47W/cm^3 with maximum energy efficiency of 97%. This transformer has been evaluated successfully in the resonant converter topology within the switching frequency range of 3 – 4.5MHz. The peak energy efficiency of the converter is reported to be 92% and the converter has been tested for the maximum power level of 45W, which is suitable for consumer applications such as laptop adapters. In addition to this, a record power density transformer has been designed with a custom made pot core and has been characterized in the frequency range of 1 - 10MHz. The power density of this custom core transformer operating at 6.78MHz frequency is 67W/cm^3 and with the peak energy efficiency of 98%.

In conclusion, the research in this dissertation proposed a solution for obtaining high power density converters by designing the highly integrated, high frequency (1 - 10MHz) coreless and core based planar magnetics with energy efficiencies in the range of 92 - 97%. This solution together with the latest semiconductor GaN/SiC switching devices provides an excellent choice to meet the requirements of the next generation ultra flat low profile switch mode power supplies (SMPS).

SAMMANDRAG

Det vore önskvärt att kunna öka effekttätheten och samtidigt behålla, eller till och med reducera, tillverkningskostnaden i många olika kraftelektronikapplikationer. Högre effekttäthet kan uppnås genom att ökad switchfrekvens då stora reaktiva komponenter kan bytas ut mot mindre då mindre energi behöver lagras i varje switchcykel. Där blir små planara transformatorer en viktig komponent för att uppnå dessa skalfördelar i moderna switchade nätaggregat (SMPS) jämför med konventionella lindade transformatorer. Ett problem som uppstår när man ökar switchfrekvensen från några hundra kHz till MHz området är att flera förlustmekanismer såsom skin- och närhets-effekt, inducerade eddy-strömmar i lindningarna samt obalanserat magnetiskt flöde ökar. Dessutom ökar även kärnförlusterna vid högre frekvenser. Denna avhandling adresserar och bidrar med lösningar till olika problemställningar inom transformatorer för högfrekventa spänningsomvandlare med hög effekttäthet.

Den första delen koncentrerar sig på design och undersökningar av kärnfria ”step-down” kretskortstransformatorer med låg bygghöjd där kursförlusterna kan elimineras helt. Med hjälp av en resonant teknik så kan men med denna typ av transformatorer uppnå hög kopplingskoefficient, hög ingångsimpedans, bra verkningsgrad samt stor bandbredd. Transformatorer med flera olika omsättningstal har designats och utvärderats. Tillverkade transformatorer i flerlagers kretskort för olika PoE applikationer för 8, 15 och 30 W visar en volymreduktion av 40-90% går att uppnå jämfört med existerande kärnbaserade transformatorer och med en bibehållen hög verkningsgrad kring 90-97%. Uppskattat EMI strålning från dessa transformatorer är lägre än för tidigare tillverkade transformatorer i två lager p.g.a. den mindre storleken.

Designregler för flerlagers kärnfria kretskorts transformatorer för en given applikation föreslås. Designade transformatorer med 10mm radie har karakteriserats till 50 W med en rekordhög effekttäthet av 107W/cm^3 med en verkningsgrad upp till 96%. Utöver detta har designregler för signaltransformatorer för gate-drivning av MOSFET transformatorer med flytande source föreslagits. Uppmätt effektförbrukning för en drivkrets för en high-side MOSFET med denna transformator är 0.37W vilket ligger nära den teoretiska gränsen vid denna frekvens. Både signal och effekttransformatorer har utnyttjats i en resonant omvandlare arbetande i frekvensområdet 2.4-2.75MHz upp till 34.5W där en maximal verkningsgrad av 86.5% har uppnåtts.

Avhandlingen har också undersökt indirekta effekter av laminatets dielektriska egenskaper på magnetfältets intensitet och fördelning av strömtätheten genom finita element analys (FEA). Fördelar med högfrekvensmaterial jämfört med traditionella FR4 material med avseende på verkningsgrad har också undersökts experimentellt.

Lindningsstrategin har en betydande effekt för högfrekvensegenskaperna i magnetiska komponenter. Olika strategier har undersökts och en konventionell lindning har jämförts med parallella lindningar i en planar transformatorer och föreslagen teknologi har visat sig bättre än existerande i MHz området.

Avhandlingens andra del behandlar en ny planar kärnbaserad transformator som har designats och utvärderats i MHz frekvenser. Designregler för högfrekventa kärnbaserade effekttransformatorer har föreslagits. Tillverkade planara transformatorer har karakteriserats upp till 50W vilket ger en effekttäthet på 47W/cm^3. En resonant omvandlare som nyttjar denna transformator och arbetar i frekvensområdet 3-4.5MHz har karakteriserats upp till 45W med en verkningsgrad upp till 92% och skulle kunna användas för olika konsumentprodukter t.ex omvandlare för en laptop. En transformator för ännu högre frekvenser har också konstruerats och vid 6.78MHz så har en verkningsgrad av 98% uppmätts och en effekttäthet av 67W/cm^3.

Sammanfattningsvis så presenterar denna avhandling olika lösningar för högfrekvents transformatorer med och utan kärna för området mellan 1-10MHz och verkningsgrader upp till 98%. Dessa transformatorer kommer att vara mycket betydelsefulla för att kunna dra fördelar av nya halvledarkomponenter i kiselkarbid (SiC) och GalliumNitrid (GaN) för nästa generations ultra kompakta/flata spänningsomvandlare.

ACKNOWLEDGMENT

This thesis would not have been possible without the guidance of several individuals who have contributed and extended their invaluable assistance in one way or the other. It's a great pleasure for me to take this opportunity to thank each and everyone in this acknowledgment.

First of all, I offer the utmost gratitude towards my supervisor Associate Professor Kent Bertilsson for believing my potential and giving me the opportunity to pursue my doctoral studies at Mid Sweden University, Sundsvall, Sweden. I would also like to thank him for his advice, guidance and support from day one of my PhD studies to the present date. The good advice, support and friendship of my second supervisor, Prof. Bengt Oelmann, has been invaluable for which I am extremely grateful.

I would also like to thank my other Power Electronics group members Abdul Majid, Jawad Saleem, Stefan Haller and Hari Babu Kotte who have also contributed to the research work presented in terms of publications.

I gratefully acknowledge Krister Alden for his kind friendship, Fanny Burman, Carolina Blomberg and Lotta Frisk for their kind administrative support, Cheng Peng for having good technical discussions. I also thank my colleague Muhammad Anzar Alam for spending his valuable time with me and Hari for discussing many things.

Many thanks also go to Benny Thörnberg, Göran Thungström, Najeem Lawal, Johan Siden, Mikael Bylund, Brian Johnston, Naeem Ahmad, Magnus Engholm, Henrik Andersson, Claes Mattsson, David Krapohl, Omeime Esebamen, Meng Xiaozhou and Prerna Kumar for extending their help during the thesis work in one way or the other. Further, I would also like to express my gratitude towards all my other colleagues of Electronics Design Department at Mid Sweden University who have directly or indirectly contributed to my thesis work. Also the timely help by Anne Åhlin and Christina Olsson are greatly appreciated.

I would also like to acknowledge Mid Sweden University, VINNOVA, The Swedish Energy agency, County Administrative Board in Västernorrland and European Union for their financial support.

I would like to show my gratitude towards my parents and brother, Sri. Ambatipudi Seshu Madhava Rao, Smt. Lakshmi Sailaja and Murali Krishna

for their unending support, encouragement and prayers. I would also express my gratitude towards my father-in-law Sri. Kotte Krishna Murthy, mother-in-law Smt. Suseela Devi, Grandmother Seshamma Sadhu and sister-in-law Vijaya Lakshmi SomaSekhar for their never-ending showers of love towards me. I would like to thank my husband and colleague Hari Babu Kotte for his solicitude, personal and professional support and unlimited patience at all times and above all for believing my potential. His high regard for my aspiration gave me the strength to carry on. I would also thank my loving brother Ambatipudi Nagendra Prasad (Sekhar anna) for his caring towards his sister, everlasting support at all times, for his encouragement and motivation in all aspects of my life. Without his support, this would not have been possible.

I would also express my sincere gratitude towards my guru Sri. S. Kamakshaiah garu. The support and help offered by my former colleague and brother Kosaraju Kiran Kumar is greatly acknowledged. My dearest friends Sujatha and Rama Devi's constant love, support and caring attitude towards me from the past 15 years were greatly appreciated for which I am greatly indebted.

Last but not the least, I am greatly indebted to my well wishers and guides Sri. C. Rommel uncle, Sri. Krishnendra Santani who has shown the path for the spiritual bliss and it was the greatest achievement of mine here in Sundsvall, Sweden.

Sundsvall, May 2013
Radhika Ambatipudi

TABLE OF CONTENTS

ABBREVIATIONS AND ACRONYMS

AC	Alternating Current
CAD	Computer Aided Design
CISPR	Comité International Spécial des Perturbations Radioélectriques
CLPCB	Coreless Printed Circuit Board
DC	Direct Current
DSP	Digital Signal Processing
DVD	Digital Versatile Disc
EMC	Electro Magnetic Compatibility
EMI	Electro Magnetic Interference
ETD	Economic Transformer Design
FCC	Federal Communications Commission
FEA	Finite Element Analysis
FFT	Fast Fourier Transform
FR4	Flame Retardant 4
GaN	Gallium Nitride
HEMT	High Electron Mobility Transistor
IEC	International Electrotechnical Commission
IP	Internet Protocol
IGBT	Insulated Gate Bipolar Transistor
IPM	Intelligent Power Modules
kHz	Kilo Hertz
LCD	Liquid Crystal Display
LTCC	Low Temperature Co-fired Ceramic
MEEF	Maximum Energy Efficiency Frequency
MHz	Mega Hertz
MIF	Maximum Impedance Frequency
MMF	Magnetomotive Force
MnZn	Manganese Zinc
MOSFET	Metal Oxide Semiconductor Field Effect Transistor
MRC	Multi Resonant Converter
NiZn	Nickel Zinc
PCB	Printed Circuit Board
PoE	Power over Ethernet
PQ	Power Quality
PRC	Parallel Resonant Converter
PSU	Power Supply Unit
RF	Radio Frequency
RFI	Radio Frequency Interference
RM	Rectangular Modular

Si	Silicon
SiC	Silicon Carbide
SMPS	Switch Mode Power Supplies
SPICE	Simulation Program with Integrated Circuit Emphasis
SPRC	Series Parallel Resonant Converter
SRC	Series Resonant Converter
WLAN	Wireless Local Area Network
ZVS	Zero Voltage Switching

LIST OF FIGURES

LIST OF TABLES

LIST OF PAPERS

This thesis is mainly based on the following nine publications, herein referred to by their Roman numerals:

Paper I **Comparison of Two Layered and Three Layered Coreless Printed Circuit Board (PCB) Step-down Transformers**
Radhika Ambatipudi, Hari Babu Kotte, Kent Bertilsson
Proceedings of 2010 3rd International Conference on Power Electronics and Intelligent Transportation System, Shenzhen, China, November 2010, Vol. IV, pp. 314 – 317, ISBN 978-1-4244-9162-9.

Paper II **Coreless Printed Circuit Board (PCB) Step-down Transformers for DC-DC Converter Applications**
Radhika Ambatipudi, Hari Babu Kotte, and Kent Bertilsson
Proceedings of World Academy of Science Engineering and Technology (WASET), Paris, France, October 2010, Issue. 46, pp. 379-388, ISSN 1307-6892.

Paper III **Radiated Emissions of Multilayered Coreless Printed Circuit Board Step-Down Power Transformers in Switch Mode Power Supplies**
Radhika Ambatipudi, Hari Babu Kotte and Kent Bertilsson
Proceedings of 8th International Conference on Power Electronics, ICPE 2011 - ECCE Asia, The Shilla Hotel, and Jeju, South Korea, May 30-June 3, 2011, pp.960 -965.

Paper IV **High Speed (MHz) Series Resonant Converter (SRC) Using Multilayered Coreless Printed Circuit Board (PCB) Step-Down Power Transformer**
Hari Babu Kotte, **Radhika Ambatipudi** and Kent Bertilsson
Power Electronics, IEEE Transactions on, vol.28, no.3, pp.1253-1264, March 2013.

Paper V **Effect of Dielectric Material on the Performance of Planar Power Transformers in MHz Frequency Region**
Radhika Ambatipudi, Hari Babu Kotte and Kent Bertilsson
Proceedings of INDUCTICA 2012 Coil Winding, Insulation and Electrical Manufacturing International Conference and Exhibition (CWIEME), Berlin, Germany 26 – 28, June 2012.

Paper VI **A ZVS Half Bridge DC-DC Converter in MHz Frequency Region Using Novel Hybrid Power Transformer**
Hari Babu Kotte, **Radhika Ambatipudi**, Stefan Haller and Kent Bertilsson
Proceedings of International Conference on Power Electronics and Intelligent Motion (PCIM Europe 2012), Nuremberg, Germany, 08 - 10 May 2012, pp.399-406. ***(This paper has been chosen for the PCIM 2012 Conference YOUNG ENGINEER AWARD sponsored by European Center for Power Electronics (ECPE), Infineon Technologies and Mitsubishi Electric)***

Paper VII **Effect of Air Gap on the Performance of Hybrid Planar Power Transformer in High Frequency (MHz) Switch Mode Power Supplies (SMPS)**
Radhika Ambatipudi, Hari Babu Kotte, and Kent Bertilsson
Proceedings of INDUCTICA 2012, Coil Winding, Insulation and Electrical Manufacturing International Conference and Exhibition (CWIEME), Berlin, Germany 26 – 28, June 2012.

Paper VIII **Design and Analysis of 45W Multi Resonant Half Bridge Converter in MHz Frequency Region using GaN HEMTs**
Hari Babu Kotte, **Radhika Ambatipudi** and Kent Bertilsson
Submitted for publication in Journal of Power Electronics (JPE), Korea (Under revision)

Paper IX **High Performance Planar Power Transformer with High Power Density in MHz Frequency for Next Generation Switch Mode Power Supplies**
Radhika Ambatipudi, Hari Babu Kotte and Kent Bertilsson
Proceedings of 28th Annual IEEE Applied Power Electronics Conference & Exposition, APEC 2013, Long Beach, California, USA, March 17 – 21, 2013, pp.2139-2143.

Related papers not included in thesis

Paper 1 **Analysis of Solid and Parallel Winding Structures in MHz Planar Transformers Suitable for Switch Mode Power Supplies**
Radhika Ambatipudi**, Hari Babu Kotte** and Kent Bertilsson
Submitted for Publication in Journal of Electrical Engineering and Technology, South Korea.

Paper 2 **High Speed Series Resonant Converter Using Multilayered Coreless Printed Circuit Board (PCB) Step-Down Power Transformer**
Hari Babu Kotte, **Radhika Ambatipudi** and Kent Bertilsson
Proceedings of IEEE 33rd International Telecommunications Energy Conference, Amsterdam, The Netherlands, 9-13 October 2011.

Paper 3 **A 45W LLC Resonant Converter in MHz Frequency Region for Laptop Adapter Application Using GaN HEMTs**
Hari Babu Kotte, **Radhika Ambatipudi** and Kent Bertilsson
Proceedings of International Conference on Power Electronics and Intelligent Motion (PCIM Europe 2013), Nuremberg, Germany, 14-16 May 2013, pp.1029-1035.

Paper 4 **Design and Implementation of EMI Filter for High Frequency (MHz) Power Converters**
Abdul Majid, Jawad Saleem, Hari Babu Kotte, **Radhika Ambatipudi**, and Kent Bertilsson
Proceedings of International Symposium on Electromagnetic Compatibility (EMC Europe 2012), Rome, Italy, September 17 - 21, 2012.

Paper 5 **A ZVS Flyback DC-DC Converter Using Multilayered Coreless Printed –Circuit Board (PCB) Step-down Power Transformer**
Hari Babu Kotte, **Radhika Ambatipudi** and Kent Bertilsson
Proceedings of World Academy of Science, Engineering and Technology, Paris, France, Issue 70, October 2010, ISSN: 1307-6892, pp. 148-155.

Paper 6 **Comparative Results of GaN And Si MOSFET in a ZVS Flyback Converter Using Multilayered Coreless Printed Circuit Board Step-Down Transformer**
Hari Babu Kotte, **Radhika Ambatipudi** and Kent Bertilsson
Proceedings of "2010 3rd The International Conference on Power Electronics and Intelligent Transportation system (PEITS 2010)", November 20-21, 2010, Shenzhen, China, Vol. IV, pp. 318- 321, ISBN 978-1-4244-9162-9.

Paper 7 **High Speed Cascode Flyback Converter Using Multilayered Coreless Printed Circuit Board (PCB) Step-Down Power Transformer**
Hari Babu Kotte, **Radhika Ambatipudi** and Kent Bertilsson

Proceedings of 8th International Conference on Power Electronics, ICPE 2011 - ECCE Asia, May 30- June 3, 2011, The Shilla Hotel, and Jeju, Korea, pp.1856-1862.

Paper 8 **Analysis of Feedback in Converter using Coreless Printed Circuit Board Transformer**
Abdul Majid, Jawad Saleem, Hari Babu Kotte, **Radhika Ambatipudi,** Stefan Haller and Kent Bertilsson
Proceedings of International Aegean Conference on Electrical Machines and Power Electronics & Electromotion Joint Conference (ACEMP), Istanbul, Turkey, September 8 - 10, 2011, pp.601-604.

Paper 9 **High Frequency Full Bridge Converter Using Multilayer Coreless Printed Circuit Board Step Up Power Transformer**
Jawad Saleem, Abdul Majid, **Radhika Ambatipudi**, Hari Babu Kotte and Kent Bertilsson
Proceedings of 2011 20th European Conference on Circuit Theory and Design (ECCTD), Linköping, Sweden, August 29 - 31, 2011 pp.805-808.

Paper 10 **Energy Efficient Multi Resonant Half Bridge Converter in MHz Frequency Region Using Novel Hybrid Planar Power Transformer and GaN HEMTs**
Hari Babu Kotte, **Radhika Ambatipudi** and Kent Bertilsson
Submitted for Publication in Journal of Electrical Engineering and Technology, South Korea.

Paper 11 **High Frequency Half-Bridge Converter using Multilayered Coreless Printed Circuit Board Step-Down Power Transformer**
Abdul Majid, Hari Babu Kotte, Stefan Haller, **Radhika Ambatipudi**, Jawad Saleem and Kent Bertilsson
Proceedings of 8th international Conference on Power Electronics, ICPE 2011 - ECCE Asia, The Shilla Hotel, and Jeju, Korea, May 30- June 3, 2011, pp.1177-1181.

1 INTRODUCTION

The power supply unit (PSU) is an essential part of any electronic device as no electronic circuit can function without some sort of power. The ever increasing demand for slim and portable consumer electronic appliances such as laptop adapters, palmtop computers, LCD monitors, mobile and iPad chargers highlight the significance of the low profile low power converters [1]. In this regard, power electronics researchers and engineers are continuously striving to design small size, lightweight, low profile, small foot print and energy efficient converters [2], [3]. In order to achieve this task, the switching frequency of the converters has to be increased so that the size of the passive elements such as inductors, transformers and capacitors [4] - [10] gets reduced as it is required to store a lesser amount of energy in each cycle. In addition to this, by integrating the passive elements in the converter circuit, it is feasible to realize the high power density converters [9].

The majority of power electronic converter circuits employ the inductors and transformers, which are defined by their electromagnetic behavior. One of the design challenges in relation to achieving the high power density converters is the design and development of high power density magnetics (either inductor or transformers), which are usually considered as the bulkiest [10] and most expensive components in switch mode power supplies (SMPS). In a typical SMPS, the magnetics together with the heat sinks are considered to be occupying more than 80% of the total volume [11] when compared to other elements. However, the most irreplaceable components in the SMPS are considered as the magnetic elements i.e., the inductors and transformers. For example, if the non-isolated converters such as buck, boost, buck-boost and cuk converters are considered, then the inductor is one of the essential parts, in addition to the other elements of the circuit. Similarly, in the case of single/double ended isolated converter topologies such as forward, flyback, half-bridge and full-bridge converters, transformer becomes the backbone as it provides the galvanic isolation, large step down/step up conversion ratios and multiple outputs [12]. On the other hand, these are considered as complex components in terms of design, but at the same time, these have become the heart of the modern SMPS.

From the semiconductor point of view, the state-of-the-art ‘Si’ material switching devices are reaching the theoretical limits in terms of performance and reliability [13], in order to meet the current industrial demands of achieving energy efficient high power density converters [14]. In this regard, the new semiconductor material devices such as silicon carbide (SiC) schottky diodes/transistors [15] and gallium nitride high electron mobility transistors (GaN HEMTs) [16] have been introduced

into the market which makes it feasible to increase the switching frequency of converters from a few hundred kHz to the MHz frequency region.

1.1 THESIS BACKGROUND

The trend towards the high power density and low profile converters has exposed a number of limitations imposed by the traditional wire wound transformers and inductors. This is mainly due to the increased losses in these wire wound components because of the skin and proximity effects when the operating frequency is increased beyond 100 kHz [4], [6]. In this regard, in recent years, the planar magnetics have become extremely popular due to the advantages they offer for achieving the high power density converters and will be discussed in coming sections.

1.1.0 Planar transformer technology

Due to the increased switching speeds of the converter, the number of turns of primary/secondary windings in the case of planar transformers can be noticeably reduced. Generally, planar transformers use flat copper foils instead of round copper wires in order to reduce the eddy current loss, which in turn results in low skin and proximity effects [4]. A side view of an assembled planar transformer with a typical EE core [12] is illustrated in fig. 1. In these type of transformers, the distance between the primary and secondary always remains constant and hence provides a tight control of the leakage inductance between them. The insulation material used in between the windings and the core material is of Kapton or Mylar insulation [12], [17].

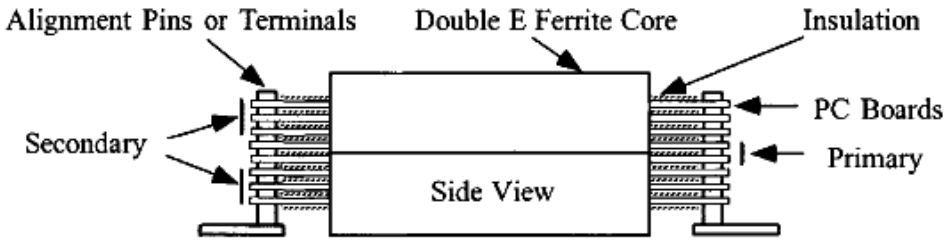

Figure 1. Side view of planar transformer with EE core [12]

The reasons for the popularity of planar transformers in modern SMPS are listed as follows [4], [12], [18].

- Low profile, lightweight
- Low leakage inductance
- Uniform construction
- High power density

- High efficiency, reliability
- Excellent repeatability
- High frequency of operation compared to wire wound transformers

Even though the planar transformers possess the above mentioned advantages, there are also some disadvantages associated with them such as high design and tooling costs for both PCBs and ferrite cores, thermal temperature rise of the magnetic materials [17], core losses, an inefficient means of terminating the wires within the board, high inter-winding capacitance, large footprint etc., In this regard, for the past few years, a great deal of research has been conducted in order to overcome the limitations of this planar transformer technology in different aspects.

Since the core loss is also one of the limiting factors for increasing the operating frequency of transformers in order to improve the power density of converter, in the early 90s, the research was concentrated on coreless transformer technology.

1.1.1 Coreless transformer technology

Under this section, the evolution of various coreless transformers and their operating principles will be discussed.

a) Twisted coil transformer

A new type of high frequency transformer without a core [19] was first introduced in 1991. This type of transformer consists of a simple twisted pair of coils as illustrated in fig. 2 (a) where its operation is based upon the skin effect of the current carrying conductor. As the operating frequency of the transformer is increased, the leakage inductance of the transformer decreases which results in the increase of the coupling coefficient and thereby the energy efficiency of the transformer can be improved. In these type of transformers, it has been demonstrated that the coupling factor is about 0.8 at an operating frequency of 1MHz. The corresponding energy efficiency of this transformer for different load resistances as a function of frequency is shown in fig. 2 (b).
It can be observed from fig. 2 (b), that the energy efficiency of these transformers is strongly dependent upon the load resistance and the operating frequency. The disadvantages of these type of transformers are

i. Difficulty in the mass production manufacturing process in relation to producing identical coils

ii. Difficulty in controlling the parameters of the twisted coils

iii. Limitations on high operating frequency region

Therefore, the motivation behind the move towards the planar windings on printed circuit board (PCB) has been increased.

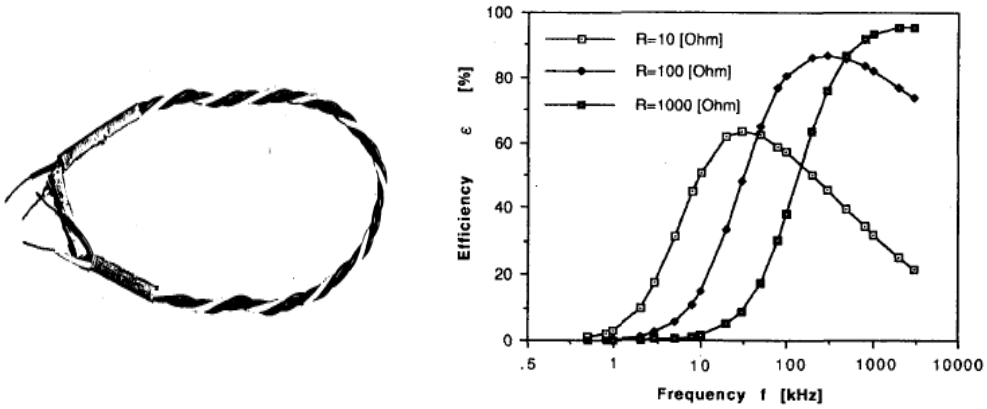

(a) (b)

Figure 2. (a) Twisted coil transformer & (b) energy efficiency [19]

b) Thin film transformer

In 1995, an interesting attempt, involved the printing of the copper windings on the PCB without any magnetic core [20] and this caused the focus of the research to be on the high frequency coreless PCB transformers. In this case, both the primary and secondary windings of the transformer are on a single layer and they are arranged coaxially as shown in fig. 3.

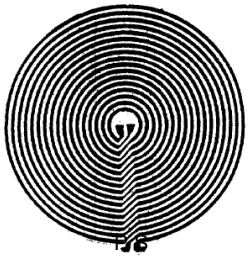

Figure 3. Thin film Transformer [20]

The principle of operation of these transformers is based on the skin and mutual effects between the windings at higher frequencies. In order to attain the parameters for the transformers, an integral equation analysis method has been utilized. However, the problems such as the low coupling factor and high leakage inductance have not been solved in these type of transformers.

c) Coreless PCB transformer

Due to the above mentioned disadvantages of the thin film transformer, an alternative approach involving printing the windings on both sides of the PCB as

shown in fig.4 was also introduced in the late 1990s [21]. The late arrival of the coreless transformers is based on the incorrect belief, that these transformers would result in a low coupling factor, low voltage gain, low input impedance and high radiated EMI due to the absence of a magnetic core. However, these misunderstandings were clarified by incorporating the resonant technique i.e., by the connection of an external resonant capacitor across the secondary terminals of the transformer, which was reported in [21], [22] and these are also explained briefly in this section.

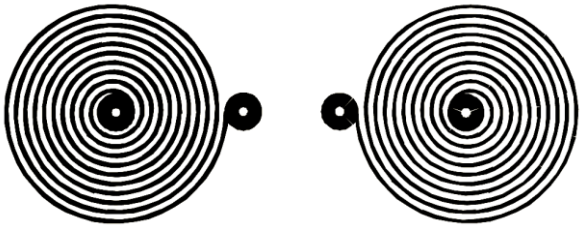

(a) (b)

Figure 4. (a) Top and (b) bottom view of Coreless PCB transformer [22]

Operating principle and characteristics of coreless PCB transformers

Even though the coreless PCB transformers lack the magnetic core, based on the resonant technique i.e., with the connection of an external resonant capacitor across the secondary winding as said earlier, the aforementioned misunderstandings can be clarified.

Voltage gain: The voltage gain is defined as the ratio of the secondary voltage to that of the primary voltage under no load condition. The voltage gain of coreless PCB transformer as a function of frequency [22] is illustrated in fig. 5.

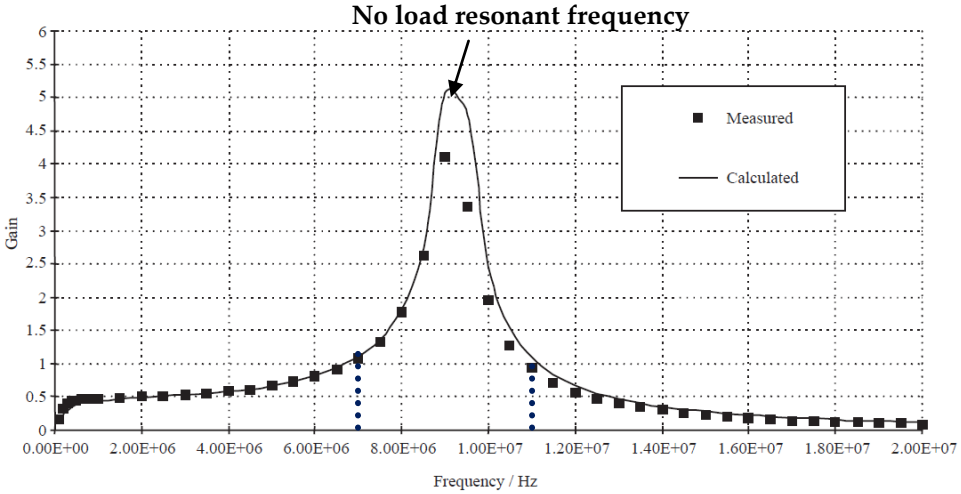

Figure 5. Voltage gain of unity turn's ratio coreless PCB transformer [22]

The frequency at which the voltage gain is at its maximum is known as the no load resonant frequency as shown in fig.5 and it depends on the equivalent inductance and the capacitance of the circuit. From fig. 5, it can be observed that the voltage gain of the unity turn's ratio transformer is greater than unity in the frequency region, 6.5 – 11MHz represented by the dotted line, which shows that the voltage gain can be improved with the assistance of an external resonant capacitor. Obtaining the voltage gain greater than unity also proves that the disadvantage of having a higher leakage inductance as compared to the core based transformers became an apparent advantage in case of coreless PCB transformer.

Low input impedance: Due to the low number of turns in case of core less PCB transformers, there is a belief that they act as short-circuit windings. However, due to the resonance phenomenon, these transformers consist of sufficient amount of input impedance as shown in fig.6 [22].

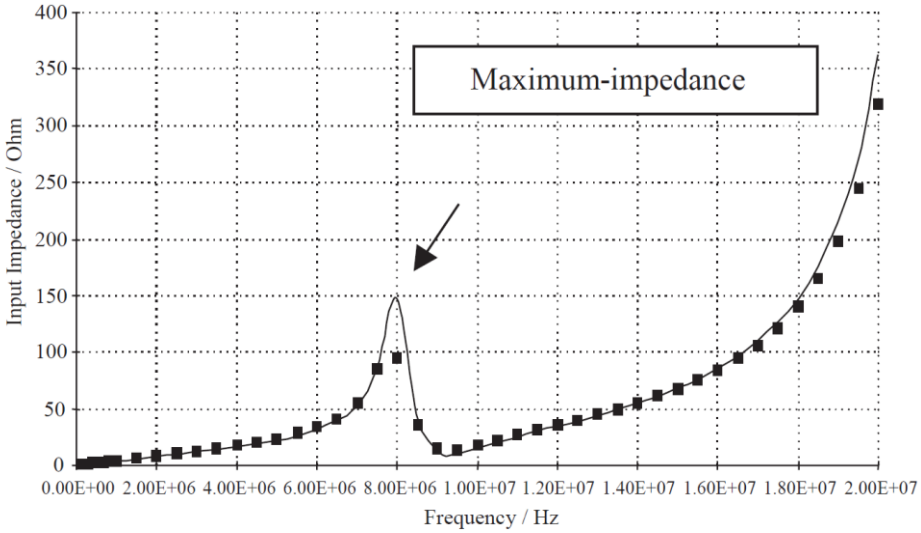

Figure 6. Input impedance of coreless PCB transformer [22]

Here, from this figure, it can be observed that the transformer possess sufficiently high input impedance (>50Ω) in the frequency region of 7 - 8.5MHz, proving that these transformers do not behave as short circuit windings. The frequency at which the input impedance of transformer is at a maximum is known as the maximum impedance frequency (MIF) and from figures 5 and 6, it can be observed that MIF is less than that of the no load resonant frequency.

Energy efficiency: Due to the low coupling factor and low voltage gain of the coreless PCB transformer, it is presumed that the energy efficiency of these transformers is very low compared to those of the core based counterparts.

However, because of the high voltage gain and input impedance obtained by the resonant technique, it is also possible to achieve higher energy efficiencies for these coreless PCB transformers.

For example, the energy efficiency of the unity turn's ratio transformer at different load resistances for a power transfer application is illustrated in fig. 7. From this figure, it can be observed that the energy efficiency of the coreless PCB transformer is greater than 90% for different load conditions.

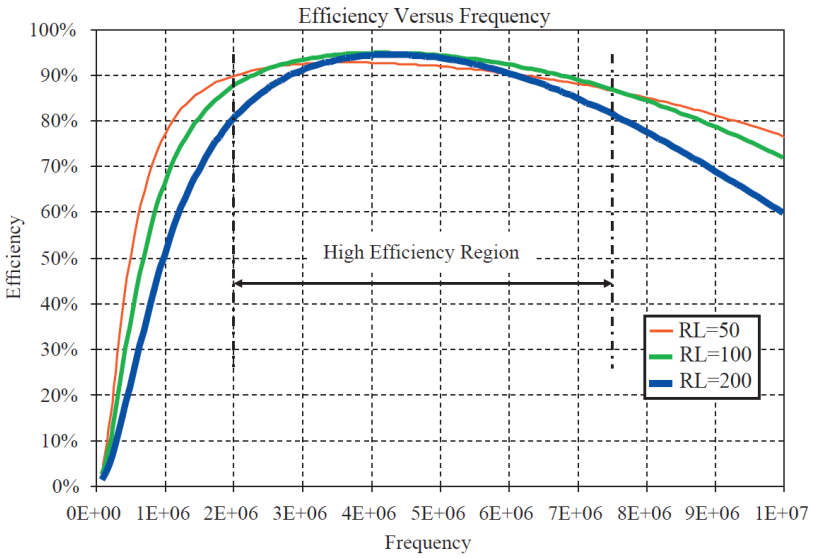

Figure 7. Energy efficiency of unity turn's ratio coreless PCB transformer [22]

When the load power is very low i.e., for signal transfer applications, the maximum energy efficiency frequency (MEEF) approaches MIF [23] whereas, for power transfer applications, MEEF is less than MIF. The desired operating frequency of the transformer can be obtained by varying the resonant capacitor across the secondary terminals of the transformer [23].

Radiated EMI: Since, the coreless PCB transformers are not covered by any magnetic core, it is presumed that the magnetic field which is not confined, results in serious radiated emissions. However, according to antenna theory, a good loop radiator must possess a radius which is closer to that of the wavelength corresponding to the operating frequency [24]. For these coreless PCB transformers, the radius is of a few mm compared to that of the wavelength corresponding to the operating frequency, which is in the order of several meters. Hence, the radiated emissions from these transformers, by considering the fundamental component, have been proved to be negligible [24].

Apart from clarifying the aforementioned misconceptions, these coreless PCB transformers offer the following advantages [22]

- *Operating Frequency*: There is no high frequency limitation imposed on these type of transformers unlike the core based transformers. However, a lower operating frequency limit does exist because of the low magnetizing reactance/impedance of the transformer which increases the primary winding current.

- *Magnetic Saturation*: Since these type of transformers do not contain any core material, no magnetic saturation and core losses exist, as in the case of core based transformers.

- *High Power Density*: As there is no core, there is a drastic reduction in the vertical dimension of the transformer which results in a high power density along with the potential to meet the stringent height requirements of the converters.

- Easy to manufacture low profile transformers with high power density and repeatability.

- Elimination of manual winding and Bobbin.

- Cost effective solution compared to core based transformers due to the elimination of expensive core material.

Due to the aforementioned advantages of coreless PCB transformers, a great deal of research has been focused on designing the magnetics for high frequency signal and power transfer applications without using any magnetic core. On the other hand, the coreless PCB transformers discussed in various literatures [21], [22], [25] - [29] are of unity turn's ratio. However, many SMPS applications demand the step-down/step-up conversion ratios and thus, it is required to investigate these transformers with different turn's ratio which can be utilized for various applications such as Power over Ethernet (PoE), telecom, laptop adapters etc.,

1.2 THESIS OBJECTIVE AND MOTIVATION

The objective of the thesis is to design the high frequency (1 - 10MHz) energy efficient transformers (either coreless or core based transformers) with a high power density, suitable for various AC/DC and DC/DC converter applications for power levels less than 100W.

However, for realizing the thesis objective, there exists several challenges while designing the high frequency magnetics. The winding losses in the transformers increase as the frequency of operation is increased because of the induced eddy current in the windings, which leads to skin and proximity effects. The other major obstacles in the high frequency magnetic components are eddy currents and unbalanced magnetic flux distribution [4]. Due to the unbalanced magnetic flux distribution in the conductors of the transformers, the coupling coefficient is reduced thus resulting in localized hot spots. In addition to this, the parasitic elements of the magnetic components also play an important role in the converter operation when the operating frequency is increased.

Initially, the research was focussed on investigating the possibilities of designing the energy efficiency, high power density coreless PCB transformers for step down conversion applications. The purpose of the first part of the thesis is to discover whether or not the coreless PCB transformers for both signal and power transfer applications will be a potent alternative to the existing core based transformers in order to meet the energy efficient, stringent height low power (0.1 – 100W) applications. The question is whether these transformers offer advantages in terms of energy efficiency and high power density as compared to their commercially available core based counterparts by providing the step-down/step-up voltage conversions.

The second part of the thesis is concentrated on the design and evaluation of the core based transformers by utilizing the existing high frequency core materials (1-10MHz) [30], [31] and with the investigation of different winding strategies suitable for the next generation SMPS.

During this process of achieving the primary objective, several tasks listed below were considered as intermediate goals of the thesis.

- Determination of optimal design (layer comparison) of the step-down transformer in terms of energy efficiency and power density for the given power transfer application.

- Modelling of the coreless PCB step-down transformers for obtaining the exact electrical parameters.

- Estimating the radiated EMI from the designed coreless PCB step-down transformers.

- Design and evaluation of the coreless PCB signal transformer for achieving the low gate drive power consumption.

- Investigation of different winding strategies such as parallel winding strategy and conventional solid winding strategy and to propose the optimal winding strategy for the planar transformers operating in MHz frequency region.

- To propose the design guidelines for obtaining the energy efficient, high power density step-down coreless PCB transformer suitable for power transfer applications based upon the experimental analysis

- Investigating the effect of dielectric laminate on the performance of planar power transformers operating in MHz frequency region.

- Evaluation of the existing core materials and thereby designing the energy efficient core based transformers with high power density operating in MHz frequency region.

1.3 THESIS OUTLINE

The thesis has been divided into two parts in which the first part covers the coreless PCB transformer technology and the second part explores core based transformer technology for high frequency power conversion applications.

The content of the thesis is organized as follows. Initially, in the first chapter of the thesis, some basic background and the motivation behind the requirement of the high frequency PCB transformers for power transfer applications have been provided and this also included the objective of the thesis. In addition to this, the chapter provides the thesis outline and its content.

The second chapter provides a comparison of the designed two layered and three layered coreless PCB step down transformers for a given power transfer application together with a discussion in relation to the necessary theory. Here, the analytical equations for obtaining the desired electrical parameters of the transformer followed by the high frequency model of the coreless PCB transformers are presented. The performance characteristics required for the optimal operation of the transformer is also presented together with some experimental results relating to the two layered and three layered transformers.

In the third chapter, a comparison is made in relation to four different three layered transformers of the same series, in terms of the performance characteristics and the measured energy efficiencies with different loads and resonant capacitors. The importance of the resonant capacitor, which is a determining factor for the optimal operating conditions of the designed transformers and a modelling

procedure to obtain the actual parameters of the designed step-down transformer are also described.

In the fourth chapter, a comparison is made with regards to the transformers discussed in chapters 2 and 3 in terms of radiated emissions. Here, the theoretical estimation of the radiated emissions of these transformers was made for various excitation voltages and presented. In addition to this, the comparative results of the near field measurements for the designed transformers at a give output power was also covered.

In the fifth chapter, the design guidelines for the multilayered coreless PCB gate drive transformers, useful for driving the high side MOSFET in double ended converter topologies, is discussed.

The design guidelines of a multilayered coreless PCB power transformer, its characteristics and application of the designed transformer in a double ended converter topology have been covered in chapter six.

Chapter seven covers the importance of high frequency dielectric material in the design of planar power transformers suitable for the next generation SMPS.

In the eighth and ninth chapters of the thesis, the design details and the performance characteristics of energy efficient novel core based transformers in MHz frequency region and different winding strategies are discussed.

Chapter ten covers the summary of publications and the author's contribution.

In chapter eleven, the contents of the thesis are summarized together with conclusions and future work.

Finally, chapter 12 covers the references cited in the thesis.

At the end of the thesis, the papers related to the work presented in the dissertation have been included.

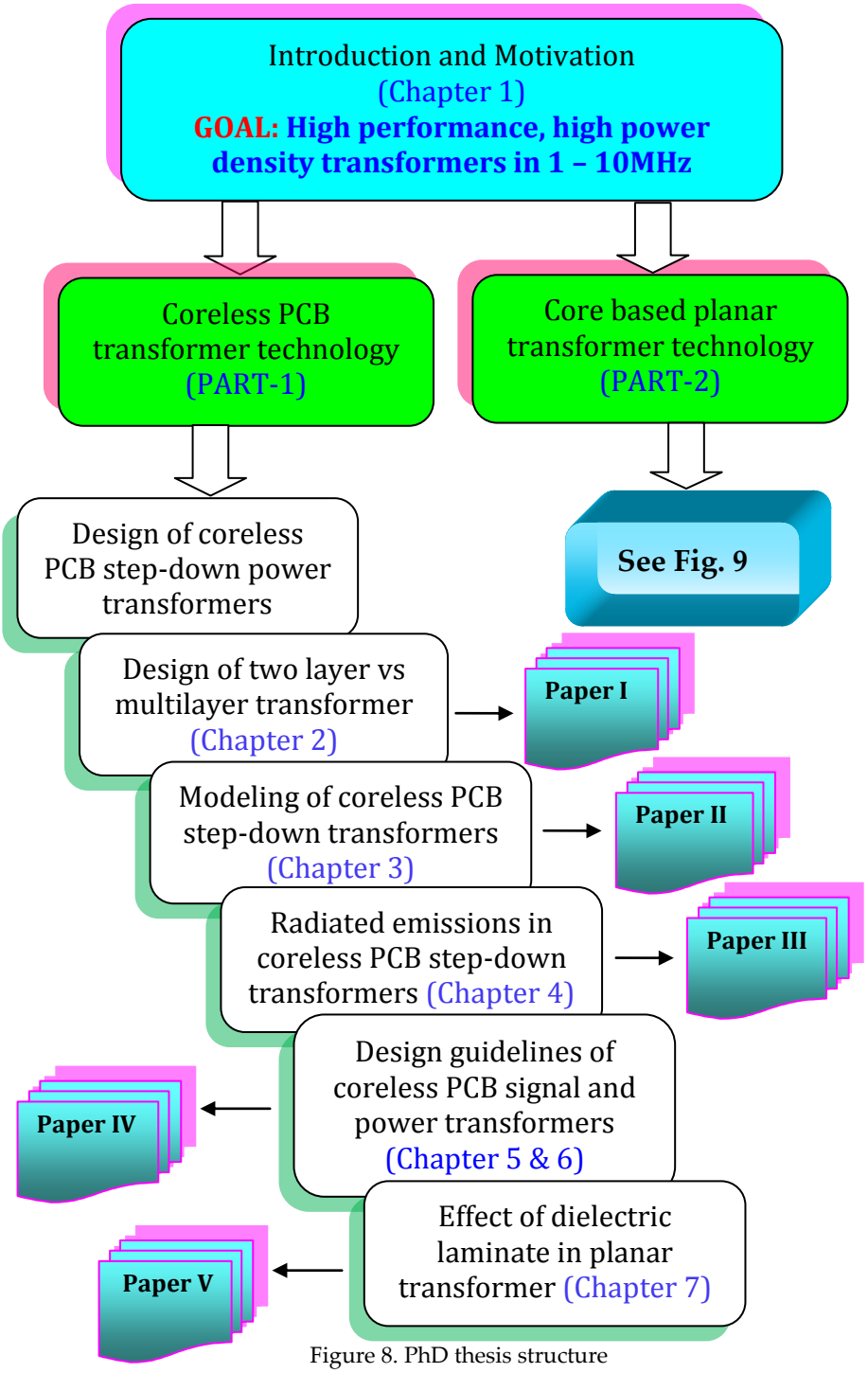

Figure 8. PhD thesis structure

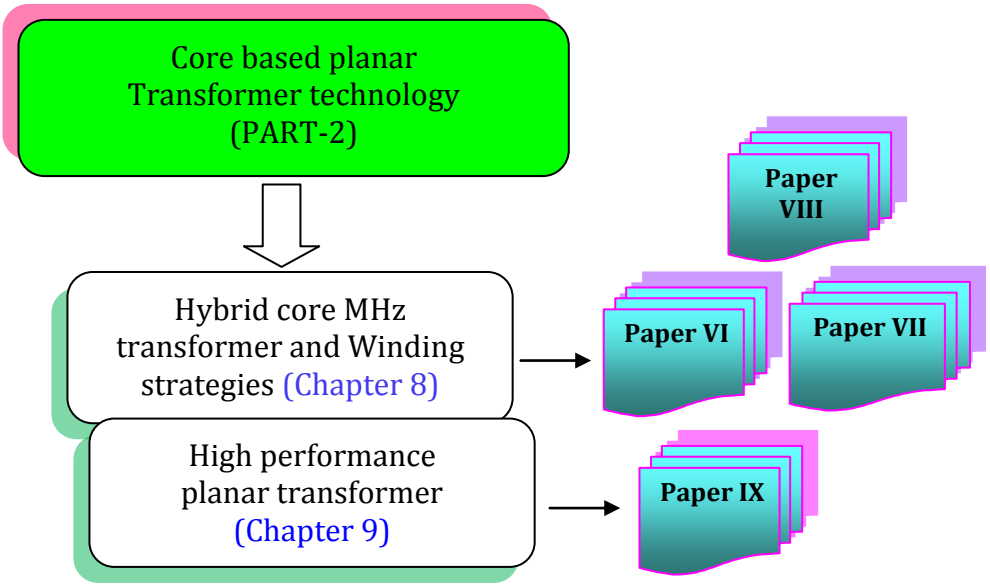

Figure 9. PhD thesis structure (contd..)

PART – 1

Coreless PCB Step-down Transformers for Power Transfer Applications

2 CORELESS PCB STEP-DOWN POWER TRANSFORMERS

As discussed in introduction, the first part of the thesis covers the coreless PCB step-down transformers suitable for power transfer application. The earlier research on coreless PCB transformers shows that these transformers can be used as an isolation transformer for both signal [32] and power transfer applications [33], [34]. However, various DC/DC converter applications such as Power over Ethernet (PoE), wireless local area network (WLAN) Access-points, IP phones and a wide variety of telecom applications demand a high frequency transformer for different step-down ratios so as to obtain compact and stringent height SMPS. For this reason, it is required to estimate different possibilities in relation to obtaining the energy efficient, high frequency step down transformer for the given power transfer application. In this regard, initially the design of the 2:1 step down transformer has been considered for simplicity. In order to evaluate the performance of the 2:1 step down transformer, one of the transformers has been designed in a two layered PCB whereas the other has been designed in a four layered PCB. However, in the latter transformer, three layers were only utilized for the primary/secondary windings and the other layer is used for the external connection. These transformers have been designed in such a way that they possess almost the same inductance in order to compare their performance for the given power transfer application. For both the transformers, the electrical parameters such as inductances, capacitances and resistances have been measured at a particular frequency of 1MHz and a comparison has been made in terms of these measured parameters. The performance characteristics, such as the transfer function $H(f)$, input impedance Z_{in} and energy efficiency η under the same conditions have been measured and compared. Based on these electrical parameters and performance characteristics, an analysis has been made for both the transformers, which will be discussed in the coming sections.

2.1 DESIGN OF TWO LAYERED AND THREE LAYERED 2:1 STEP-DOWN TRANSFORMER

A coreless PCB transformer consists of two parts, namely the dielectric material and copper tracks. The most commonly used electrical insulator is the FR-4 dielectric material whose breakdown strength is 50kV/mm [35]. The primary and secondary windings of the transformer are etched on both sides of the PCB laminate. The dimensions of the designed two layered and the three layered transformers on a four layered PCB of thickness (T) of approximately 1.48 mm are illustrated in fig. 10.

In the two layered transformer, the primary and secondary windings are in the second and third layers of the four layered PCB with primary/secondary turns of 24/12 respectively. In the three layered transformer, the two primaries are on the second and fourth layer of the PCB and these are connected in series with the

assistance of the first layer. Here, from fig.10, it can be observed that the primary and secondary windings of the three layered transformer are fully aligned unlike the two layered transformer.

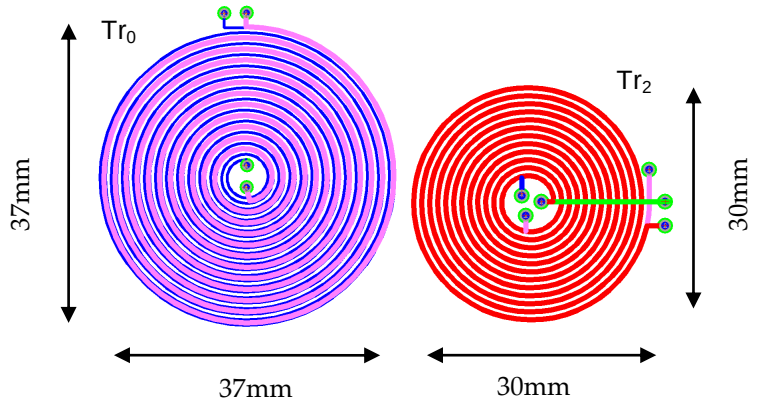

Figure 10. Dimensions of (a) two layered & (b) three layered transformers

The 3D view of both the transformers is illustrated in fig.11. In the three layered transformer, the secondary winding is sandwiched in between the two primaries as shown in fig. 11 (b). The primary/secondary number of turns of the three layered transformer as per the layer arrangement are 12/12/12.

As per IEC950 safety standards, for mains insulation, it is required to have a distance of 0.4mm [36] between the primary and secondary windings if FR-4 dielectric material is used. In the case where the transformers are utilized for DC/DC converter applications, it can be further reduced to 0.2mm. However, in both these transformers, the distance between the primary and secondary windings (Z) is considered as 0.4mm.

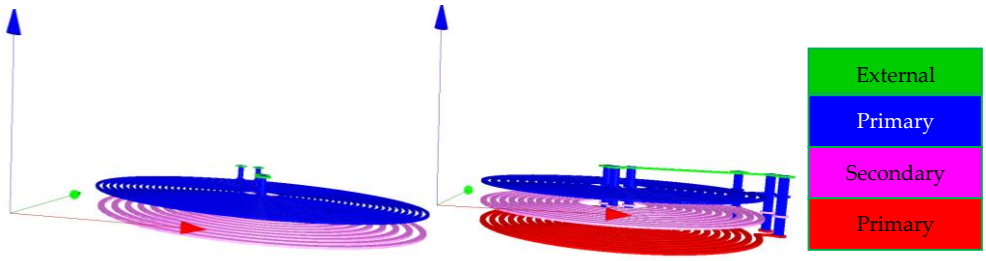

Figure 11. 3D view of (a) two layered and (b) three layered transformers

Since no core material exists in the coreless PCB transformers, the electrical parameters of these transformers purely depend on the geometrical parameters. The parameters that are influencing the performance of the coreless PCB transformers [37] are listed as follows.

- Shape of the winding
- Number of turns of primary/secondary winding of the transformer (N_P)/(N_s)
- Width of the conductor (W)
- Height of the conductor (H)
- Distance between the PCB layers (Z)
- Track separation (S)
- Inner/outermost radius (R_i/R_o)

The geometrical parameters of the above designed two transformers are tabulated and given in Table 1.

Table 1. Geometrical parameters of two layered & three layered transformer

	N_P:N_s	W_P/W_s[mm]	H[μm]	Z[mm]	S_P/S_s[mm]	R_o[mm]	Shape
Tr_0	24:12	0.3/0.64	70	0.4	0.37/0.74	18.5	Circular spiral
Tr_2	12:12:12	0.6/0.6	70	0.4/0.4	0.4/0.4	15	Circular spiral

Regarding the shape of the winding, for the given geometrical parameters, the rectangular spiral winding structure possess the higher value of inductance when compared to other structures such as hoop type, meander and closed type coils [38]. Additionally, for the given amount of inductance, the spiral structure of the transformer provide a lower value of resistance compared to the other above mentioned structures. However, among the entire possible spiral winding structures [39] - [41] such as rectangular, hexagonal, octagonal and circular spiral structures shown in fig.12, the circular spiral winding structure possess a higher inductance and lower inter-winding capacitance. Apart from this, the circular spiral winding structure possess a low DC resistance due to the decreased length of the winding and less overlap area compared to other structures [18]. Therefore, in this thesis, a circular spiral winding structure is considered for the primary/secondary windings of the transformers.

For the given power transfer application, based upon the topology, it is required to obtain the desired amount of inductance of the transformers. For achieving this task, there exists several possibilities of the design depending on the requirements such as power density, energy efficiency, degree of complexity, manufacturing capability, radiated emissions and so on. However, it is not possible to achieve all the desirable features discussed earlier at the same time since there exists trade-off among all these factors. The width of the windings is determined by the value of the current flowing through the conductors and the maximum allowed current density. From table 1, it can be observed that the width of the winding in two layered and three layered transformers are differed, due to the following reason.

For example, in case of the two layered transformer, the width/separation of the primary/secondary windings can be considered as the same as that of the three layered transformer in order to reduce the DC resistance. However, by doing so, the outermost radius of the transformer gets increased to 24mm from 18.5mm for the same amount of inductance, which in turn decreases the power density of the transformer and increases the amount of radiated emissions, since the radiated emissions depend on the outermost radius of transformer which will be discussed in later chapters. For the same amount of load power of 30W, the resulting power density of the transformer is 2.79W/cm^2 for a transformer with 18.5mm radius whereas it is only 1.65W/cm^2 for the transformer with 24mm outermost radius. This results in 40% improvement of the power density in the transformer with 18.5mm outermost radius. Therefore, in order to have high power density of transformer, the geometrical parameters of the two layered transformer are considered as given in table.1.

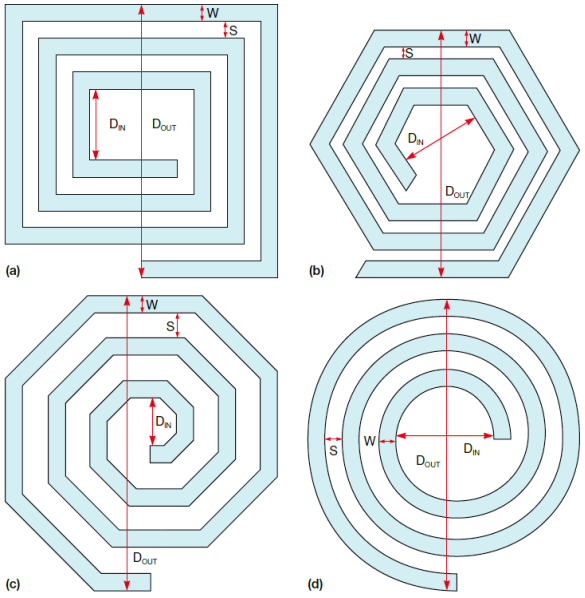

Figure 12. Planar winding of (a) rectangular (b) hexagonal (c) octagonal and (d) circular spiral shapes [39].

The spacing between the copper tracks should be as close as possible in order to obtain the higher inductance which is determined by the manufacturing capability and the cost of production. In general, it is considered to be more than 150μm.

2.2 ELECTRICAL PARAMETERS OF THE TRANSFORMERS

By using the above mentioned geometrical parameters, the electrical parameters such as the resistance, inductance and capacitance of these designed coreless PCB step-down transformers can be estimated with the following methods.

I. Analytical equations given by the Hurley and Duffy method [42] – [44] which can be implemented by using MATLAB program.

II. Finite Element Analysis (FEA) method [29], [45]

Since, FEA is a time consuming method particularly for multilayered coreless PCB transformers, the above parameters were estimated by using method I. The required analytical equations to obtain the electrical parameters of these transformers are discussed in this section. For estimating the self and mutual inductances of a transformer, the spiral windings are approximated to the concentric circles as shown in fig. 13, which are connected in series infinitesimally [37], [42]. The self and mutual inductance calculations using the Hurley and Duffy method are discussed in the coming sub sections.

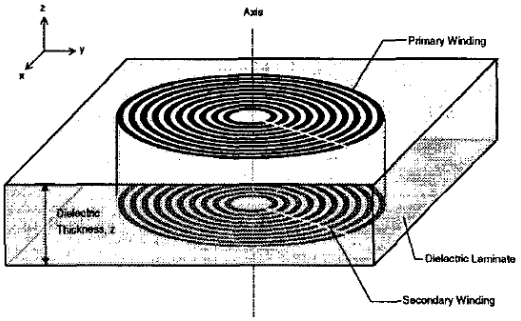

Figure 13. Representation of spiral conductors as approximated infinitesimally series connected concentric circles [37]

2.2.1 Inductance calculations

A transformer consisting of 'N_p/N_s' number of turns on the primary/secondary windings, possess total self inductance [37] which is given as the summation of the mutual inductances between the two concentric circular coils M_{ij} where i, j runs from 1 to N. Therefore, the self inductance of the primary and secondary windings (L_p/L_s) can be obtained as follows:

$$L_p = \sum_{j=1}^{N_p} \sum_{i=1}^{N_p} M_{ij} \tag{1}$$

$$L_s = \sum_{j=1}^{N_s} \sum_{i=1}^{N_s} M_{ij} \tag{2}$$

The mutual inductance of the transformer between the primary and secondary windings is given as the summation of the mutual coupling inductance between them and is given by equation (3)

$$M_{ps} = \sum_{j=1}^{N_p} \sum_{i=1}^{N_s} M_{ij} \tag{3}$$

The mutual inductance between two circular tracks is given as

$$M_{ij} = \frac{\mu_0 \pi}{H_1 \ln\left(\frac{R_{o2}}{R_{i2}}\right) H_2 \ln\left(\frac{R_{o1}}{R_{i1}}\right)} \int_0^{\infty} S(kR_{o2}, kR_{i2}).S(kR_{o1}, kR_{i1}).Q(kH_1, kH_2) e^{-k|Z|} dk \tag{4}$$

where,

$$S(kR_{o2}, kR_{i2}) = \frac{J_0(kR_{o2}) - J_0(kR_{i2})}{k} \tag{5}$$

$$S(kR_{o1}, kR_{i1}) = \frac{J_0(kR_{o1}) - J_0(kR_{i1})}{k} \tag{6}$$

$$Q(kH_1, kH_2) = \frac{2}{k^2}\left(\cosh k\frac{H_1 + H_2}{2} - \cosh k\frac{H_1 - H_2}{2}\right), where' Z' > \frac{H_1 + H_2}{2} \tag{7}$$

$$Q(kH_1, kH_2) = \frac{2}{k}\left(H - \frac{e^{-kH} - 1}{k}\right), where' Z' = 0, H_1 - H_2 = H \tag{8}$$

Here,

μ_0	permeability of vacuum
J_0 ()	first kind Bessel function of order zero
R_{i1}/R_{i2}	inner radius of i^{th}/j^{th} circular track
R_{o1}/R_{o2}	outermost radius of i^{th}/j^{th} circular track
H_1/H_2	height of the conductors
Z	distance between the layers

Therefore, the primary/secondary leakage inductances of the transformer are obtained by subtracting the mutual inductance 'M_{ps}' from their corresponding self inductances and turn's ratio 'n'.

$$L_{lkp} = L_p - M_{ps} \cdot n \tag{9}$$

$$L_{lks} = L_s - \frac{M_{ps}}{n} \tag{10}$$

$$n = \sqrt{\frac{L_p}{L_s}} \tag{11}$$

2.2.2 DC resistance calculations

The DC resistances of the primary/secondary windings of the transformer can be calculated by knowing the length, cross sectional area of the winding and the resistivity and is given as follows.

$$R = \frac{\rho \cdot l}{A} \tag{12}$$

where,

ρ resistivity of copper conductor, 1.68×10^{-8} Ω-m
l length of the conductor (m)
A cross sectional area of copper tracks given by the product of width and the height of the conductor (m^2)

2.2.3 Capacitance calculations

The inter-winding capacitance of the coreless PCB transformers i.e., the capacitance between the primary/secondary windings of the transformer can be calculated by assuming two planar windings as two parallel conducting plates [46] and is given by the following equation.

$$C_{ps} = \frac{\varepsilon \cdot A_p}{Z} \tag{13}$$

$$\varepsilon = \varepsilon_o \cdot \varepsilon_r \tag{14}$$

where,

ε_o permittivity of air, 8.854×10^{-12} F/m
ε_r relative permittivity of dielectric material, 4.4 for FR-4
Z distance between two parallel plates (dielectric thickness)
A_p area of conducting plates

Since, the above equation (13) is valid for the plates, which are densely packed and as it also does not take fringing effects into account, the following equation [46] can be utilized for determining the capacitance between the parallel plates in the case of coreless PCB transformers.

$$C_{ps} = \frac{\varepsilon(w + 0.5Z) \cdot l}{Z} \tag{15}$$

where,

l length of the parallel plate (m)

For both the transformers, the aforementioned electrical parameters are calculated by solving the analytical equations (1) – (15) with the assistance of MATLAB.

2.3 HIGH FREQUENCY MODEL OF CORELESS PCB TRANSFORMER

The high frequency model of a coreless PCB power transformer operating in MHz frequency region is shown in fig. 14. In this case, the intra-winding or self capacitance of both the primary (C_{pp}) and secondary (C_{ss}) windings [21] are very small, typically in the range of a few pFs, and hence can be ignored. The primary/secondary mutual inductances of the transformer by knowing the self and leakage inductances can be calculated as follows:

$$L_{mp} = L_p - L_{lkp} \tag{16}$$

$$L_{ms} = L_s - L_{lks} \tag{17}$$

Therefore, the mutual inductance of the transformer which is a geometric mean of 'L_{mp}' and 'L_{ms}' is obtained as follows.

$$L_m = \sqrt{L_{mp} \cdot L_{ms}} \tag{18}$$

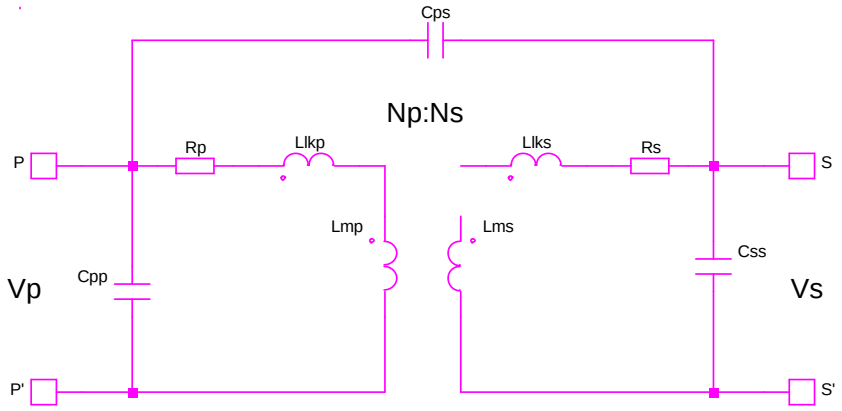

Figure 14. High Frequency model of coreless PCB step-down transformer

Here,

R_p/R_s	primary/secondary AC resistance of transformer
L_{lkp}/L_{lks}	primary/secondary leakage inductance of transformer
L_{mp}/L_{ms}	primary/secondary mutual inductance of transformer
C_{ps}	inter-winding capacitance of transformer
C_{pp}/C_{ss}	primary/secondary intra-winding capacitance

In order to obtain the optimal design of a coreless PCB transformer, consideration has to be given to two important parameters i.e., the coefficient of coupling (K) and the winding resistance (R_p/R_s) of the transformer.

2.3.1 Coupling coefficient, (K)

The coefficient of coupling 'K' for the transformers can be obtained by using the following equation

$$K = \frac{L_m}{\sqrt{L_p \cdot L_s}} \tag{19}$$

2.3.2 AC Resistance

The winding resistance of the transformer increases as the operating frequency of the currents is increased because of both the skin and proximity effects. However, the proximity effects in the case of the two layered transformer is very small compared to the multilayered transformers. By approximating the rectangular spiral to a circular spiral winding [47], the AC resistances of the primary/secondary

windings for the designed transformers, considering only the skin effect, were calculated by using the following equation (20).

$$R_{ac} = \frac{R_{dc} \cdot H}{\delta\left(1 - \exp\left(\frac{-H}{\delta}\right)\right)} \tag{20}$$

where,

R_{dc} DC resistance of winding
H height of the conductor
δ skin depth

The equation for skin depth or depth of penetration of the conductor by magnetic flux is given as follows:

$$\delta = \frac{1}{\sqrt{\pi f \mu \sigma}} \tag{21}$$

f operating frequency
μ permeability of medium
σ conductivity

However, the above mentioned equation (20) for calculating the AC resistance includes only the skin effect in the transformer. Since, in multilayered coreless PCB transformers, the AC resistance increases due to both the skin and proximity effects, it can be calculated by the following equation [48] - [50].

$$R_{ac} = \underbrace{R_{dc} \cdot \frac{\Delta}{2}\left[\frac{\sinh\Delta + \sin\Delta}{\cosh\Delta - \cos\Delta}\right]}_{T_1} + \underbrace{R_{dc} \cdot \frac{\Delta}{2}\left[(2m-1)^2 \cdot \frac{\sinh\Delta - \sin\Delta}{\cosh\Delta + \cos\Delta}\right]}_{T_2} \tag{22}$$

where,

$$\Delta = \frac{H}{\delta} \tag{23}$$

m number of layers in a winding section where MMF reaches from 0 to maximum value

Here, the first term 'T_1' corresponds to the skin effect whereas the second term 'T_2' represents the proximity effect. Since, the structure of the three layered transformer is primary-secondary-primary (PSP), the term 'm' tends to unity [49].

2.4 PERFORMANCE CHARACTERISTICS OF CORELESS PCB TRANSFORMERS

In order to determine the operating frequency of the coreless PCB transformers, the performance characteristics such as the transfer function $H(f)$, input impedance 'Z_{in}', corresponding phase angle 'ϕ' and energy efficiency 'η' are required. These characteristics can be obtained by using the high frequency equivalent circuit of the transformer referred to primary side [22] as depicted in fig.15.

2.4.1 Transfer function *H(f)* and input impedance *(Z_{in})*

The transfer function *H (f)* of the transformer is defined as the ratio of secondary voltage *(V_s)* to that of the primary voltage *(V_p)* under loaded conditions and is given as follows.

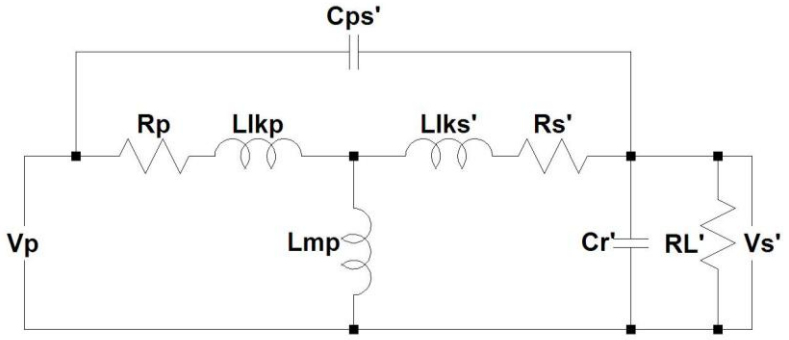

Figure 15. High frequency model of coreless PCB transformer referred to primary

$$H(f) = \frac{V_s}{V_p} = \frac{(1/X_1) + j(2\pi f)C_{ps}'Y_1}{nY} \tag{24}$$

The input impedance (Z_{in}) of the coreless PCB transformer can be obtained as follows

$$Z_{in} = \frac{1}{sC_{ps}'(1 - n\cdot\frac{V_s}{V_p}) + \frac{(1-A)}{X_1} + sC_{pp}'} \tag{25}$$

$$R_s' = n^2 R_s \tag{26}$$

$$L_{lks}' = n^2 L_{lks} \tag{27}$$

$$C_{pp}' = C_{pp} + \frac{n-1}{n} C_{ps} \tag{28}$$

$$C_r' = \frac{1}{n^2} C_r + \frac{1-n}{n^2} C_{ps} \tag{29}$$

$$C_{ps}' = \frac{1}{n} C_{ps} \tag{30}$$

$$X_1 = R_p + sL_{lkp} \tag{31}$$

$$X_2 = R_s' + sL_{lks}' \tag{32}$$

$$Y_1 = X_2\left[\frac{1}{X_1} + \frac{1}{sL_{mp}}\right] + 1 \tag{33}$$

$$Y_2 = \frac{1}{X_2} + sC_{ps}' + sC_r' + \frac{1}{n^2 R_L} \tag{34}$$

$$Y = -\frac{1}{X_2} + Y_1 Y_2 \tag{35}$$

$$A = \frac{sC_{ps}' + \frac{X_2}{X_1} Y_2}{Y} \tag{36}$$

2.4.2 Maximum gain frequency, f_r

The frequency at which the transfer function is maximum is known as the maximum gain frequency, f_r.

$$f_r = \frac{1}{2\pi\sqrt{L_{eq} \cdot C_{eq}}} \tag{37}$$

where

$$L_{eq} = L_{lks}' + L_{mp} \,||\, L_{lkp} \tag{38}$$

$$C_{eq} = C_r' + C_{ps}' \tag{39}$$

2.4.3 Maximum Impedance Frequency (*MIF*)

The frequency at which the input impedance of the transformer is maximum is known as the maximum impedance frequency (MIF). It is always less than the maximum gain frequency (f_r) of the transformer.

2.4.4 Maximum Energy Efficiency Frequency (*MEEF*)

The frequency at which the energy efficiency of the transformer is maximum is known as the maximum energy efficiency frequency (MEEF). It is always less than the f_r and MIF of the transformer. Therefore, the relationship between the maximum gain frequency, maximum impedance frequency and the maximum energy efficiency frequency can be given as follows.

$$MEEF \leq MIF < f_r \tag{40}$$

For signal and low power applications, the maximum energy efficiency frequency (MEEF) of the transformer is equal to the maximum impedance frequency (MIF).

2.5 MEASUREMENT OF ELECTRICAL PARAMETERS OF THE DESIGNED CORELESS PCB STEP-DOWN TRANSFORMERS

The initial electrical parameters of the designed coreless PCB transformers were measured at 1MHz using the HP4284A high precision RLC meter. The primary/secondary self inductances and resistances are obtained by open circuiting the opposite winding of the transformer, whereas the leakage inductances L_{lkp}/L_{lks} are obtained by short circuiting the opposite winding of the transformer. Apart from this, the four wire measuring method can also be used for obtaining the

leakage inductances of the transformer which are less than 1μH [51]. By using this method the leakage inductance can be obtained as follows.

$$L_{lk} = \left(\frac{50}{2\pi f}\right)\left(\frac{V_{dut}}{V_{50\Omega}}\right) \tag{41}$$

where,

L_{lk}	leakage inductance
f	excitation frequency
V_{dut}	voltage across device under test
$V_{50\Omega}$	voltage across 50Ω resistor

For obtaining the precise parameters of the transformers, the initial measured parameters using RLC meter were passed into the above high frequency model shown in fig.15 and fine tuned such that the measured performance characteristics, such as $H(f)$, and Z_{in} are in good agreement with that of the modelled ones. Hence, the actual parameters of the transformers can be obtained with the assistance of initial measured parameters, the high frequency model and measured performance characteristics. The comparison of the actual parameters obtained from measurements and modelling together with the analytical parameters obtained by using MATLAB are shown in Table 2.

Table 2. Analytical and actual electrical parameters of 'Tr_0' and 'Tr_2'

	L_p	L_s	L_{lkp}	L_{lks}	L_{mp}	L_{ms}	L_m	$R_{p\_dc}[\Omega]$	$R_{s\_dc}[\Omega]$	C_{ps}[pF]	K
Tr_0(A)	9.49	2.71	0.7	0.19	8.8	2.52	4.7	1.68	0.4	79	0.92
Tr_0(M)	9.65	2.54	0.9	0.28	8.75	2.26	4.53	1.9	0.47	96	0.91
Tr_2(A)	8.44	2.27	0.37	0.1	8.07	2.17	4.18	0.75	0.35	109	0.95
Tr_2(M)	8.25	2.2	0.4	0.18	7.85	2.02	3.98	0.84	0.41	119	0.93

L_p, L_s, L_{lkp}, L_{lks}, L_{mp}, L_{ms}, L_m – *in* μH

A – Analytical parameters; M – Actual parameters of transformers

The percentage deviations of the analytical values from the modelled ones in terms of self inductances L_p/L_s of the two layered transformer were found to be 1.6/6.6% respectively. In the case of the three layered transformer, this was found to be 2.3/3.1% respectively for L_p/L_s. In both cases, the deviations in the inter-winding capacitance 'C_{ps}' were found to be 17.7/8.4% respectively for two/three layered transformers. From table 2, it can be verified that the parameters obtained by solving the analytical equations using MATLAB are, to a certain extent, in good agreement, in terms of the self inductances of the transformers with that of the modelled parameters. This gives an initial idea of the required primary/secondary inductances for the given power transfer application prior to the physical design of the transformer.

The DC resistance of the primary/secondary winding of both the transformers is given in table 2 and their corresponding calculated AC resistances in the frequency

range of 100 kHz – 10MHz using the equations (20) - (22) are shown in fig. 16. It can be observed that the AC resistance, in the case of primary/secondary winding of the two layered transformer, is higher than that of the three layered transformer. This is due to the increased length of the winding and reduced width of the conductor of the primary winding in the case of the two layered transformer. It can be observed from the fig. 16, that the rate of rise of the AC resistance is increasing in nature in the case of the three layered transformer after a certain frequency range, due to the proximity effect, which is dominant compared to the skin effect in the case of the multilayered transformers.

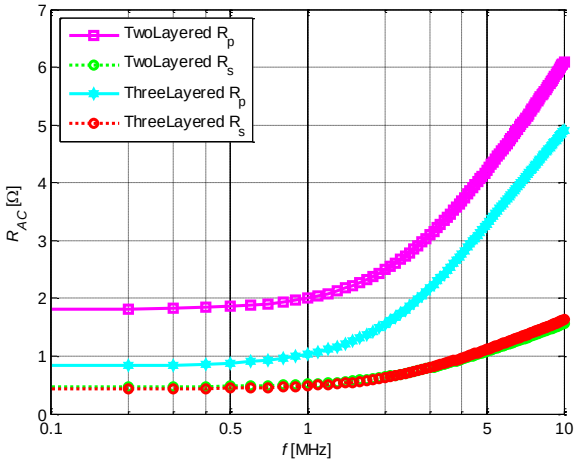

Figure 16. Calculated AC resistance of coreless PCB step down transformers

2.6 EXPERIMENTAL SET-UP AND POWER TESTS OF DESIGNED CORELESS PCB STEP-DOWN TRANSFORMERS

The experimental flow diagram in order to characterize the transformers for power transfer applications is illustrated in fig. 17.

In order to evaluate the performance of these power transformers in terms of their transfer function *H(f)*, input impedance *(Z_{in})* and energy efficiencies *(η)*, power tests were conducted by using EMPOWER BBM0A3FKO radio frequency power amplifier. This power amplifier is capable of delivering 100W with an adjustable frequency range of 0.01MHz - 230MHz. The input given to the power amplifier can be adjusted by varying the amplitude, frequency and the type of excitation such as sinusoidal, square wave etc., from the signal generator, HP 33120A. The output of the power amplifier is fed to the designed transformers (DUT) and the above mentioned performance characteristics of the transformers are determined by retrieving the primary and secondary voltages/currents from a Tektronix TPS2024 oscilloscope, consisting of four isolated channels with 200MHz bandwidth and 2Gs/sec sampling rate.

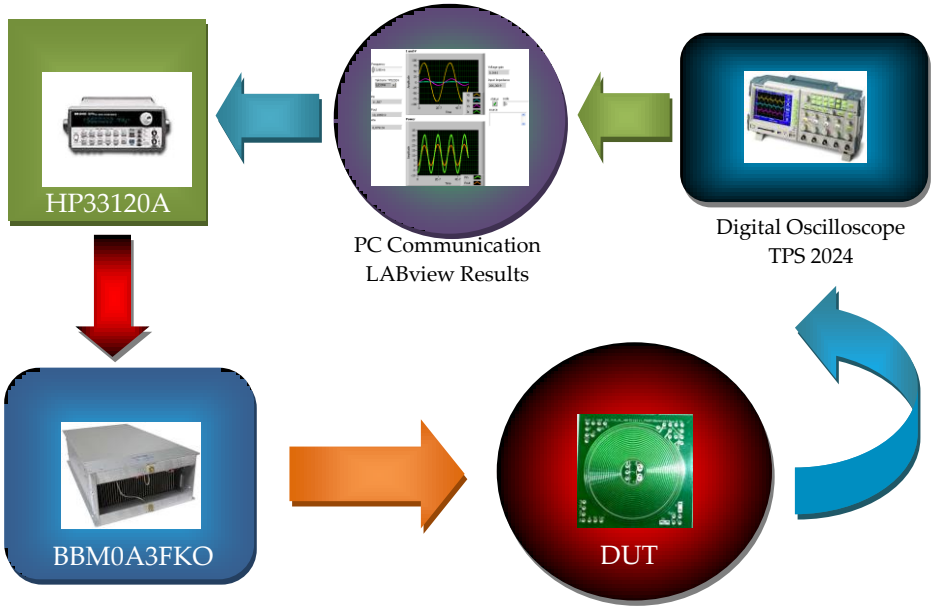

Figure 17. Block diagram representation of experimental flow to characterize transformers

The experimental setup and the schematic diagram of the coreless PCB transformer together with the resonant capacitor under loaded condition are shown in fig. 18. The primary/secondary currents 'I_{pri}/I_{sec}', flowing through the transformer were measured by utilizing Tektronix AC current probes CT2 [52] of 1.2 kHz – 200 MHz bandwidth and with propagation delay of 6.1ns. Similarly, the primary/secondary voltages 'V_{pri}/V_{sec}' of the transformer were measured by using Tektronix P2220 passive probes [53] whose bandwidth is in the range of DC - 200MHz with a typical probe capacitance of 17pF. The retrieved primary/secondary voltages and currents from the oscilloscope were processed by using the LABVIEW 8.5 professional software from which the performance characteristics such as transfer function, input impedance and energy efficiency of transformers can be obtained.

The measured performance characteristics $H(f)$ and Z_{in} of the two layered and three layered transformers with a load resistance 'R_L' of 500Ω and a resonant capacitor 'C_r' of 1.2nF is illustrated in figs. 19 (a) and (b) respectively. The measured maximum gain frequencies of the two/three layered transformers are 7.5/9MHz respectively, which can be observed from fig. 19 (a). Here, the maximum gain frequency of the three layered transformer for a given resonant capacitor is higher compared to that of the two layered transformer because of the reduced leakage inductance. From fig.19 (b), it can be observed that the maximum gain frequencies of both the transformers are 2.9/3.4 MHz respectively. From fig.19 (a) and (b), it can be verified that the maximum impedance frequency (MIF) of both these

transformers is lower compared to their corresponding maximum gain frequencies (f_t), as discussed earlier.

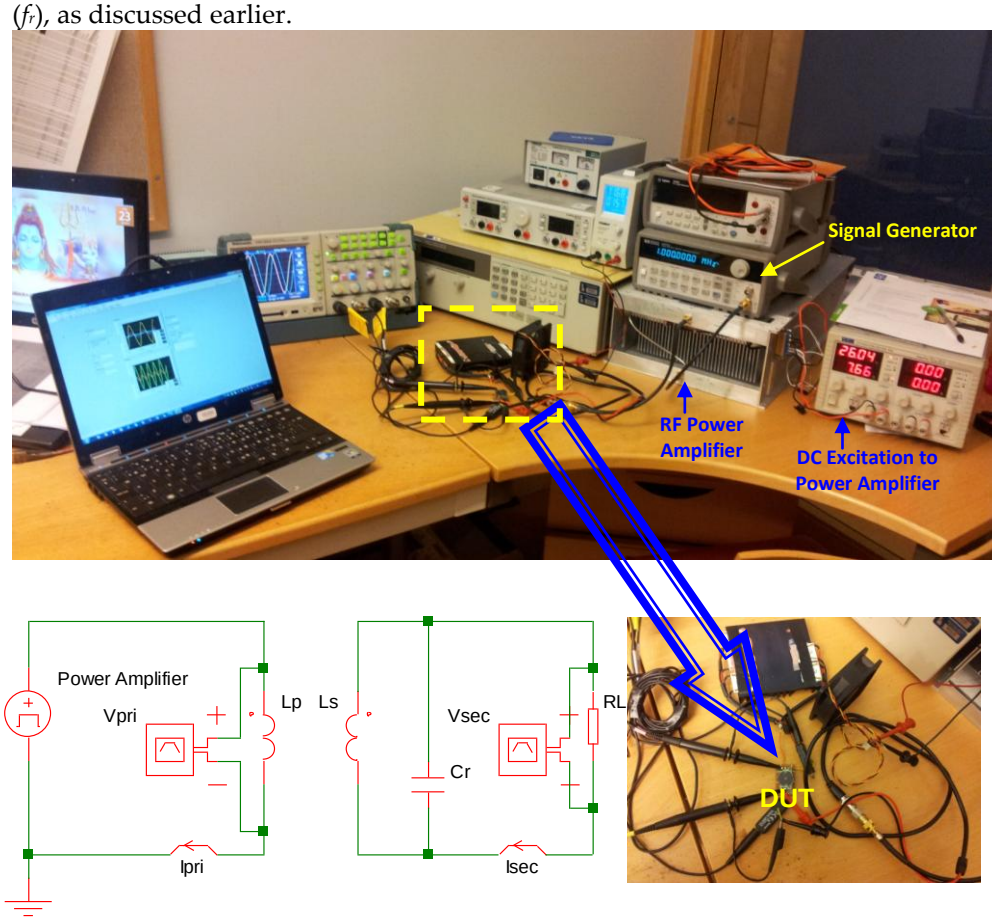

Figure 18. Experimental set-up for the power tests of designed transformers

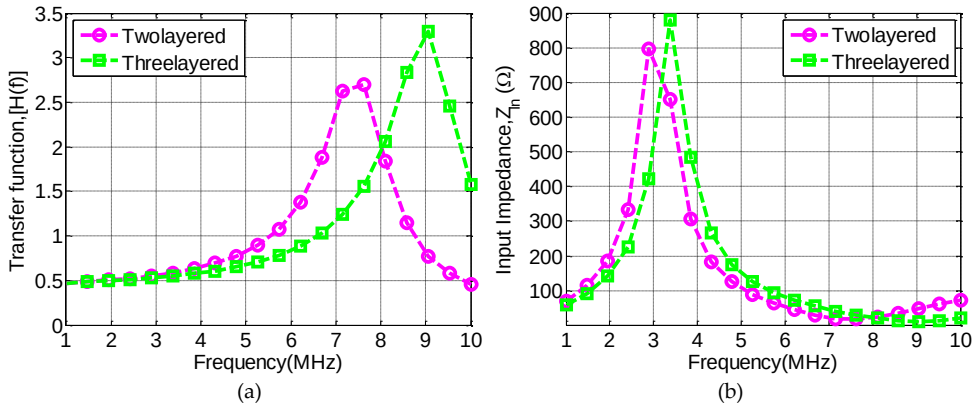

Figure 19. Measured (a) transfer function $H(f)$ and (b) input impedance of two/three layered transformers with R_L=500Ω and C_r=1.2nF

The measured average input/output powers per cycle of the designed transformers are obtained from the instantaneous voltage and current waveforms and are given by the following equations.

$$P_{in} = \frac{1}{T}\int_0^T v_{pri}(t)\cdot i_{pri}(t)dt = \left|V_{pri}\right|^2 \cdot \Re\left(\frac{1}{Z_{in}}\right) \tag{42}$$

$$P_{out} = \frac{1}{T}\int_0^T v_{\sec}(t)\cdot i_{\sec}(t)dt = \frac{\left|V_{\sec}\right|^2}{R_L} \tag{43}$$

Therefore, by knowing the average input and output powers, the energy efficiency of the transformers can be obtained by using the following equation (44).

$$\%\eta_{meas} = \frac{P_{out}}{P_{in}}\cdot 100\% \tag{44}$$

The measured energy efficiency of the two layered and three layered transformers with a load resistance R_L of 30Ω and 50Ω is illustrated in fig. 20. Here, a resonant capacitor of 1.2nF was placed across the secondary winding of the transformers in order to bring the maximum energy efficiency frequency into the range of 2 – 4MHz.

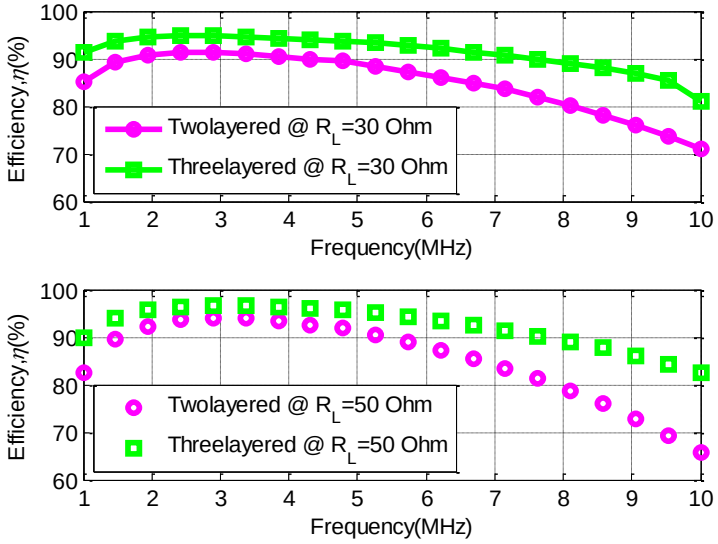

Figure 20. Measured efficiency of transformers for different load conditions

It can be observed from fig. 20, that the energy efficiency of the three layered transformer is higher for both loads as compared to the two layered transformer despite of having comparatively large inter-winding capacitance. This can be explained by two major factors, namely, the coupling coefficient (K) and the AC resistances of the transformers. From fig. 16, it can be observed that the AC resistance of the two layered transformer is higher as compared to that of the three

layered transformer which results in increased copper losses in the two layered transformer. Also from table 2, it can be observed that the coupling coefficient of the three layered transformer is higher because the secondary winding of the transformer is sandwiched in between the two primary windings and also due to the perfect alignment of the primary and secondary conductors.

The designed coreless PCB power transformers are tested at their maximum energy efficiency frequencies (*MEEF*) up to the power level of about 25W and the corresponding results are depicted in fig. 21. It can be also observed from fig. 21 that for the entire load power range, the three layered transformer is better as compared to the two layered transformer. Here, the peak energy efficiency of the two layered/three layered transformers is 92% and 94.5% respectively.

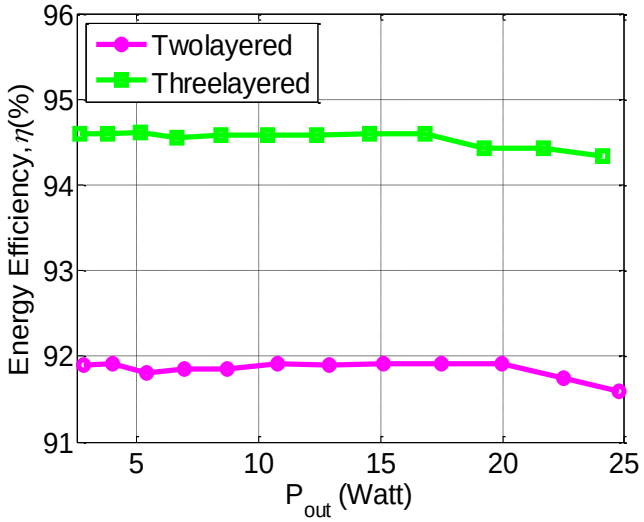

Figure 21. Measured efficiency of transformers at MEEF

3 MODELLING, OPTIMIZATION AND APPLICATION POTENTIALS OF CORELESS PCB STEP-DOWN POWER TRANSFORMERS

From the analysis of chapter 2, it was found that for a given power transfer application, the three layered 2:1 transformer is better in terms of energy efficiency as compared to the two layered 2:1 transformer due to the increased coupling coefficient (*K*) and the reduced copper losses. By possessing a low coupling coefficient of transformer, the current drawn from the primary and hence the secondary winding gets increased and thereby by the conduction losses increases. On the other hand, in order to have higher coupling coefficient, the size of the transformer has to be increased which leads to increased AC resistance and reduced power density of transformer. Therefore, the coefficient of coupling '*K*' and the AC resistance both have an impact on the performance of the coreless PCB transformer which demands the optimized coupling coefficient and AC resistance.

For the given power transfer application, the coupling coefficient of the transformer can be improved by increasing the area of the transformer with or without increasing the number of turns [37]. However, if the area of the transformer is increased by increasing the number of turns, the rate of increase of the self inductance of the transformers is higher in comparison to its leakage inductance which leads to high coupling coefficient. Therefore in this regard, a series, consisting of four different three layered 2:1 step-down transformers shown in fig. 22 were designed. These transformers were compared in terms of their self, leakage and mutual inductances, AC resistances, coupling coefficient, and energy efficiencies.

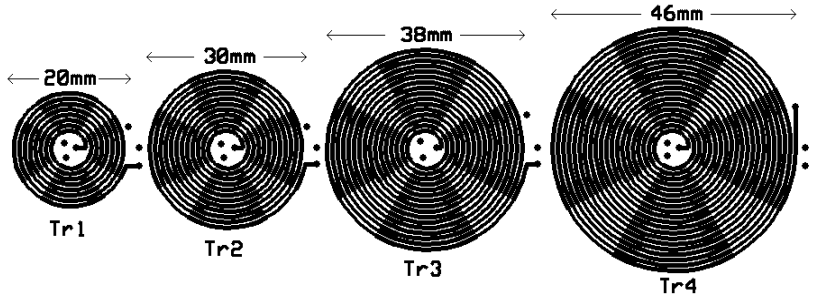

Figure 22. Dimensions of same series coreless PCB step-down transformers with different turns

Here, the geometrical parameters of the coreless PCB step-down transformers are considered as follows: conductor width (W) of 0.6mm, track separation (S) of 0.4mm, conductor height (H) of 70μm and total height of PCB as 1.48mm. The corresponding number of turns in each layer of these transformers T_{r1}, T_{r2}, T_{r3} and T_{r4} are 8/12/16/20.

3.1 MODELLING OF CORELESS PCB STEP-DOWN TRANSFORMERS

As the coreless PCB transformers operate with the assistance of resonance phenomena, it is very crucial to obtain precise electrical parameters for the designed transformers to make it easier in relation to analyzing the transformer behavior in the converter circuit. Therefore, as mentioned in chapter 2, the initial parameters of these transformers such as self and leakage inductances, resistances, capacitances, were measured with the assistance of high precision RLC meter at 1MHz. The measured performance characteristics of the designed transformers such as $H(f)$, Z_{in}, and phase angle ϕ, were obtained by following the experimental procedure described in section 2.6 of chapter 2. Then the initial measured electrical parameters were passed into the high frequency equivalent circuit shown in fig 15 and are then fine tuned in order to match the measured and modelled performance characteristics of these transformers. In this way, the actual parameters of the transformers were obtained.

Case (i): Transfer function *H(f)*

By following the above mentioned modelling procedure and from the measured performance characteristics, the magnitude of the transfer functions $H(f)$ for two different resonant capacitors of 1.5nF and 2.2nF at a load resistance of 470Ω for all the transformers are obtained and are illustrated in fig. 23 (a) and (b) respectively.

From fig.23, it can be observed that the measured transfer function of the transformers is in good agreement with those calculated by using the analytical equations discussed in chapter 2. From fig. 23(a) and (b), it can be observed that both the magnitude of the peak and the resonant frequencies decrease as the number of turns increases. According to equation (37), the resonant frequency of the transformers decreases for larger resonant capacitors across the secondary winding of the transformers. This phenomenon can be observed from fig. 23 (a), that the resonant frequency of the transformer Tr_1 with C_r=1.5nF is close to 9.7MHz whereas in fig. 23(b) it is 8.0MHz when C_r=2.2nF.

Case (ii): Input impedance 'Z_{in}' and phase angle 'ϕ'

Under the load condition R_L of 470Ω and an external resonant capacitor of 1.5nF, the measured and modelled input impedance (Z_{in}) and the phase angle (ϕ) of the transformers (Tr_1-Tr_4) are plotted in fig. 24 (a) and (b) respectively.

From fig. 23 (a), the maximum gain frequency of transformer Tr_1 is approximately 9.7MHz. For the same transformer Tr_1, from fig. 24 (a) it can be observed, that the input impedance peaks at 4.8MHz approximately, which is known as MIF. From

figs. 23 (a) and 24 (a), the maximum impedance frequency of the transformer is less than the no load resonant frequency which agrees well with the expression (40). From fig. 24 (b), it can be observed that before MIF, the transformer is highly inductive in nature.

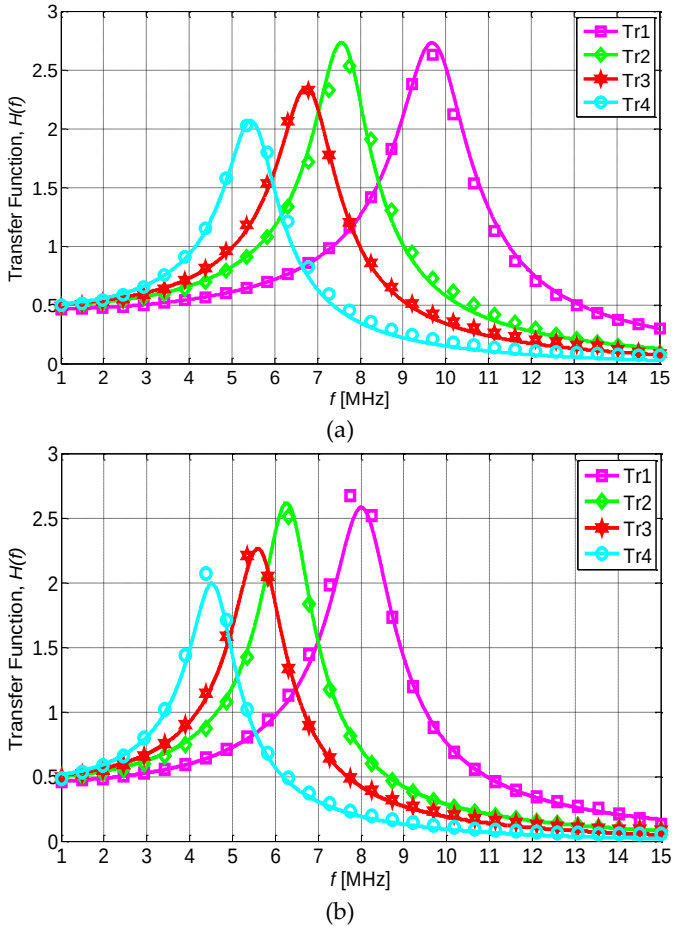

Figure 23. Modelled (solid line) and measured (markers) transfer function $H(f)$ of the transformers with R_L=470 Ω, (a) C_r=1.5nF and (b) C_r=2.2nF

The operating frequency region of the transformer is considered as the region where the transformer possesses sufficient input impedance and also where it is highly inductive in nature. Hence, for power transfer applications with these coreless PCB step-down transformers, the maximum impedance frequency i.e., MIF determines the operating frequency region. The input impedance of the transformer Tr_1 at 3MHz is sufficiently high and has a magnitude of approximately 85Ω and thus the corresponding operating frequency region of this transformer lies approximately in the frequency range of 3 - 4.8MHz. After this frequency region,

the input impedance of the transformer decreases as shown in fig. 24 (a) and additionally the transformer is not inductive in nature as illustrated in fig. 24 (b), hence it is not possible to operate the transformer after MIF. The same phenomenon i.e., the MIF, operating frequency region is observed for the remaining transformers Tr_2 - Tr_4. The input impedance of the transformers Tr_1-Tr_4 is observed to be increasing in nature as shown in fig. 24 (a) because of the increased inductance of the transformers.

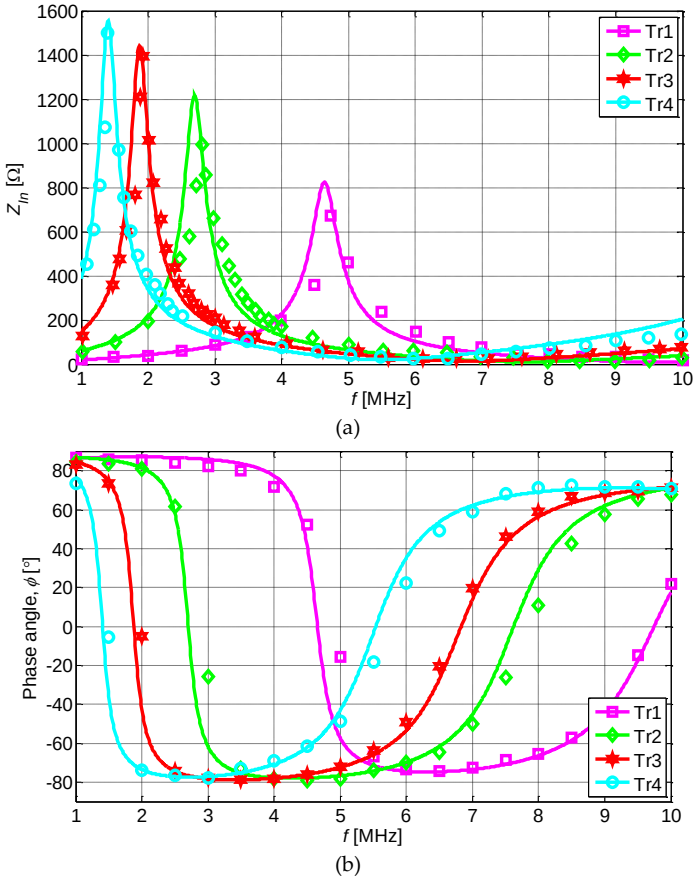

Figure 24. Modelled (solid line) and measured (markers) (a) input impedance Z_{in} and (b) phase angle with C_f=1.5nF and R_L=470 Ω

By matching the measured and modelled performance characteristics, the actual parameters of transformers Tr_1 - Tr_4 were obtained and are given in table.3. From this table, it can be observed that the inter-winding capacitance C_{ps} of the transformer is increasing in nature because of the increased area of the plates (A_p) since the distance between the plates (Z) is maintained constant. In addition to this, from table.3, it can be observed that the rate of rise of leakage inductance w.r.t self

inductance is decreasing in nature as the number of turns of the transformer gets increased as discussed earlier.

Table 3. Modelled/Actual electrical parameters of transformers

Parameters	R_p	R_s	L_p	L_s	L_{lkp}	L_{lks}	L_m	C_{ps}	$\%L_{lkp}/L_p$	$\%L_{lks}/L_s$
Tr_1	0.62	0.3	2.86	0.78	0.35	0.09	1.3	57	12.24	11.54
Tr_2	0.84	0.41	8.25	2.2	0.4	0.18	3.97	119	4.85	8.18
Tr_3	1.1	0.55	17.3	4.54	0.46	0.23	8.5	176	2.66	5.07
Tr_4	1.62	0.82	31.9	8.1	0.72	0.35	15.5	260	2.26	4.32

L_p, L_s, L_{lkp}, L_{lks}, L_m – in μH; R_p, R_s – in Ω; C_{ps} – in pF

3.1.1 AC resistance and coupling coefficient of transformers Tr_1-Tr_4

The AC resistances of the designed transformers including both skin and proximity effects were calculated by using equations (22) & (23) for all the transformers and is shown in fig. 25 (a). Similarly, the calculated coupling coefficients from the measured parameters of the transformers according to equation (19) are illustrated in fig. 25 (b). From this figure, it is evident that the coupling coefficient '*K*' is increasing in nature as the area of the transformer increases. The coupling coefficient is highest for the transformer Tr_4; however, the AC resistance from fig. 25 (a) is also greatest for that transformer and, in addition, the inter-winding capacitance is higher according to table 4. Therefore, for the given power transfer application, the first two transformers Tr_1, Tr_2 were considered since they possess low winding resistance and inter-winding capacitance as compared to the other transformers Tr_3 and Tr_4 and the power tests were conducted by following the procedure discussed in chapter 2.

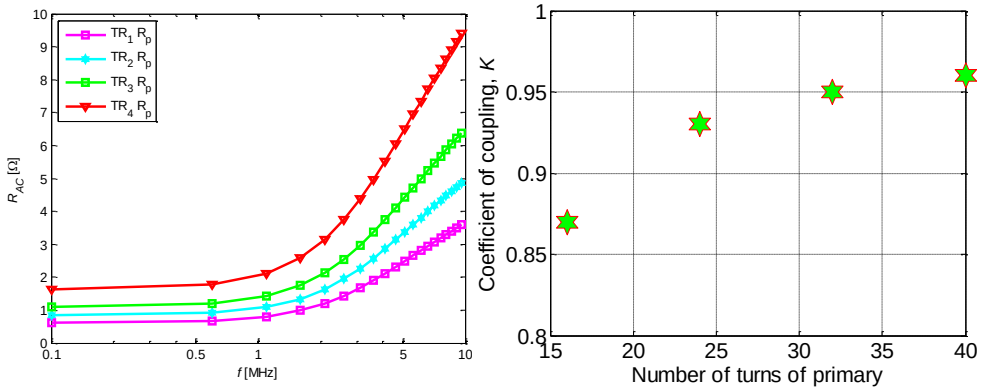

(a) (b)

Figure 25. Calculated (a) primary winding AC resistance and (b) coupling coefficient of transformers Tr_1-Tr_4

3.2 EFFICIENCY OF TRANSFORMERS WITH DIFFERENT LOADS (R_L)

The measured energy efficiency of the transformers Tr_1, Tr_2 with different load resistances and an external resonant capacitor of 1.5nF are depicted in fig. 26 (a) and fig. 26 (b) respectively.

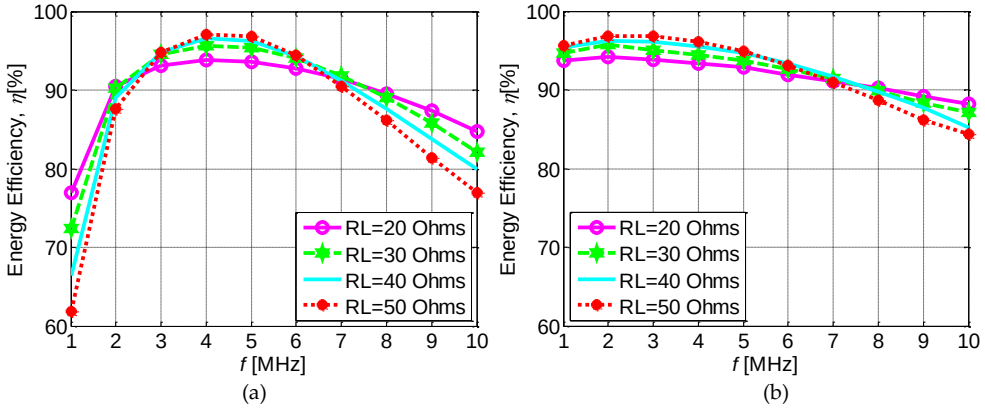

Figure 26.Measured efficiency of (a) Tr_1 & (b) Tr_2 at C_r=1.5nF with different loads

From these figures, it can be observed that the maximum energy efficiency frequencies (MEEF) of Tr_1 and Tr_2 are found to be 4MHz and 2MHz respectively. From these figures, it is also verified that the MEEF is less than the MIF according to expression (40). The MEEF is independent of the load conditions for both the transformers and can be examined from these figures. The maximum energy efficiency of transformers Tr_1/Tr_2 is found to be 97% at their corresponding MEEF with respective load powers of 12W/10W approximately. The efficiency of transformers Tr_1/Tr_2 at their corresponding MEEF is found to be approximately 93.8%/94.5% at an output power of 23W/20W.

3.3 EFFICIENCY OF TRANSFORMERS WITH DIFFERENT CAPACITORS (C_R)

As an external resonant capacitor across the secondary winding plays an important role in these transformers, the energy efficiency was also measured for both the transformers with two different resonant capacitors at a load resistance of 30Ω and is depicted in figs. 27 (a) and (b). From fig.27, it can be observed that MEEF moves towards higher frequencies as the resonant capacitor value is decreased, because the corresponding 'f_r' and MIF gets increased.

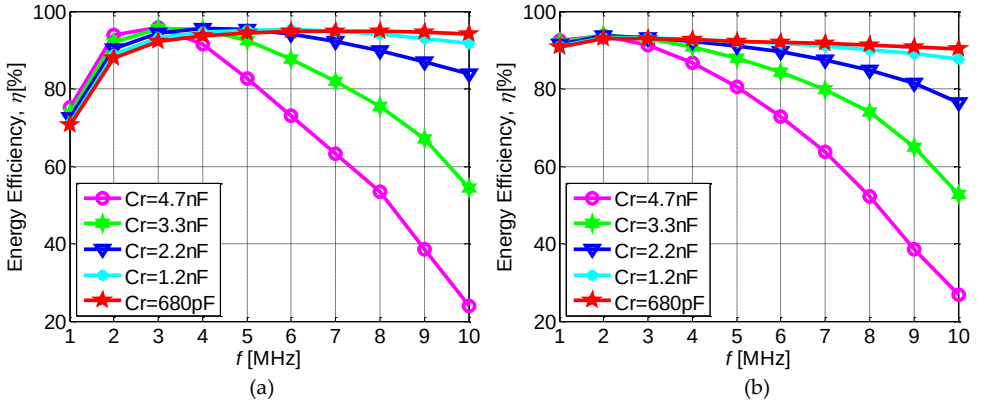

Figure 27. Measured efficiency of (a) Tr_1 & (b) Tr_2 at R_L=30Ω with different capacitors

In addition to this, it can be observed from fig.27, that with a lower value of 'C_r', the energy efficiency of the transformers remains constant for a wide range of frequencies. Thus with the proper selection of resonant capacitor across the secondary winding of the transformer, the energy efficiency of the transformer can be maintained at a high level in the desired operating frequency range.

3.4 EFFICIENCY WITH SINUSOIDAL AND SQUARE WAVE EXCITATION

For the majority of the SMPS applications utilizing single and double ended converter topologies such as flyback, forward, half bridge, and full-bridge etc., the power fed to the high frequency transformer is not sinusoidal in nature. Therefore, it is required to determine the energy efficiency of the transformers when the power processing is not sinusoidal in nature. Hence, power tests were also carried out for square wave excitations in addition to sinusoidal excitations. The comparative results of the power tests for both the transformers Tr_1 and Tr_2 under these conditions are shown in fig. 28. Here, the load resistance considered is of 30Ω with a resonant capacitor of 1.5nF. At their corresponding MEEF, the energy efficiencies of transformers Tr_1/Tr_2 are 96.0%/96.3% for sinusoidal excitations. Only a slight variation exists in terms of energy efficiency for the square and sinusoidal excitations in the case of both the transformers because of the current harmonics. The power densities of both these transformers Tr_1 and Tr_2 at the tested maximum power level of 25W are 53.8W/cm^3 and 23.9W/cm^3 respectively with the energy efficiencies greater than 95%.

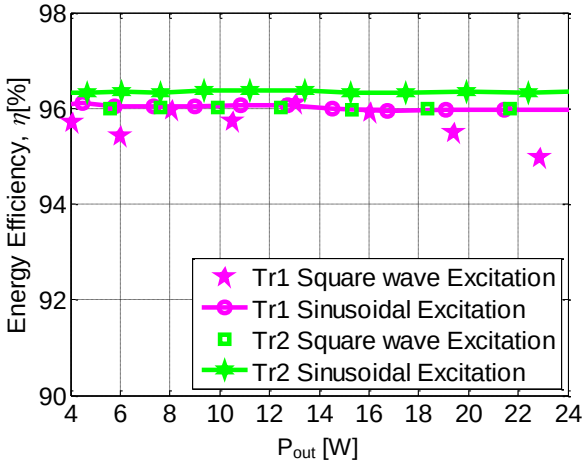

Figure 28. Energy efficiency of transformers with sine and square wave excitations

This provides the scope of utilizing these step-down transformers for low profile DC/DC converter applications, where stringent height requirements are mandatory, together with the assistance of high speed switching devices.

3.5 APPLICATION POTENTIALS OF DESIGNED TRANSFORMERS

The designed three layered 2:1 coreless PCB step-down power transformers were compared to the existing core based ones [54] for various power levels such as 8, 15 and 30 W which can be utilized for telecom and PoE applications. The core based transformers in terms of their dimensions, electrical characteristics such as input/output voltage; load current and power were tabulated and are listed in table.4. When compared to existing core based transformers, the %volume reduction of the designed coreless PCB transformers was also estimated approximately and listed in the last two columns of table.4. It can be observed that the percentage volume of the coreless PCB transformers is drastically reduced as compared to the core based transformers. With these coreless PCB transformers, the height of the transformer can be reduced from a maximum of 12mm to 1.48 mm, which leads to a huge reduction in the volume of the transformer as shown in fig.29 and hence, the low profile DC-DC converters can be realized.

Table 4. Coreless and core based power transformers

V_i[V]	V_o[V]	I_o[A]	Power[W]	Dimension[mm]	Part Number	Tr_1, Tr_2
18-36	15	0.53	8	15.24x12.7x11	FCT1-150L2SLB	72, 37
36-75	15	1.00	15	17.7x13.4x12	FCT1-150M2SLB	79, 53
36-75	24	1.25	30	30x20.5x11.4	POE300F-24LB	91, 81

Part Number corresponds to parts in coilcraft.com, all dimensions are in mm

Therefore, the core based step-down transformers can be replaced by the designed coreless PCB step-down transformers in order to realize the compact SMPS.

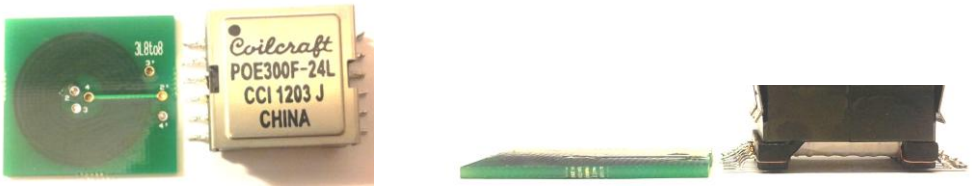

(a) (b)

Figure 29. (a) Top and (b) side view of coreless PCB transformer Tr_1 and core based transformer

4 RADIATED EMISSIONS OF CORELESS PCB STEP-DOWN POWER TRANSFORMERS

In the previous two chapters, the modelling, performance characteristics, power tests and energy efficiency of the designed coreless PCB step-down power transformers have been discussed. These high power density coreless PCB step-down transformers have proven to be highly energy efficient in the MHz frequency region for power transfer applications. However, one of the other major misconceptions of coreless transformers is that they possess a high radiated EMI, because of the absence of the core as discussed earlier. Even though the transformers do possess high energy efficiency, if it fails the electromagnetic compatibility (EMC) tests, it is of no use. Therefore, it is necessary to determine the amount of radiated emissions from these transformers when used for power transfer applications in SMPS in order to minimize the malfunctioning of the other devices in the circuit.

4.1 NEED FOR DETERMINATION OF EMI EMISSIONS OF CORELESS PCB STEP-DOWN TRANSFORMERS

Prior to the commercialization of the product, it is necessary to satisfy the requirements set by the American Federal Communication Commission (FCC), or European International Special Committee on Radio Interference (CISPR) standards, due to which it must be sent for an EMC test. If the product fails the test, it would result in a product delay and increased costs of production until the problem has been dealt with by the researchers/engineers. Hence, the prior estimation of the amount of EMI generated from the converters and its components has many advantages such as providing the solution to improvements in the design criteria, sources of EMI, remedies, recommended topologies, reduction in the cost of production of transformers and thereby the converters etc., Fig. 30 illustrates the required cost for correcting the EMI problems [55] at different stages of product development. From this figure, it can be observed that it would be more expensive if the EMC tests are carried out at the product launch stage. Therefore, in this context, the discussion will focus on the radiated emissions from the designed coreless PCB transformers in terms of different converters point of view. In earlier research work [24], the radiated emissions of coreless PCB transformers for signal transfer applications were proven to be negligible when considering the fundamental component of current through the transformer by both antenna theory and near field measurements. However, for power transfer applications in various single ended and double ended converter topologies, since the waveforms are not sinusoidal in nature, it is also required to consider the harmonic currents along with the fundamental component of the current waveform and its nature. For example in a flyback converter topology, as the currents are sawtooth in nature, it consists of both even and odd harmonic

components. Whereas, in the case of half bridge and full bridge converter topologies, the current is of a square wave in nature and consists of only odd harmonic components. Therefore, in this chapter, the simulated and measured EMI emissions of two layered and three layered coreless PCB step-down transformers for power transfer applications, with regards to different excitations, have been assessed and the relative comparison has been presented.

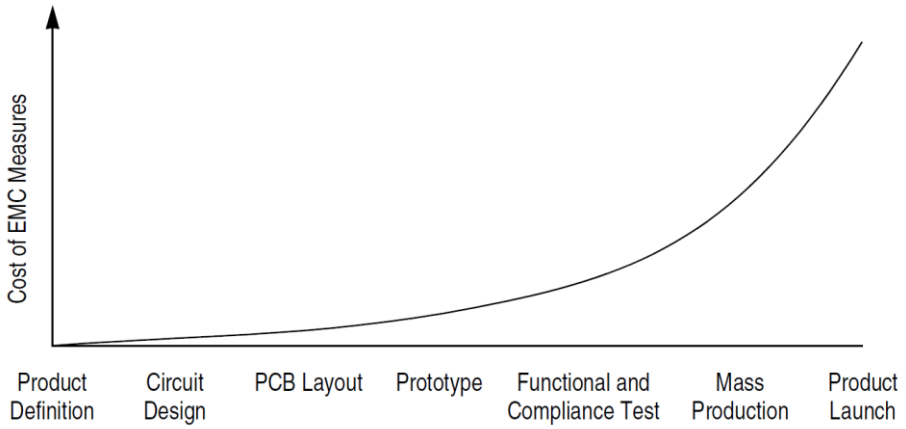

Figure 30. Cost for correcting EMI in different stages of product development [55]

4.2 FAR FIELD RADIATION- ANTENNA THEORY

The designed coreless PCB step-down transformers discussed in chapters 2 and 3 are circular spiral in shape in order to reduce the inter-winding capacitance 'C_{ps}' of the transformer. Here, each turn of the transformer can be considered as a loop antenna [56], [57]. From antenna theory [22], [24] when current flows through the loop in the X-Y plane at an angular frequency of 'ω', the energy is radiated into the air. This energy is perpendicular to the X-Y plane and possesses the intrinsic impedance of 377Ω in free space. At each frequency of operation, the associated wavelength of the radiated signal can be calculated as follows

$$\lambda = \frac{c}{f\sqrt{\varepsilon_r}} \tag{45}$$

where, 'λ' is the wavelength, 'c' is the speed of light, 'f' is the frequency of signal, 'ε_r' is the relative permittivity. In air core transformers, 'ε_r' is considered as unity. The signal and its corresponding components will be electrically large if the wavelength of the signal becomes reduced as the harmonic frequency increases. Any loop can be considered as a good radiator if the outermost radius of the loop is either equal to or half of the wavelength of the signal. For example, if the operating frequency of the transformer is considered as being 2MHz, the corresponding wavelength (λ) of the signal calculated by using equation (45) is 149.5m. However, the designed two layered coreless PCB transformer possess the outermost radius of 18.5mm, which is about 1.2×10^{-4} times the wavelength of the

signal and it is far beyond 0.5λ. For a loop antenna, the amount of time averaged radiated power 'P' is given [22] as

$$P = 160\pi^6 I_o^2 \left(\frac{rf}{c}\right)^4 \quad (46)$$

where,

I_o RMS current flowing through the loop

r Radius of the loop

From this equation, it can be observed that the radiated energy not only depends on the current and its nature as discussed earlier, but also on the frequency and radius of the transformer.

4.2.1 Estimation of radiated emissions from two layered and three layered transformers

Based on the above discussed parameters, such as the current harmonics, the nature of the current, radius and the structure of the transformer, EMI emissions for three different transformers, T_{r0}, T_{r1}, and T_{r2} were estimated by using antenna theory. The computations were carried out when the designed transformers were excited by means of both sinusoidal and square waves at a fundamental/operating frequency of 2MHz and a load power of 20W. These tests were conducted at their MEEF, which was maintained at 2MHz with the assistance of external resonant capacitor across the secondary winding of transformer. The following computations were made in order to estimate the EMI emissions from the designed step-down transformers.

1) Taking the primary/secondary currents from the measured waveforms of the transformers excited with RF power amplifier.
2) Considering the primary/secondary currents obtained from the simulations of the high frequency model of the designed step-down transformers.
3) By considering the ideal sinusoidal/square waves of primary/secondary current waveforms generated from MATLAB.

The measured waveforms of the primary/secondary voltages and currents of transformer T_{r2} (three layered 12:12:12 transformer) at its operating frequency of 2MHz for both sinusoidal and square wave excitations are depicted in figs. 31 (a) and (b) respectively.

4.2.2 Radiated power calculations for sinusoidal and square wave excitations

In order to calculate the radiated power of the transformer, the harmonics of the measured/simulated and idealized current waveforms were determined by using Fast Fourier Transform (FFT).

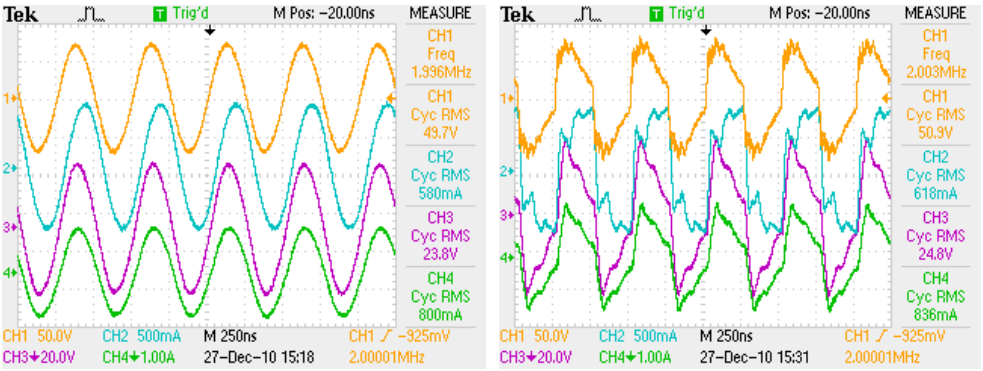

(a) (b)

Figure 31. Measured waveforms of Tr2 with R_L=30 Ω for (a) sinusoidal and (b) square wave excitations

By considering these harmonic components along with the fundamental current component in the equation (46), the radiated power of the transformers is computed. The corresponding calculated radiated power for the transformer Tr2 with the sinusoidal and square wave excitations is depicted in figs. 32 (a) and (b) respectively.

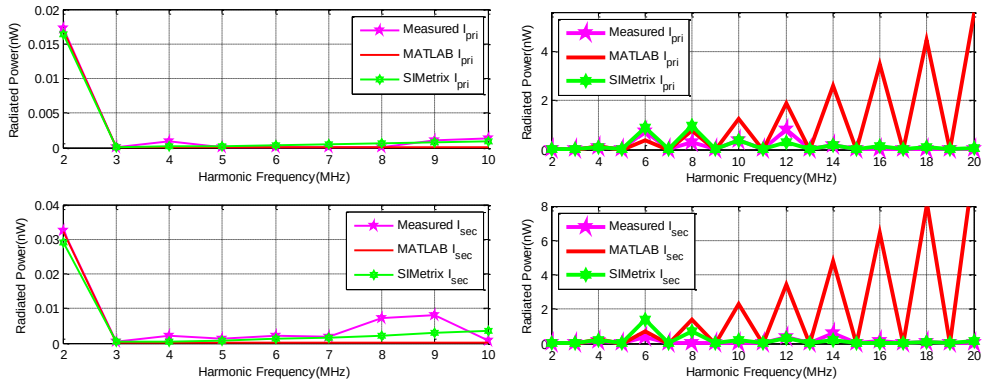

(a) (b)

Figure 32. Radiated power of Tr2 for (a) sinusoidal and (b) square wave excitations with resonant capacitor

In [22], the radiated powers of the transformer were carried out by considering the worst case condition i.e., by considering the outermost loop of the transformer. However, in this case the radiated power of the designed transformers is computed by considering all the loops of the transformer.

From fig. 32 (a), it can be observed that the radiated power obtained for the simulated, measured and MATLAB generated sinusoidal current wave forms are almost zero except at the fundamental frequency. In all the three cases, the radiated

power determined for the secondary current waveform which carries an RMS value of 0.8A at the fundamental frequency is found to be approximately 0.03 nW. From fig. 32 (b), the radiated power obtained is increasing in nature for the square wave excitation because of the presence of odd harmonic components. In this case, the measured and simulated radiated powers are considered to be in good agreement with each other compared to the MATLAB generated one because of the wave distortion. Comparing the radiated powers obtained when using the square and sinusoidal excitations reveals that, the radiated power obtained for the transformers with square wave excitation is higher compared to that of the sinusoidal waveforms.

By removing the resonant capacitor across the secondary winding, the radiated power of the transformer T_{r2} was computed for the square wave excitation. The corresponding radiated power of T_{r2} is depicted in fig.33. From this figure and fig. 32(b), it can be observed that the radiated power gets increased in case of transformer without any resonant capacitor across the secondary winding. From this, it can also be concluded that the radiated emissions can also be reduced with the aid of resonant capacitor across the secondary winding since the leakage inductance and the interwinding capacitance of the transformer along with the resonant capacitor forms a filter circuit which in turn smoothens the current waveform.

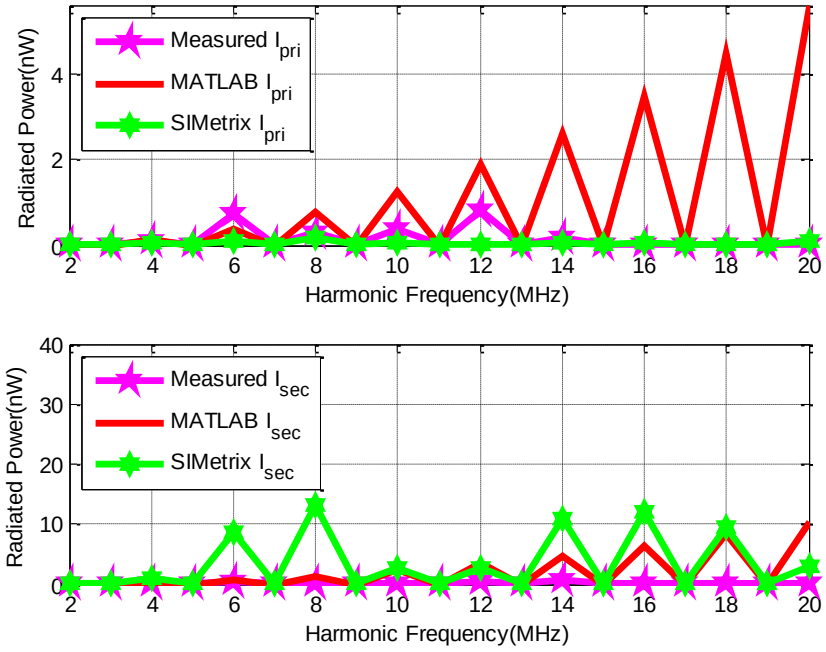

Figure 33. Radiated power of T_{r2} for square wave excitation without any resonant capacitor

Because, for class B equipment, according to FCC and CISPR regulations, the radiated limits are applicable from 30MHz – 300MHz, the radiated power for all these transformers for both sinusoidal and square wave excitations are depicted in figs. 34.

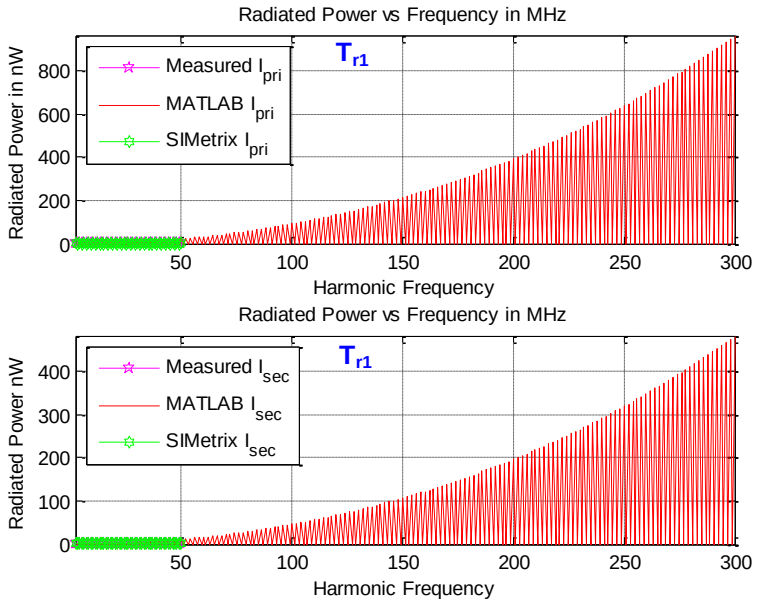

(a)

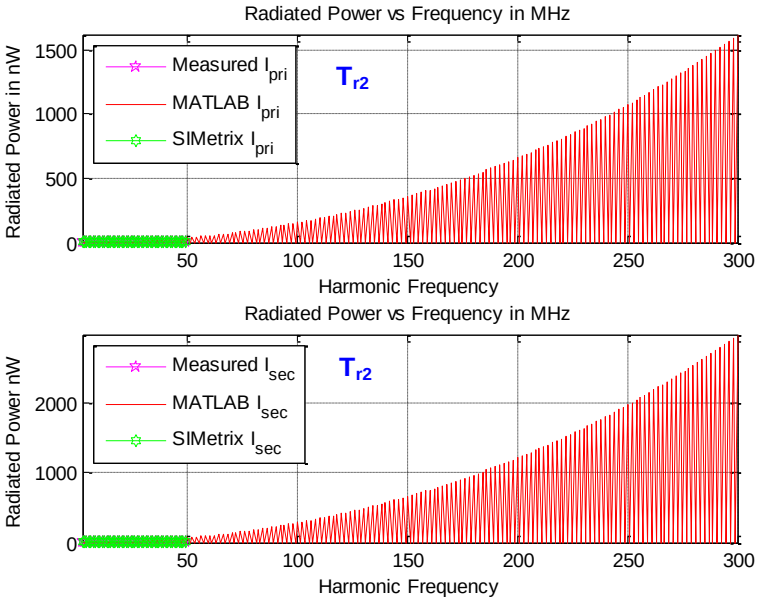

(b)

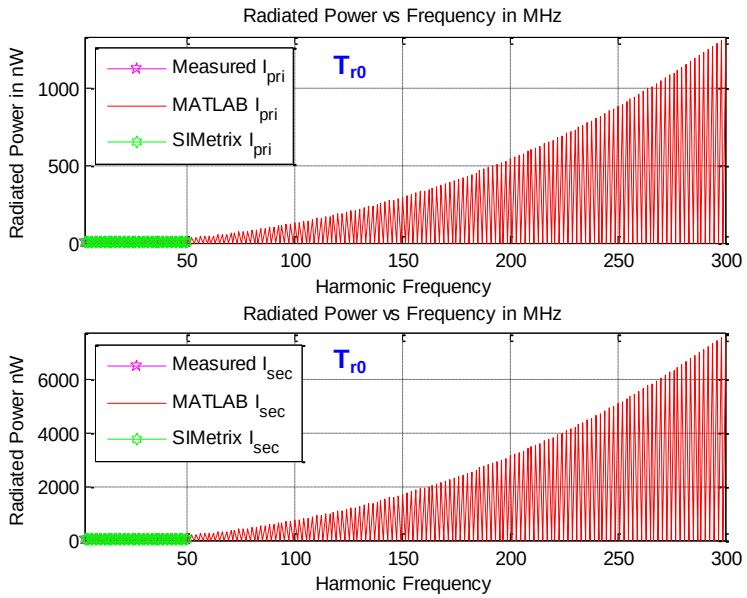

(c)

Figure 34. Radiated power of (a) Tr_1, (b) Tr_2 & (c) Tr_0 for sinusoidal & square wave excitation

From figs. 34 (a) and (b), it can be observed that the radiated power due to the harmonic components of the secondary currents from transformer Tr_1 was approximately reduced by a factor of 6 throughout the spectra compared to that of the transformer Tr_2 due to the reduced transformer outermost radius. In this case, the measured waveforms were limited to 50MHz only because of the limitation of the probe and oscilloscope bandwidths.

Similarly, from figs. 34 (b) and (c), the radiated power obtained in the case of the three layered transformer Tr_2 is lowered approximately by a factor of 2.6 as compared to that of the two layered transformer, Tr_0 due to the reduction of the outermost radius as discussed earlier.

In chapter 2, it was already proved that the energy efficiency of the transformer Tr_2 is greater than Tr_0 and also in terms of EMI point of view, the three layered transformer is better compared to the two layered transformer. Based on these two observations, it can be concluded that, for a given power transfer application; the three layered transformer is better compared to the two layered one.

4.3 MEASUREMENT OF NEAR MAGNETIC FIELDS OF TWO LAYERED AND THREE LAYERED TRANSFORMERS

Apart from the theoretical estimation of the radiated power of the designed coreless PCB step-down transformers using far field antenna theory, the measurements of the near magnetic field were carried out for comparison with the assistance of HZ552 H-field probe and HMS3000 spectrum analyzer from HAMEG instruments. The antenna was situated horizontally to the device under test (DUT) at a distance of 10cm [58] in order to obtain the relative measurements. The measurements were carried out when the load power of all the transformers is considered to be 20W. The fundamental frequency of operation of these transformers is considered as 2MHz, which was set by varying the resonant capacitors across the secondary winding of the transformers. The measurements are expressed in terms of dBμV corresponding to the voltage levels acquired by the antenna.

Initially the measurements were carried out for two layered transformer T_{r0} for both the sinusoidal and square wave excitations when the transformer delivers the load power of 20W. The near field emissions were observed in the range of 30 – 300MHz and the corresponding results are shown in fig. 35(a). From this figure, it can be observed that the emissions for coreless PCB transformer with sinusoidal excitation is negligible compared to irregular square wave excitation.

The measurements were also carried out for the two layered and three layered transformers and the relative comparison of the measurement results in the frequency range of 30 – 100MHz are depicted in fig.35 (b). From this figure, it can be observed that the emissions from two layered transformer are relatively higher compared to the three layered transformers. At a particular frequency of 30MHz, the emissions from T_{r0}, T_{r1} and T_{r2} are 59.82, 43.96 and 55.94 dBμV respectively as shown in fig. 35 (b). Here, it should be noted that the transformers are excited by an irregular square waveform.

In order to suppress the EMI emissions of the two layered transformer, two EMI absorbers FM1 from Kolektor Magma and IFL10M from TDK Lambda were placed on both sides of the transformer and the measurements were carried out. The FM1 material from Kolektor Magma and IFL10M material from TDK lambda possesses the surface resistivity of $4x10^5$ Ω-m and 1MΩ-m respectively. The corresponding thicknesses of these sheets are 1mm and 0.02mm. The relative measurements of the transformer with and without EMI absorbers are shown in fig. 35(c). From this figure, it can be observed that with the application of the EMI absorbers on both sides of the transformer, the EMI emission gets reduced. At a particular frequency of 30MHz, the emissions without any EMI absorber, with FM1 and IFL10M are

59.82, 51.82 and 48.11 dBµV respectively. For the entire frequency range, it can be observed that the emissions by using IFL10M are relatively low compared to other two cases. Therefore, in conclusion, if the emissions from the converters using the coreless PCB step-down transformers do not meet the FCC and CISPR standard limits, with the assistance of the very thin absorption sheets, the emissions can be reduced without sacrificing the power density of the converter.

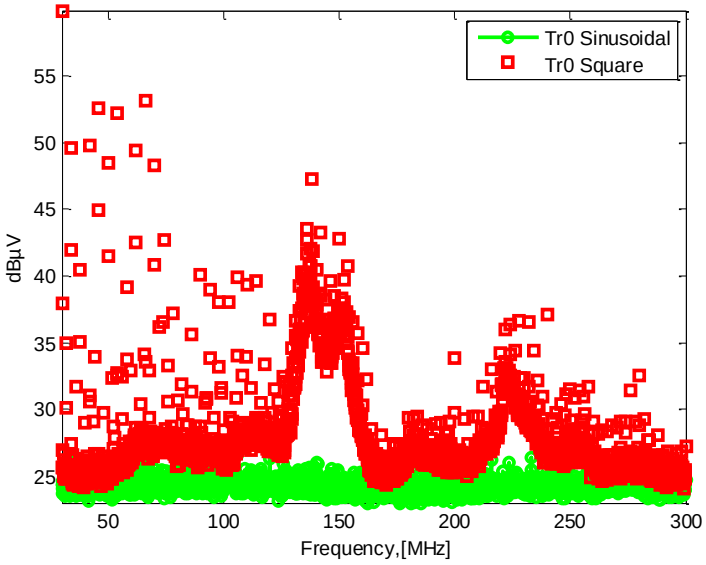

(a)

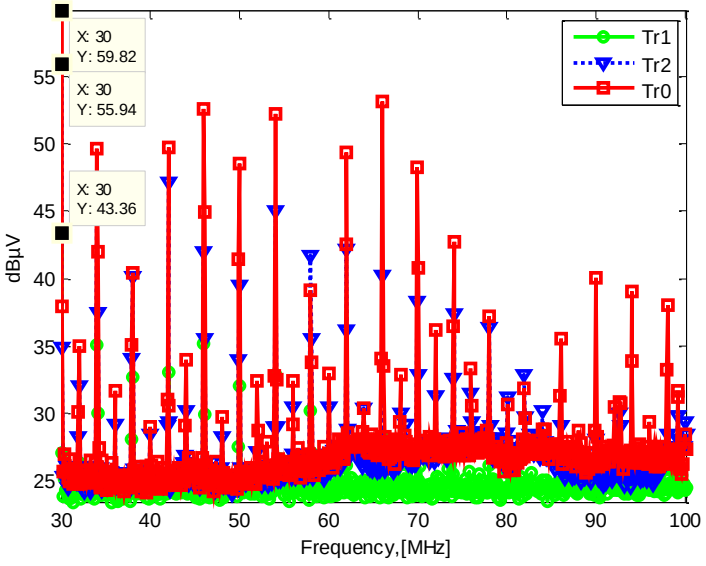

(b)

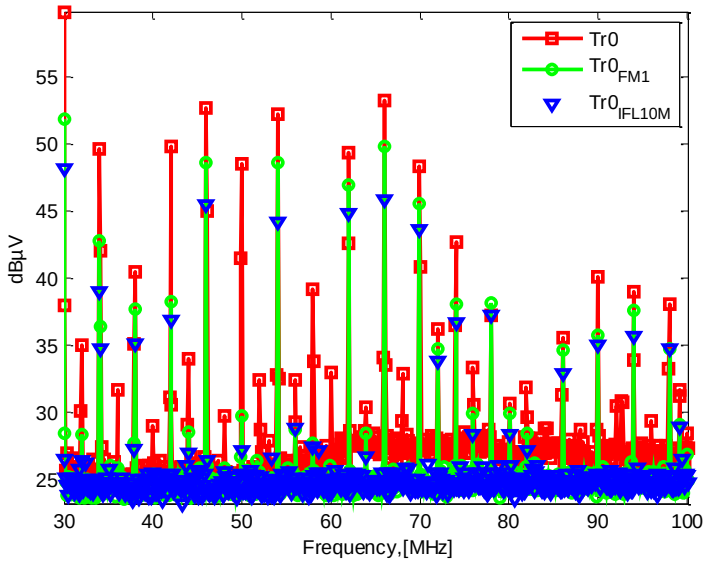

(c)

Figure 35. Measurement of near magnetic field of (a) T_{r0} for sinusoidal excitation, (b) T_{r1}, T_{r2} & T_{r0} for irregular square wave and (c) T_{r0} with and without shielding

5 MULTILAYERED CORELESS PCB SIGNAL TRANSFORMER

From the previous chapter, it can be concluded that, if the power in the converter circuit is processed in a sinusoidal manner, the radiated EMI from the power transformer gets reduced. In this regard, while employing the coreless PCB step-down transformers for power transfer applications, the resonant converter topologies such as series resonant converter (SRC), a parallel resonant converter (PRC), a series parallel resonant converter (SPRC) or LLC resonant converter topologies are beneficial when compared to single ended and double ended converter topologies such as flyback, forward, half bridge etc.,

For AC/DC and some of the DC/DC converter applications, in order to switch the high side MOSFET, a gate driver, operating at a few MHz, with galvanic isolation and at higher input voltages is required. However, the commercially available high side gate drivers for Si MOSFETs are limited to just 1MHz with an input voltage less than 125V [59]. In order to provide galvanic isolation, either the pulse transformer or optocoupler are generally utilized. However, at higher operating frequencies such as in few MHz, the influence of core losses introduced by the core material becomes dominant in pulse transformers or core based transformers.

Since, coreless PCB transformers possess good high frequency characteristics apart from its several advantages as discussed earlier, there has been a significant research over the past few years [60] - [64] for signal transfer applications. In addition to this, printing the windings on the FR-4 material provides a much higher isolation of 15 - 40kV when compared to the isolation offered by the optocoupler which is of only 1.5 - 7.5kV [65]. However, the demonstrated earlier research work on the two layered bifilar coreless PCB gate drive transformers does not provide the optimal solution in comparison to a pulse transformer in terms of gate drive power consumption [66]. Under the load conditions of 10nF capacitor parallel to 100Ω resistor, it was stated that the total current drawn by the drive circuitry for driving the inverter bridge [66] using coreless PCB transformer at 1.1MHz was found to be 0.28A (1.68W per gate drive) whereas with the core based transformer it was only 0.133A (0.8W per gate drive). This increase in the current for the coreless PCB transformer is due to the increased winding resistance for the given amount of inductance in a two layered transformer. From the chapter 2, it was concluded that the multilayered coreless PCB transformer offers low resistance compared to two layered transformer for obtaining the given amount of inductance. Therefore, in order to reduce the winding resistance and hence the gate drive power consumption, it is required to design a multilayered coreless PCB gate drive transformer suitable for low power converter applications. In addition to this, the transformer with less surface area has low radiated EMI as per the observations in the previous chapter, due to which the chances of mistriggering the

switching device can be minimized. In order to achieve these characteristics of low gate drive power consumption and low radiated EMI, multilayered coreless PCB transformers were designed and evaluated.
Therefore, in this chapter, the design guidelines, structure, geometrical, electrical parameters and performance characteristics of multilayered coreless PCB gate drive transformers are discussed.

5.1 ESTIMATION OF INDUCTANCE FOR GATE DRIVE TRANSFORMER

In this section, the procedure to estimate the amount of inductance required to design the coreless PCB gate drive transformer is presented. For the given application, the desired inductance of the transformer is determined by various factors such as input capacitance 'C_{iss}' of the MOSFET which determines the peak current 'I_{peak}' required by the MOSFET gate driver, peak input voltage 'V_{peak}' and the operating frequency of the transformer 'f_{sw}'. Here, the input capacitance of the MOSFET acts as a resonant capacitor and it determines the operating frequency of the transformer i.e., MIF. It is recommended to operate the gate drive transformer at MIF in order to reduce the gate drive power consumption of the circuit as discussed earlier. Usually, for the low power applications, the MOSFET load capacitances vary in the range of 100 – 1000 pF. If the desired operating frequency region of the gate drive circuit is in the range of 2 – 4 MHz, from the initial estimations using the above design parameters, ideally, it is required to have the transformer self inductance in the range of 1.5 – 3 μH.

5.2 DESIGN OF MULTILAYERED CORELESS PCB GATE DRIVE TRANSFORMER

After knowing the required amount of inductance, two different multilayered coreless PCB transformers (Tr_A and Tr_B) with the following geometrical parameters were designed by using the analytical method described in chapter 2 and then evaluated. The geometrical parameters of the designed gate drive transformers are given in table 5.

Table 5. Geometrical parameters of the gate drive transformers, Tr_A and Tr_B

	N	W[mm]	S[mm]	R_{in}/R_{out}[mm]
Tr_A	16	0.22	0.18	1.3/4.3
Tr_B	20	0.19	0.17	1.0/4.4

The designed transformer is circular spiral in shape so as to reduce the inter-winding capacitance, which results in high bandwidth when compared to other shapes [62]. The transformers are designed on a four layered PCB laminate where the primary winding is distributed on two layers and the remaining two layers are occupied by the secondary winding. These transformers were also covered by using high frequency ferrite plates, which is similar to a large air gapped core, in

order to reduce the gate drive power consumption and to increase the self inductance. The prototype of the designed gate drive transformers with and without high frequency flat ferrite plates are illustrated in fig. 36 (a) and (b) respectively. The flat ferrite plates are of high frequency Ni-Zn, 1F core material whose initial permeability is 80.

The ferrite plates possess a radius of 10mm and a thickness of approximately 1.5mm.

(a) (b)

Figure. 36. Prototype of gate drive transformer T_{rA} with and without ferrite plates

The measured primary DC resistance of the transformers T_{rA}/T_{rB} are 0.43/0.94Ω respectively. The remaining electrical parameters for the transformers, with and without the ferrite plates at 1MHz, using an RLC meter are given in table 6.

Table 6. Electrical parameters of the gate drive transformers, T_{rA} and T_{rB}

	L_P[µH]	L_{lkp}[µH]	L_s[µH]	L_{lks}[µH]	C_{ps}[pF]	K
T_{rA}	0.91	0.34	1.16	0.44	11	0.624
T_{rA} (Ferrite)	1.95	0.45	1.85	0.44	11	0.766
T_{rB}	1.56	0.56	1.89	0.71	11	0.626
T_{rB} (Ferrite)	3.39	0.72	3.4	0.72	11	0.788

From table 6, it can be observed that the self and mutual inductance of the transformers using the ferrite plates increase while the leakage inductance of the transformers remains more or less the same. Since this gate drive transformers are designed with the aim of driving the power MOSFETs, the load is considered as the parallel combination of both the resistor and the capacitor. The input capacitance of the MOSFET determines the bandwidth of the coreless PCB gate drive transformers since they act as the resonant capacitors across the secondary winding of drive transformer.

5.3 PERFORMANCE CHARACTERISTICS OF GATE DRIVE TRANSFORMERS

The performance characteristics of the designed gate drive transformers such as the voltage gain/transfer function, input impedance and phase angle discussed in chapter 2 have been presented for the designed coreless PCB gate drive transformer in this section. These characteristics were obtained by considering the load resistor of 100Ω and the capacitor of 680pF. For the measured parameters of the transformers, a 680pF capacitor is considered across the secondary winding so that the operating frequency region of the gate drive transformers falls within the range of 1 - 4MHz. The calculated voltage gain/transfer function and input impedance of the transformers obtained from the measured parameters under

these conditions is illustrated in fig. 37 (a) and (b) respectively. The maximum voltage gain of the transformers T_{rA} and T_{rB} were found to be approximately 1.1 and 1 respectively at their corresponding maximum gain frequencies of 6 and 4.5MHz. The maximum gain frequencies of the transformers, with and without ferrites, were unchanged because there was no significant difference in the leakage inductance of the transformers. The maximum impedance frequency (MIF) of the transformers is found to be less than that of the maximum gain frequency as discussed in chapter 2. The phase angles of these transformers under the same load conditions are shown in fig. 38 (a).

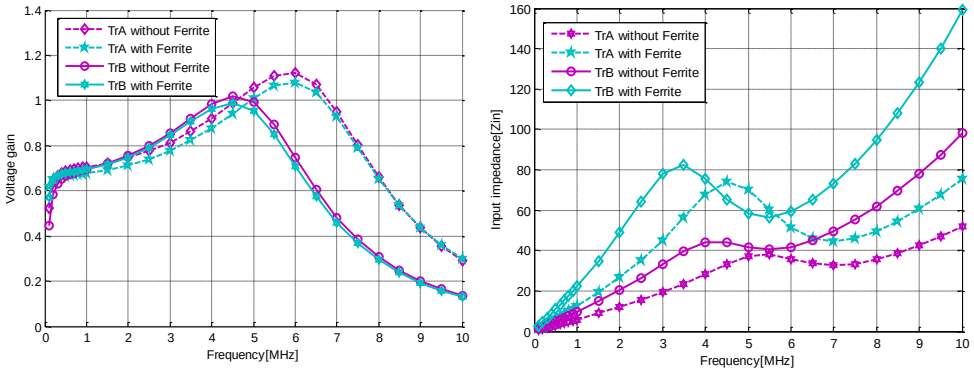

(a) (b)

Figure 37. (a) Voltage gain and (b) input impedance of gate drive transformers T_{rA} and T_{rB}

From fig.38 (a), it can be observed that, before MIF, the phase angle of the transformers is found to be sufficiently high to ensure that the transformers are inductive in nature. By operating the transformers at MIF, the gate drive power consumption of the circuit can be minimized as discussed earlier which is considered as a desirable characteristic in case of SMPS. The calculated energy efficiency of these gate drive transformers under the same load conditions for a sinusoidal signal is depicted in fig. 38(b).

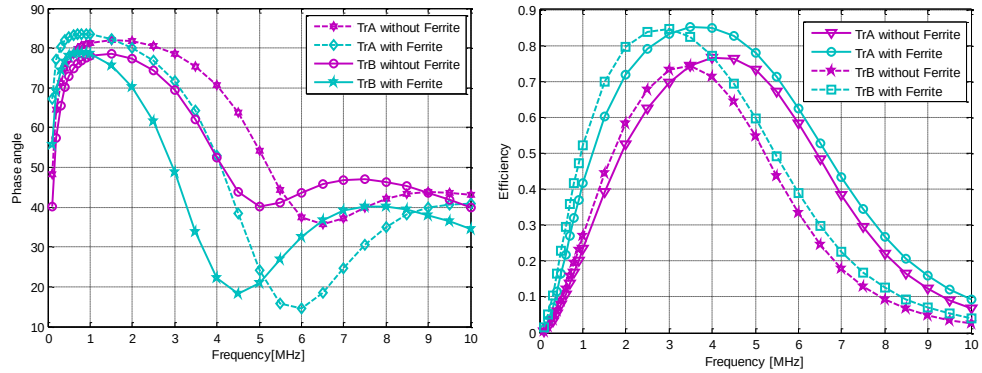

(a) (b)

Figure 38. (a) Phase angle and (b) energy efficiency of gate drive transformers T_{rA} and T_{rB}

The efficiency with regards to these transformers is within the range of 60 - 85% in the desired operating frequency region. From fig. 37(b) and 38 (b), it can be observed that the input impedance and energy efficiency of the transformers were improved by means of the ferrite material, resulting in reduced gate drive power consumption. From fig 38(b), it can be observed that the energy efficiency in the case of T_{rB} is less than that for T_{rA} due to the increased resistance of the windings. Hence, transformer T_{rA} is considered for further analysis.

5.3.1 Estimation of maximum impedance frequency, MIF

It is necessary to determine the maximum impedance frequency (MIF) of the transformers for different load conditions since, the MOSFETs utilized for different applications do in fact vary and, additionally, these capacitances are considered as non-linear in nature. Therefore, MIF of the gate drive transformer T_{rA} was estimated for several combinations of load resistors and capacitors and is illustrated in fig. 39 (a). In this case, the load resistors are varied from 100 - 1000Ω and the capacitors from 100 - 1500pF. In addition to this, the maximum energy efficiency of transformer T_{rA}, for the same load conditions is estimated and plotted in fig. 39 (b).

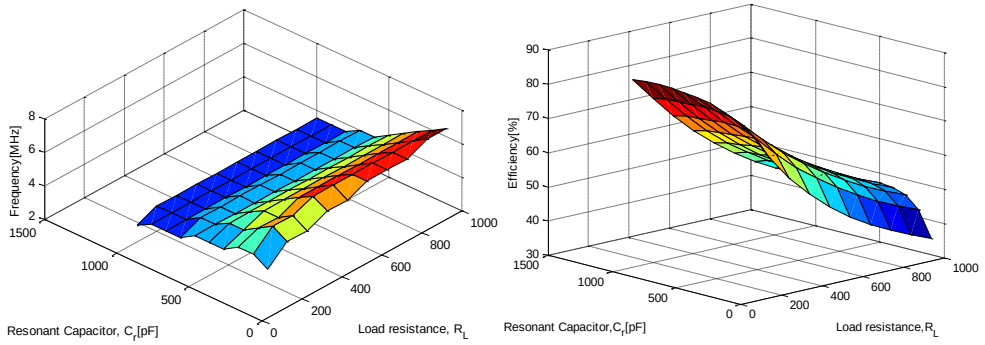

(a) (b)

Figure 39. (a) MIF & (b) maximum energy efficiency of transformer T_{rA} for different R_L and C_r

5.4 SIMULATED AND MEASURED GATE DRIVE SIGNALS USING MULTILAYERED CORELESS PCB TRANSFORMER, T_{RA}

After designing and characterizing the transformer, it has been simulated and evaluated in high frequency double ended converter topologies such as, a half bridge converter [67] and a series resonant converter (SRC) [68] in order to drive the high side MOSFET. Here, the low side MOSFET was directly driven from one of the outputs of the MOSFET gate driver LM5111 whereas the high side MOSFET was driven by using the passive gate drive circuitry with the assistance of the designed multilayered coreless PCB transformer 'T_{rA}' and a level shifting circuit as

discussed in [68]. The simulated and measured gate drive signals corresponding to the low side and the high side MOSFETs are illustrated in fig. 40 (a) and (b) respectively. In this case, the typical input capacitance of the MOSFET used in SRC i.e. ZXMN15A27K is 169pF which acts as a load to the gate drive circuitry. In fig. 40 (a) and fig. 40 (b), the yellow signal (CH1) represents the low side MOSFET gate signal whereas the pink signal (CH1) represents the high side gate drive signal. The rise/fall times of the low side and high side signals are 12.0/12.75ns and 17.53/19.92ns respectively. Under these conditions the simulated/measured gate drive power consumption of the high side gate drive circuitry using the designed multilayered coreless PCB transformer was found to be 0.35/0.37W.

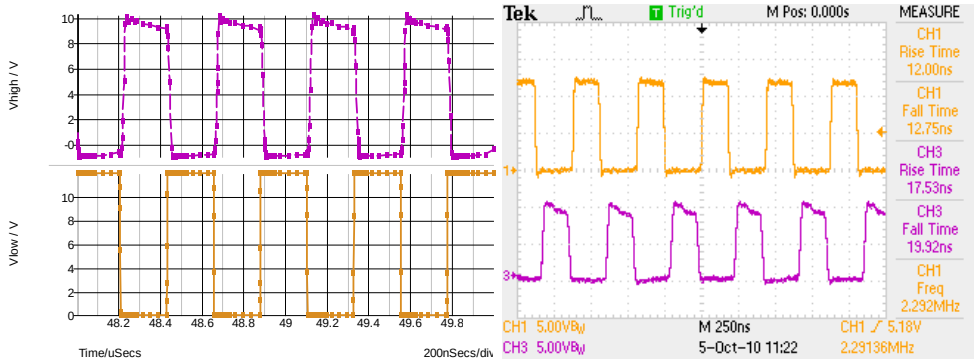

(a) (b)

Figure 40. (a) Simulated and (b) measured gate drive signals at 2.3MHz using T_{rA} with ferrite plates

6 DESIGN GUIDELINES AND PERFORMANCE OF CORELESS PCB CENTER TAPPED STEP-DOWN POWER TRANSFORMER

In the earlier chapter, the design guidelines of the multilayered coreless PCB signal transformer for driving the high side MOSFET in double ended converter topologies have been covered. For the given power transfer application and operating frequency region, the size of the transformer in double ended converter topologies gets reduced as compared to the transformer in single ended ones [69], [70] due to the full utilization of the transformer. Even though the half bridge and full bridge converter topologies are recommended for high power applications in the literature [71] - [73], due to the aforementioned reason, these converters have recently gained popularity for low-medium power applications [70], [74]. Since the entire losses in these coreless PCB transformers are contributed by the copper losses, unlike the core based transformers, it becomes an additional benefit to use these transformers in the double ended converter topologies due to the reduction of the copper utilization. Hence, this chapter deals with the design guidelines of the multilayered coreless PCB center tapped power transformer, its characteristics and the results obtained by employing it in a series resonant converter (SRC) topology.

6.1 DESIGN GUIDELINES OF CORELESS PCB STEP-DOWN TRANSFORMER

Since, there exists no straightaway design rule in case of coreless PCB step-down power transformers, the design process requires some iterative procedure and with few assumptions.

For the given power transfer application, by knowing the input/output voltage specifications, topology and operating frequency range, and the required inductances of the transformer can be obtained by the following procedure. Since, the coreless PCB transformer operation is based on the resonant phenomenon between the leakage inductance and the external resonant capacitor; it is required to estimate the desired resonant capacitor across the secondary winding for operating the transformer in the desired frequency range. The selected resonant capacitor across the secondary winding is configured in such a way that the no-load resonant frequency is greater than MEEF of the transformer (i.e., operating frequency region). Therefore, in order to estimate the capacitor, a leakage inductance of 10% of the self inductance is assumed and simulated in the circuit to achieve the desired power levels on the secondary side with the maximum possible energy efficiency. By following this procedure, for the input/output voltage specification of 120/20V dc, for the load power of 50W and the operating frequency range of 2 - 4MHz, the estimated primary inductance of the center tapped power transformer is in the range of 6 - 8μH by assuming the turn's ratio 'n' of 4:1. After knowing the required amount of inductance, the transformers can be designed by using the analytical equations given in chapter 2. However, several possibilities

exist with regards to achieving the desired amount of inductance in terms of various geometrical parameters such as inner (R_{in})/outermost radius (R_{out}), track height '*H*', width of the winding '*W*', separation between tracks '*S*', different no. of turns '*N*' and PCB layer structures.

6.1.1 Geometrical parameters of transformer

In this section, the design guidelines for selecting the required geometrical parameters for obtaining the desired inductance are discussed.

Inner/outermost radius of transformer: Here, in order to achieve high power density of the transformer, the outermost radius of the transformer is fixed as 10mm. A hollow winding factor, which is defined as the ratio of the inner radius to the outermost radius is recommended for coreless printed spiral winding structures in the case of inductors [75] in order to increase the quality factor. Here, by eliminating few inner turns of the winding, which contributes less to the total amount of inductance, the DC and AC resistances of the winding can be reduced and thus the quality factor '*Q*' of the winding given by equation (47) can be increased.

$$Q = \frac{\omega L}{R} \tag{47}$$

where, $\omega=2\pi f$

L Inductance of inductor

R Resistance of the winding

The optimal hollow factor range of the winding is considered [75] as 0.45 – 0.55. The same design guideline is followed for the coreless PCB step-down transformer in order to reduce the winding resistance. Therefore, a hollow winding factor of 0.45 is considered in the design of the transformer resulting in an inner radius of 4.5mm.

Width of the winding: In order to increase the effect of the hollow winding factor in case of coreless PCB inductor, the width of the winding should be considered as being at least 10 times the skin depth [75], corresponding to the operating frequency. In the desired operating frequency region of 2 – 4MHz, the calculated skin depths of the winding are in the range of 45 – 32μm respectively. Therefore, the width of the primary winding is considered as 0.34mm and also by considering the current carrying capability depending upon the specifications. Here, in the case of the secondary winding, the two tracks were paralleled resulting in the secondary winding width as 0.68mm.

Separation between the tracks: In order to obtain a higher amount of inductance with a low AC resistance and a high quality factor, the separation between the tracks should be as close as possible and should be within the manufacturing

capability. Here, in this case, the separation between the tracks is considered to be half of the width of the winding thus resulting in 0.17mm. Usually the manufacturing limits for track separation ranges from 0.15 – 0.2mm.

No. of turns: Based on knowledge of the inner/outermost radius, width and separation between the windings, the required no. of turns/layer can be determined by the following equation.

$$N = \frac{R_{out} - R_{in} - S}{W + S} \tag{48}$$

6.1.2 Structure of transformer

From the above known geometrical parameters, the required no. of turns for achieving the primary inductance was estimated with the assistance of the analytical equations provided in chapter 2. By considering a four layer PCB, where the two primaries are distributed on two different layers, the total number of turns required to attain the desired inductance is found to be 24. Each layer consists of 12 number of turns with the above mentioned geometrical parameters and thus the two primaries are connected in series. Here, the structure of the four layered PCB is considered as a primary-secondary-secondary-primary (PSSP). The two primaries are distributed on the first and fourth layers whereas the two secondaries are distributed on the second and third layers of the PCB. The cross sectional view of the designed multilayered PCB transformer together with its 3D view is depicted in figs. 41 (a) and (b) respectively.

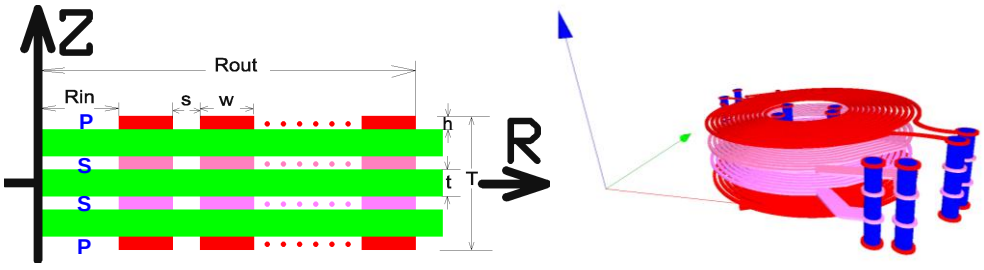

(a) (b)

Figure 41. (a) Cross-sectional view of transformer in RZ plane and (b) 3D view of the transformer

In the case of resonant converter topologies, the leakage inductance plays an important role in determining the switching frequency as well as the zero voltage switching (ZVS) condition of the converter. Based on the various structures possible, such as PSSP, secondary-primary-primary-secondary (SPPS), primary-secondary-primary-secondary (PSPS), the PSPS structure (interleaved) possess a lower leakage inductance when compared to both the PSSP and SPPS [76]

structures. Therefore, this interleaved structure is not considered, in order to avoid the external inductor which is required in resonant converter topologies for achieving zero voltage switching (ZVS) of the converter [77]. From the remaining structures, i.e., PSSP and SPPS, the PSSP structure is considered since it consists of a low resistance and high leakage inductance compared to SPPS.

The measured total primary and half of the secondary winding DC resistances of the transformer are 1.04/0.1Ω respectively and the corresponding calculated AC resistance obtained by using equation (22) is illustrated in fig.42. From this figure, it can be observed that the AC resistance of the winding is increasing rapidly from 1MHz due to both skin and proximity effects as discussed earlier.

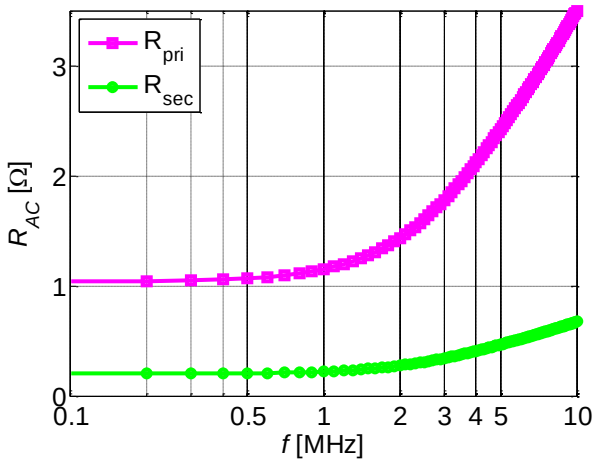

Figure 42. Calculated AC resistance of the primary/secondary winding of transformer

The prototype of the designed transformer together with the signal transformer discussed in chapter 5 and the PCB inductors is illustrated in fig.43.

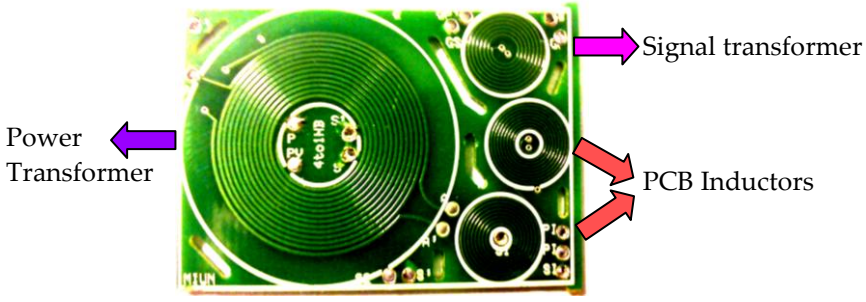

Figure 43. Prototype of signal & power transformer with PCB inductors

6.2 ELECTRICAL PARAMETERS OF DESIGNED POWER TRANSFORMER

The measured electrical parameters of the designed power transformer using a sine phase impedance analyzer are given in table.7

Table 7. Measured electrical parameters of power transformer@1MHz

L_p[μH]	L_{lkp}[μH]	L_s[μH]	L_{lks}[μH]	C_{ps}[pF]	K	R_p[Ω]	R_s[Ω]
7.89	1.95	0.64	0.16	30	0.76	1.4	0.14

The calculated turn's ratio of the transformer using equation (11) from the measured electrical parameters is 3.51.

6.3 PERFORMANCE CHARACTERISTICS OF POWER TRANSFORMER

For the considered power transfer application, in order to operate the transformer in the desired frequency region, a resonant capacitor of 6.8nF is considered. The measured performance characteristics i.e., $H(f)$, Z_{in} and η of the designed transformer with a load resistance of 10Ω are depicted in fig.44.

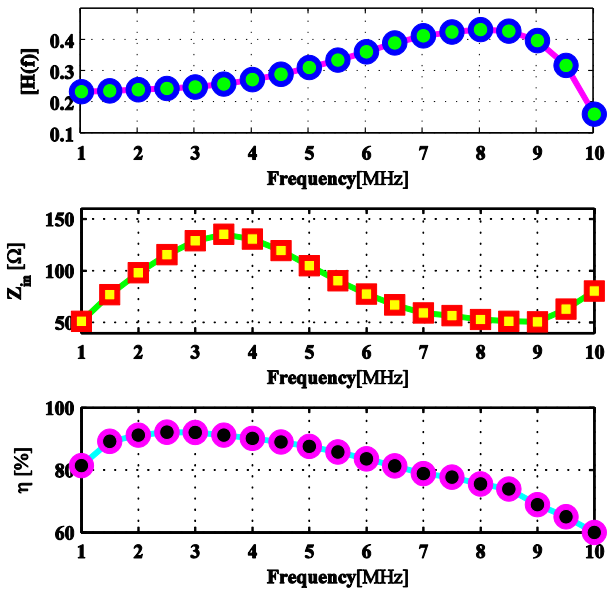

Figure 44. Measured performance characteristics of power transformer

From this figure, it can be observed that the MIF of transformer is 3.5MHz and the MEEF is around 2.6MHz, which falls within the desired operating frequency region of the converter. The energy efficiency of the transformer at MEEF is 92% with the power level of 10.5W. Since the designed transformer possess the desired characteristics in the operating frequency region, the power tests were conducted from the low power to the full load conditions at MEEF of 2.6MHz.

The energy efficiency of the transformer as a function of the load power and the thermal profile of the transformer at a load power of 20W are illustrated in fig.45 (a) and (b) respectively. From fig.45 (a), the energy efficiency of the transformer at

2.6MHz is found to be within the range of 87 – 96% for the load power range of 0.1 – 50W. For the maximum tested power level of 50W, the power density of the transformer is reported to be 107W/cm^3. The spot temperature of the power transformer at the output power level of 20W is 55.3^{o}C, with an ambient temperature of 25^{o}C. The maximum temperature of 55.7^{o}C shown in the scale is that of the resonant capacitor across the secondary winding.

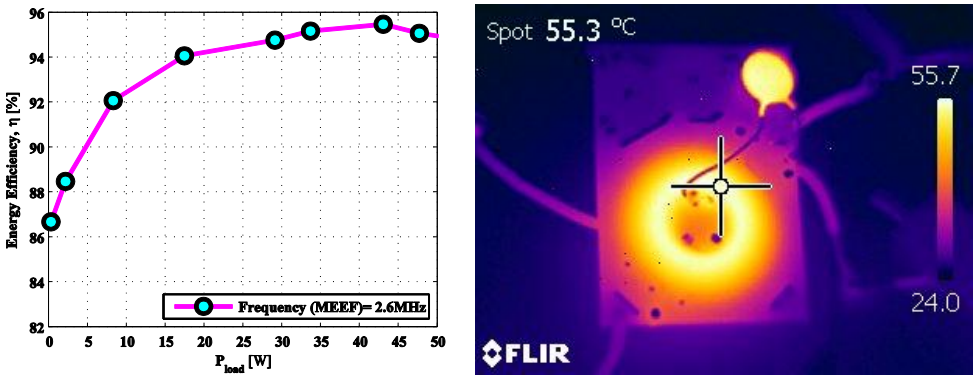

(a) (b)

Figure 45. (a) Energy efficiency and (b) thermal profile of center tapped power transformer

6.4 ENERGY EFFICIENCY OF SRC WITH THE CORELESS PCB SIGNAL AND CENTER TAPPED POWER TRANSFORMER

The designed power transformer, together with the signal transformer discussed in chapter 5, has been evaluated in a series resonant converter (SRC) in the MHz frequency region for the aforementioned converter specifications.

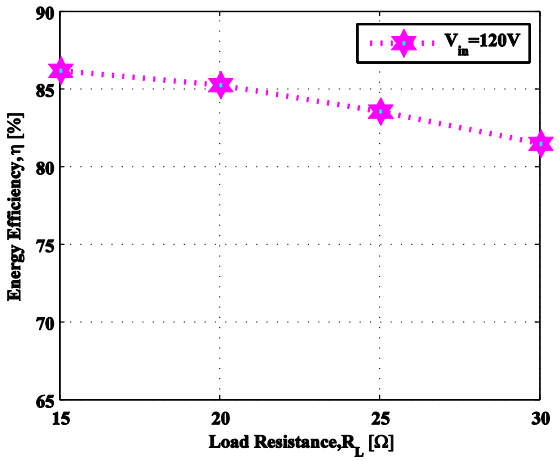

Figure 46. Energy efficiency of regulated series resonant converter (SRC) [77]

The SRC has been initially simulated using high frequency model of the coreless signal and power transformer [77] and the measurements have been carried out on the designed converter prototype. The energy efficiency of the open loop regulated SRC using a constant off time frequency modulation technique is illustrated in fig.46.

Here, the input voltage of the converter is considered as $120V_{dc}$ and the output voltage is regulated to $20V_{dc}$ with ±2% tolerance band with a peak energy efficiency of converter as 86.5%.

7 IMPACT OF DIELECTRIC MATERIAL ON PERFORMANCE OF PLANAR TRANSFORMERS

For the majority of the SMPS applications, the requirement is to have the step-down ratio of the transformer as discussed earlier. However, as the turn's ratio becomes larger such as 4:1, 6:1, 8:1 etc., several series and parallel combinations of the primary/secondary windings are required. This result in an increased number of PCB layers and therefore the stray capacitances become elevated together with the reduced coupling coefficient between the primary and secondary windings of the transformer, depending on their winding arrangements. Hence, as the turn's ratio of the transformer increases, the operating frequency bandwidth and the energy efficiency of the transformer gets lowered. Also, the proximity effect becomes pronounced at higher operating frequencies in addition to the skin effect as discussed in chapter 2, as the number of transformer winding layers increases.
As discussed previously, the coreless PCB transformer is composed of a dielectric material and copper windings. The majority of the previous research has concentrated on the latter so as to reduce the skin and proximity effects, leakage inductance as well as reducing the stray capacitances. However, the effect of the dielectric material on the performance of the transformer/inductor has not been covered, which also plays a vital role as the operating frequency is increased from few hundred kHz to several MHz.

In this regard, the investigation was also conducted on the impact of the dielectric material on the performance of planar power transformers, by comparing the transformer with traditional FR-4 laminate to that of the high frequency dielectric material i.e., Rogers 4450B in 1 - 5 MHz frequency region. In this thesis, the indirect effect of the dielectric material i.e., the effect of the electric field on the current distribution as well as on the magnetic field distribution of the transformer is explored apart from the inherent dielectric loss within the transformer. The comparative results of the transformers with two different dielectric materials in terms of the coupling coefficient, inductive and capacitive parameters, performance characteristics such as input impedance and energy efficiency are discussed.

7.1 TYPICAL PROPERTIES OF TRADITIONAL FR-4 AND HIGH FREQUENCY ROGERS 4450B DIELECTRIC LAMINATES

Before going to discuss the performance characteristics of the transformers with two dielectric materials, in this section, some of the typical properties of both the dielectric laminates, which are required for power transfer application, are presented.
The properties to be considered are the dielectric constant permittivity 'D_f' , loss tangent '$tan\delta$', dielectric strength 'D_s' in kV/mm and glass transition temperature

'T_g' in °C. These parameters, for the two different dielectric laminates [78] - [80], are given in table.8.

Table 8. Properties of dielectric laminates

Properties	FR-4	Rogers 4450B
D_f	4.3@1GHz	3.54@1GHz
Tanδ	0.020@1GHz	0.004@1GHz
D_s [kV/mm]	50	~39
T_g[°C]	127	>280

Dielectric constant permittivity 'D_f': It is functionally dependent on the frequency, and as the frequency increases the variation of 'D_f' of the FR-4 material is high as compared to that of the Rogers 4450B material. However, for high frequency applications, it is essential to have a stable dielectric constant as the frequency varies, so that the material loss can be reduced. Therefore, in terms of the dielectric constant, it can be stated that the Rogers 4450B laminate is suitable for high frequency applications.

Loss tangent '*tanδ*': In addition to a stable dielectric constant at higher operating frequencies, the requirement is to have a low loss tangent '*tanδ*' for the selected dielectric laminate. From table.8, it can be observed that Rogers material possess a low dielectric constant permittivity and a reduced loss tangent compared to its counterpart FR-4.

Dielectric strength 'D_s': In terms of dielectric strength 'D_s', the greater it is, the better it is for high voltage applications. From table.8, it can be observed that, in terms of the dielectric strength of the material, FR-4 possess a higher dielectric strength capability as compared to the Rogers 4450B laminate. However, both the materials are exhibiting reasonable dielectric strengths. The insulation resistance of both the transformers was measured with the assistance of a 3111V KYORITSU insulation tester. The measured insulation resistance of both the transformers at 1000VDC, with a 0.4mm separation between the primary and secondary windings of the transformers, is greater than 100MΩ. The test was conducted for 1 minute duration and the stable reading of 100MΩ was observed on the meter scale of the insulation tester.

Glass transition temperature 'T_g' and Moisture absorption property: The higher the value of 'T_g', the more stable it is in relation to the temperature variations. It is desirable to have a low moisture absorption property since this has an effect on both 'D_f' and '*tanδ*'.

7.2 MAGNETIC FIELD AND CURRENT DENSITY DISTRIBUTION OF TRANSFORMERS WITH DIFFERENT DIELECTRIC MATERIALS

Initially a 2-D model of a two layered 1:1 coreless PCB transformer is considered for determining the dielectric material effects on magnetic field intensity and current density distribution at higher operating frequencies as compared to the conventional operating frequency of transformers. The simulations were performed with the assistance of ANSOFT Maxwell student version 3.1.04 software. In this case, as the finite element analysis (FEA) eddy current field solver provides a clear depiction of the magnetic field and current distribution, it has been utilized for analyzing the performance of the transformers. Here, for both the transformers, the geometrical parameters were maintained at a constant value and the analysis was conducted at a frequency of 3MHz, by passing a 1A sinusoidal current into the primary winding of the transformer. The relative permittivity 'ε_r' of FR-4 and the Rogers 4450B material are 4.3 and 3.54 respectively as mentioned in table.8. The corresponding magnetic field intensities of the FR-4 and Rogers 4450B transformers are illustrated in fig.47.

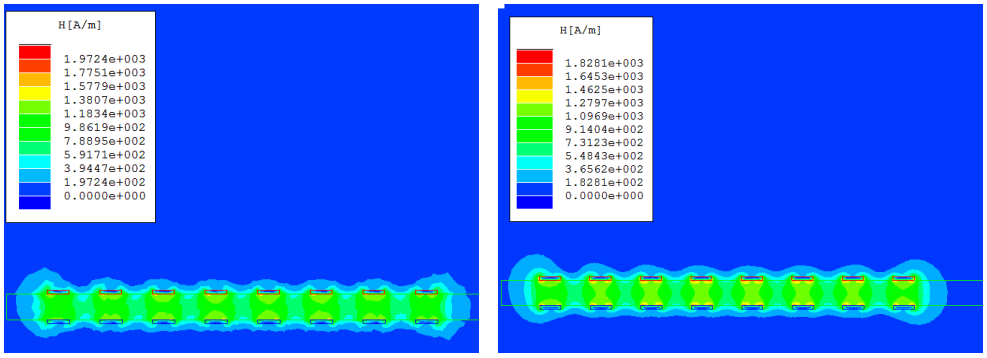

Figure 47. Magnetic field intensity of transformer with FR-4 (left) and Rogers 4450B (right) at 3MHz

From fig.47, it can be observed that the magnetic field intensity '*H*', which is a measure of leakage inductance of the transformer [76], is higher in the case of the transformer with the FR-4 material as compared to the transformer with the Rogers 4450B laminate. This results in a higher coupling coefficient '*K*' in the latter case as compared to the transformer with the FR-4 laminate.

Under the same conditions, the current density distribution of the transformers, which is a measure of conduction losses [76] (due to AC resistance), obtained from simulations, for transformer with FR-4 laminate and Rogers 4450B laminate are illustrated in fig. 48 (a) and fig. 48 (b) respectively.
Here, from fig. 48(a) and (b), it can be observed that current density distribution which is a measure of conduction losses in case of transformer with the high

frequency dielectric laminate is lower [76] as compared to the transformer with the FR-4 laminate, which results in reduced AC resistance of the transformer with Rogers 4450B material.
The simulations were carried out in the frequency range of 1 – 5MHz, and the same phenomenon was observed, which shows that the transformer with the dielectric material of low permittivity possess a high coupling coefficient and low resistive losses as compared to the transformer with the dielectric material of high permittivity.

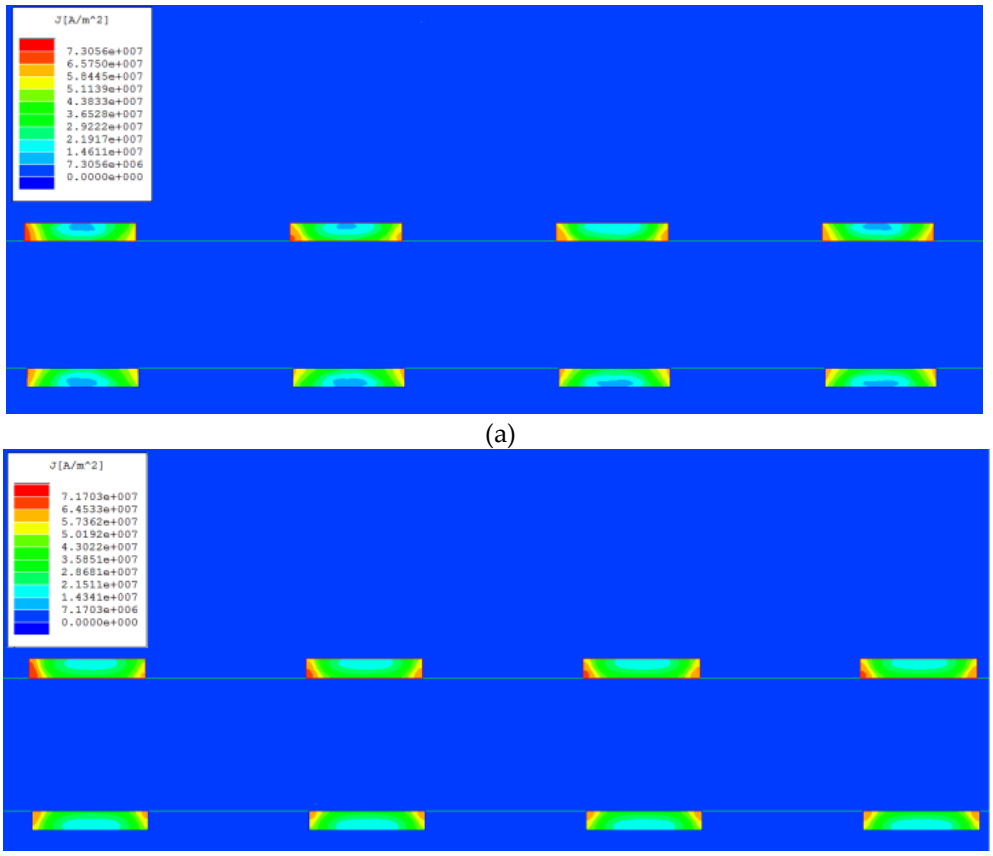

Figure 48. Current density distribution of planar PCB transformer with (a) FR-4 and (b) Rogers 4450B laminates at 3MHz

7.3 ELECTRICAL PARAMETERS OF TRANSFORMERS USING 'S' PARAMETERS

Based upon the simulations, two multilayered coreless PCB step-down transformers of 8:1 turn's ratio, which are suitable for power transfer applications, were designed on both FR-4 and Rogers 4450B dielectric laminates. Here, both the transformers were characterized by using the 'S' parameters obtained from the

network analyzer. The experimental set-up including the designed transformers possessing the same geometrical parameters for determining the AC behavior using the network analyzer is illustrated in fig.49.

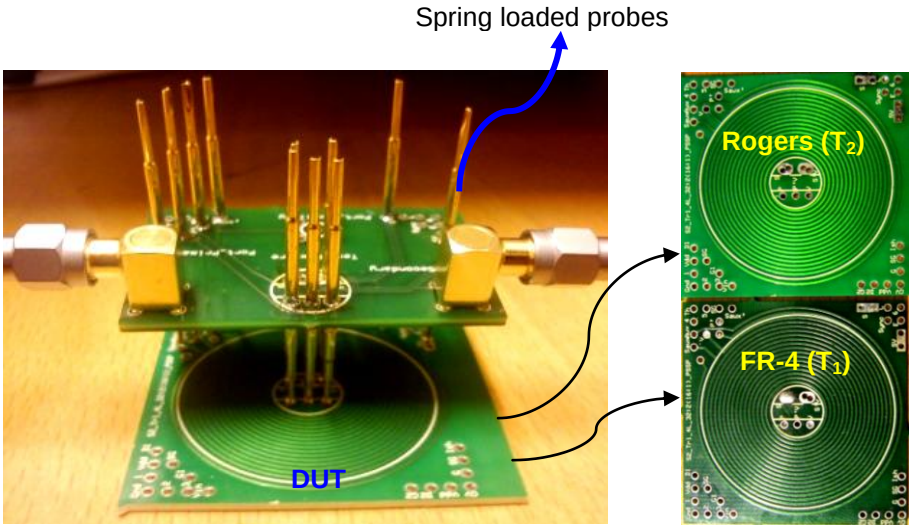

Figure 49. Experimental setup for characterizing transformers with network analyzer

Since the transformer is considered as a two port network, the electrical parameters were obtained by considering the 'S' parameters [81], [82] using the network analyzer E5070B. Here, the device under test (DUT) i.e., the transformer, was connected using high frequency spring loaded test probes as shown in fig.49 and '*S*' parameters were measured in the frequency range of 300 kHz - 10 MHz. The smith charts in real/imaginary format for both the transformers were taken and the '*S*' parameters were transformed into the complex impedance '*Z*' parameters by following the procedure described in [83], [84].

From the transformed 'Z' parameters, the electrical parameters such as self (L_{pri}/L_{sec}) and mutual inductances (L_m) are obtained as follows.

$$L_{pri} = imag(Z_{11})/\omega \tag{49}$$

$$L_{\sec} = imag(Z_{22})/\omega \tag{50}$$

$$L_m = imag(Z_{12})/\omega \tag{51}$$

where, $\omega=2\pi f$

By knowing the self and mutual inductances of the transformers, the turn's ratio 'n' can be obtained from equation (11), and the leakage inductances of the primary/secondary windings are calculated from equations (9) and (10). Since the required transformers operating frequency is within the range of 1 - 3 MHz, with the assistance of an external resonant capacitor across the secondary winding, it is desirable to know the inductance behavior in this region. From the measured

primary/secondary self inductances of both the transformers, it was observed that they are relatively close because of their same geometrical parameters.
However, in terms of leakage inductance, a deviation exists between both the transformers. The leakage inductance in the case of the transformer with the FR-4 material 'T_1' is high [85] when compared to that of the transformer with the Rogers material 'T_2' due to the high magnetic field intensity 'H' ,as discussed at an earlier stage. From the obtained self/mutual inductances of the transformer, the coupling coefficient 'K' can be obtained by using equation (19) and the corresponding coupling coefficient of both the transformers, calculated from the measured parameters, are illustrated in fig.50 (a). Here, at 1MHz the coupling coefficient 'K' of transformer with FR-4 laminate (T_1) is 0.78 whereas for transformer with Rogers 4450B laminate (T_2) it is 0.83. From this, it can be observed that, at a particular frequency of operation, an improvement of approximately 5% in the coupling coefficient can be achieved by changing the dielectric material.

From fig.50 (a), it can be stated that the Rogers material has better signal transfer characteristics in the operating frequency region of the transformer as compared to that for the FR-4 material.

Since, in coreless PCB transformers, the loss is contributed mainly by the AC resistance of the primary/secondary winding of transformers, the measured AC resistances obtained from the 'S' parameters are illustrated in fig.50 (b).

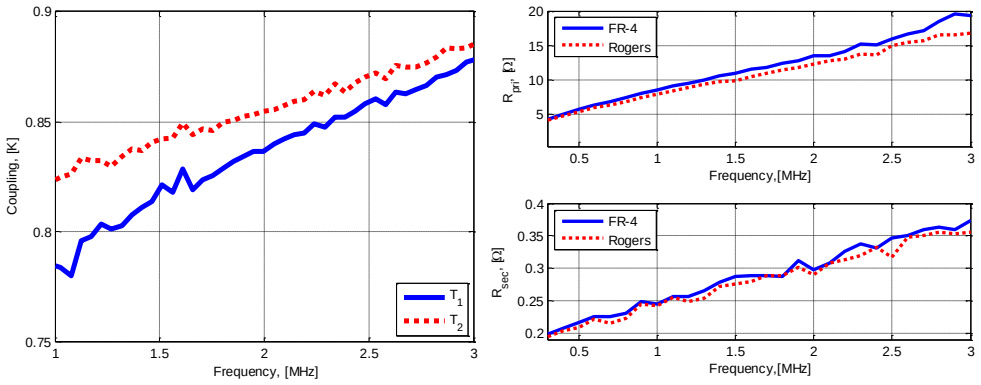

(a) (b)

Figure 50. (a) Coupling coefficient and (b) AC resistance of T_1 & T_2

Here from fig. 50(b), it can be observed that a difference exists, in terms of the AC resistance in relation to both the primary and secondary windings, when the dielectric material is changed due to the change in skin and proximity effects, which is a functional dependent of D_f. This can be confirmed from the FEA analysis in the previous sections where the current density 'J' in the case of the

transformer with the Rogers material is less than that of the transformer with traditional FR-4 laminate.

In order to validate the electrical parameters derived from the network analyzer, the parameters were also measured with the assistance of a high precision RLC meter at 1MHz and then compared. It was observed that the parameters obtained in both cases were in good agreement with each other. The measured inter-winding capacitances 'C_{ps}' of the transformers T_1 and T_2 using the RLC meter are 146pF and 123pF respectively. The difference in 'C_{ps}' is due to the change in the relative permittivity/dielectric constant permittivity (D_f) of the materials, while other parameters such as area (A) and distance between plates (d) are kept at a constant value. Since the inter-winding capacitance of the transformer with Rogers material is less as compared to the FR-4 dielectric laminate, the bandwidth of the transformer operating frequency region gets increased.

7.4 ENERGY EFFICIENCY OF TRANSFORMERS WITH DIFFERENT DIELECTRICS

The performance of the transformer can be determined by having knowledge of its energy efficiency in the desired operating frequency region. Therefore, in this regard, the maximum attainable energy efficiency/power gain 'η_{max}' of the transformer, by assuming an optimum load condition for various operating frequencies in terms of 'S' parameters [86], is obtained as follows.

$$\eta = \frac{|S_{21}|}{|S_{11}|}\left(K - \sqrt{(K^2 - 1)}\right) \tag{52}$$

where,

$$K = \frac{1 - |S_{11}|^2 - |S_{22}|^2 + |S_{11}S_{22} - S_{12}S_{21}|^2}{2|S_{12}S_{21}|} \tag{53}$$

As discussed in earlier chapters, the resonant capacitor 'C_r' across the secondary winding plays a vital role in the case of a coreless PCB transformer. Therefore, a capacitor of 4nF was connected in order to bring the operating frequency of the transformer within the desired range. The small signal maximum attainable energy efficiency/power gain of the transformers obtained from the 'S' parameters using equations (52) and (53), with and without a resonant capacitor 'C_r', are illustrated in fig.51 (a). From this fig., it can be observed that the energy efficiency of T_2 is greater than T_1 in both cases, i.e., with and without resonant capacitors.

In addition, the power tests were conducted using an RF power amplifier for these transformers in the frequency range of 1 – 6MHz. Here, the maximum tested output power in both cases was 7W. The measured energy efficiencies of these transformers, with load resistance of 10Ω and 'C_r' of 4nF, are shown in fig.51 (b).

It can be observed that from both the small signal analysis and the power tests of the transformers, the energy efficiency in the case of transformer with the Rogers material was improved by 2 - 5% in the MHz frequency region. At an operating frequency of 3MHz, for the given excitation voltage of 70V RMS and the same load power of approximately 7W, the energy efficiency of the transformers 'T_1' and 'T_2' are 84.2/86.3% respectively.

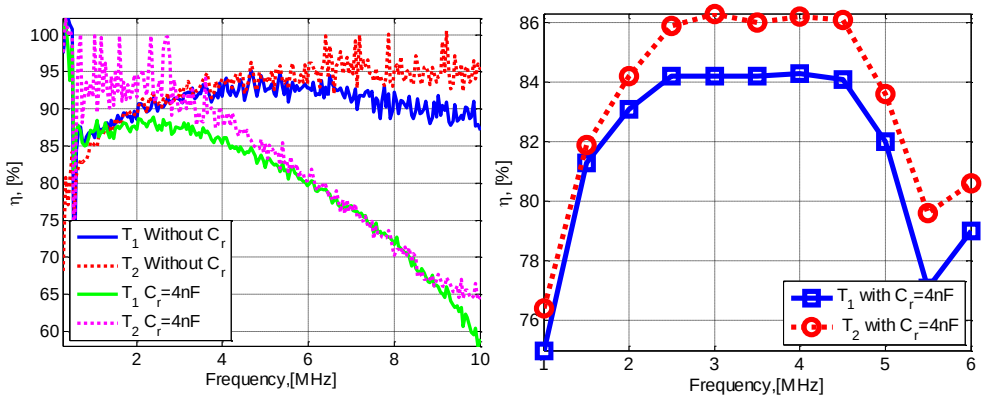

Figure 51. (a) Maximum attainable gain & (b) energy efficiency of T_1 & T_2

From figs. 50 (a) and (b), at a particular frequency of 3MHz (MEEF), a deviation in the coupling coefficient and the primary/secondary AC resistances exists, which resulted in the variation of the energy efficiency of transformers. The input impedance 'Z_{in}' of the transformers 'T_1' and 'T_2' at this operating frequency are 384 and 387Ω respectively because of the variation in the dielectric constant of the medium. According to [87], if the material has a low dielectric constant, it is possible to increase the trace width of the primary/secondary windings in order to obtain the same control impedance parameter. This results in a reduced DC resistance and hence the copper losses by lowering the skin and proximity effects of the transformers and thus it become possible for further improvement of energy efficiency of the transformer. The estimated dielectric losses at these operating frequencies are not very visible at these frequencies, which are as low as a few MHz. The dielectric losses become more prominent as the operating frequency moves towards some GHz. For wide operating frequency range of the transformers, consideration must be given to all these parameters.

From both the small signal analysis and the power tests of the transformers, it can be concluded that the energy efficiency of the transformer can be improved by changing the dielectric material of the transformer from the traditional FR-4 laminate to a high frequency Rogers 4450B. The cost of the dielectric material from the Rogers Corporation is approximately twice [88] that of the FR-4 material. However, the exceptional features of having a low inter-winding capacitance,

reduced skin and proximity effects and a better power gain/energy efficiency can be achieved by utilizing high frequency dielectric material rather than the traditional FR-4 laminate which is beneficial for the future generation high frequency transformers/inductors (both coreless and core based). Especially, as the power rating of the transformer gets increased, high frequency dielectric materials are more beneficial as they possess better thermal management property, more reliable operation in thermally dynamic environments compared to that of the FR-4 dielectric laminate [88].

PART – II

Core based Planar Transformers for Next Generation SMPS

8 NOVEL HYBRID CORE PLANAR POWER TRANSFORMER

In the earlier chapters, the potential of multilayered coreless PCB transformers for both signal and power transfer applications have been discussed. In addition to this, the impact of geometrical parameters, dielectric effects on the performance of transformer and also the design guidelines of signal and power transformer for the given application have been presented. The achieved power density of the coreless PCB step-down power transformers discussed in the thesis for the maximum tested load power of 50W is reported to be 107W/cm^3 with an energy efficiency of approximately 95%. However, in order to further increase the energy efficiency of the power transformers and to evaluate the existing high frequency core materials, the research was also focussed on the design and evaluation of the core based planar transformer. The desired operating frequency region of transformer is in the range of 1 – 10MHz, by utilizing the latest high frequency core materials available in the market. In this context, this chapter deals with a discussion on the selection of core material, core shape, winding strategies, design guidelines, application of designed transformer in resonant converter topologies and performance of a transformer w.r.t different air gaps.

8.1 DESIGN SPECIFICATIONS OF HIGH FREQUENCY PLANAR POWER TRANSFORMER

In order to miniaturize the existing core based flat profile planar power transformers for various consumer applications such as laptop adapter etc., initially, an attempt has been made to design a core based transformer with the following specifications.

- Half bridge converter topology
- Input voltage specifications : 85Vac – 130Vac
- Output voltage specifications : 22V$_{dc}$
- Frequency of operation : 3 - 5MHz
- Targeted converter energy efficiency : >90%
- Targeted transformer energy efficiency : >95%
- Output power level : 45W

In the coming sections, the procedure followed to design the planar power transformer to meet the aforementioned requirements is described.

8.1.1 Selection of high frequency core material

In order to be able to design a high frequency core based transformer, the initial step is to select the optimal core material. As the operating frequency of the transformer increases, an inevitable core loss exists as shown in fig. 52(a) [89] due to the increased eddy current phenomenon. Therefore, the requirement is to choose

the optimal core material for operating the transformer in a high frequency region. The combination of manganese and zinc i.e., MnZn or nickel and zinc (NiZn) materials possess the desirable characteristics in order to operate the magnetics at higher frequencies i.e., in the 1 to several MHz frequency region when compared to other existing magnetic materials. Some of the popular manufacturers of these high frequency magnetic materials are Ferroxcube, Magnetics Inc, TDK-EPC, MMG Canada Ltd and Kolektor Magma. MnZn materials ie., 3F4 and 3F45 can be utilized in the frequency range of 1 – 2MHz [90] whereas the material 3F5 possess the desirable characteristics in the frequency range of 2 – 4MHz [90]. For operating the magnetics above 4MHz, the recommendation is to use the NiZn - 4F1 material, which possess good magnetic properties from 4 – 10MHz. In this case, 1F material from Kolektor Magma which is equivalent to 4F1 material from ferroxcube and K1 material from EPCOS etc., [91] is considered. The important characteristics such as complex permeability, maximum flux density, initial permeability, Curie temperature, specific power loss density and other parameters can be obtained from the core material's datasheet. Specific power loss density is a strong function of the operating temperature of the transformer/inductor. The specific power loss density as a function of temperature for 1F/4F1 material [89] is illustrated in fig. 52(b). From this figure, it can be observed that the optimal operating temperature 'T_{opt}' of the magnetics, at a frequency of 10MHz with maximum flux density 'B_{max}' of 7.5mT, is 60°C whereas for 'B_{max}' of 5mT it is around 70°C. This corresponds to minimum loss point of the core, which is generally obtained from the U shaped loss curves as shown in fig.52 (b).

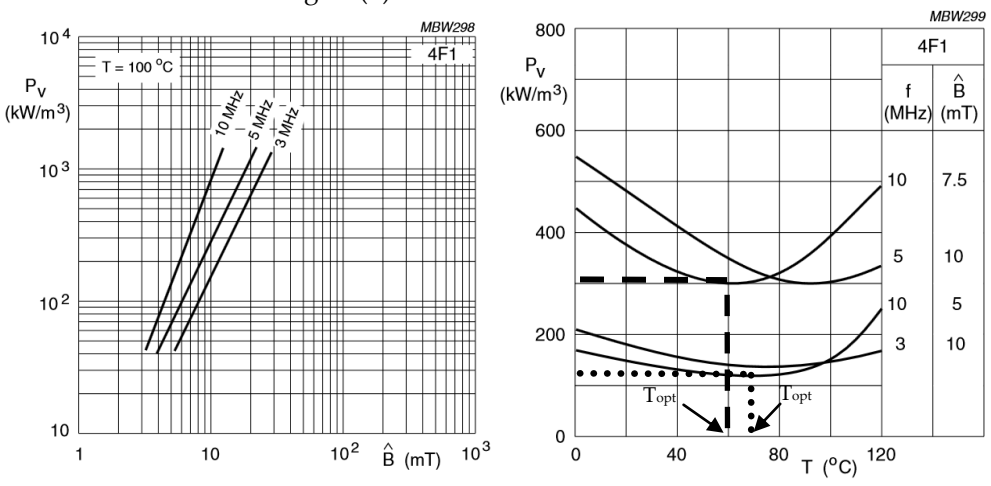

(a) (b)

Figure 52. 4F1 material specific power loss density [89] as a function of (a) 'B_{max}' and (b) temperature

In this regard, for the given power transfer application, the MnZn-3F5 material and NiZn-4F1 material were evaluated for the same geometrical parameters of the

transformer and the corresponding measured energy efficiency of the transformer as a function of frequency is shown in fig.53.

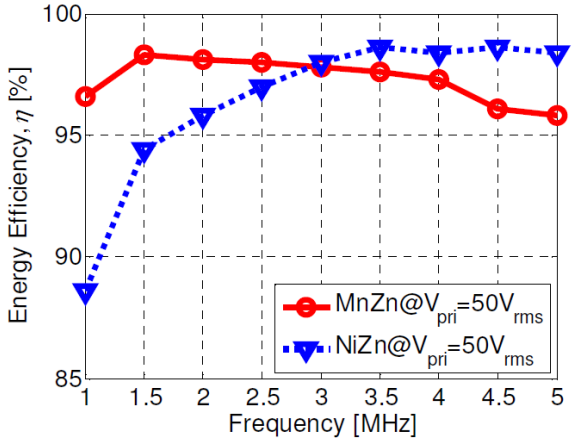

Figure 53. Characterization of MnZn & NiZn material as a function of frequency

From this figure, it can be observed that the transformer with the MnZn-3F5 material has a comparatively high energy efficiency in the frequency range of 1-3MHz, whereas the transformer with the NiZn-4F1 core material has a better performance from 3MHz for the given sinusoidal excitation voltage of $50V_{rms}$. Therefore, in order to operate the transformer within the 1 – 3MHz frequency region, the MnZn material can be utilized whereas above 3MHz, the NiZn - 4F1 material is the best choice based on the existing core materials. In addition to this, low temperature co-fired ceramic (LTCC) material can also be operated in the frequency range of 3 – 5MHz [92], [93]. However, in this thesis, the transformers were designed and evaluated by using the high frequency NiZn-4F1 core material.

8.1.2 Selection of core shape and size

Ferrite cores are available in a wide variety of geometric shapes such as pot or cup cores, EE cores, rectangular modular (RM) cores, power quality (PQ) cores, UU or UI cores, EI cores, Planar E, I cores, UR cores, economic transformer design (ETD) cores, EFD cores etc.,[94], [95]. Some of the available core geometries suitable for power transfer applications are illustrated in fig.54. No straightforward method exists with regards to the selection of the core geometry since it depends on several factors such as core cost, winding cost, winding flexibility, heat dissipation, shielding characteristics and so on and a trade off does exist between all these factors [94], [96]. Therefore, the selection of the core purely depends on user choice based up on the targeted application.

The intended application of the designed transformers is in the high frequency SMPS in order to achieve the low profile, high power density converters as discussed in chapter 1. However, as the switching frequency of the converter

increases, the electromagnetic interference (EMI) or radio frequency interference (RFI) from these transformers poses a problem if these transformers are not sufficiently shielded. Therefore, in this regard, while considering all the available core geometries, the pot core and EP cores are considered as these cores possess excellent shielding characteristics [96].

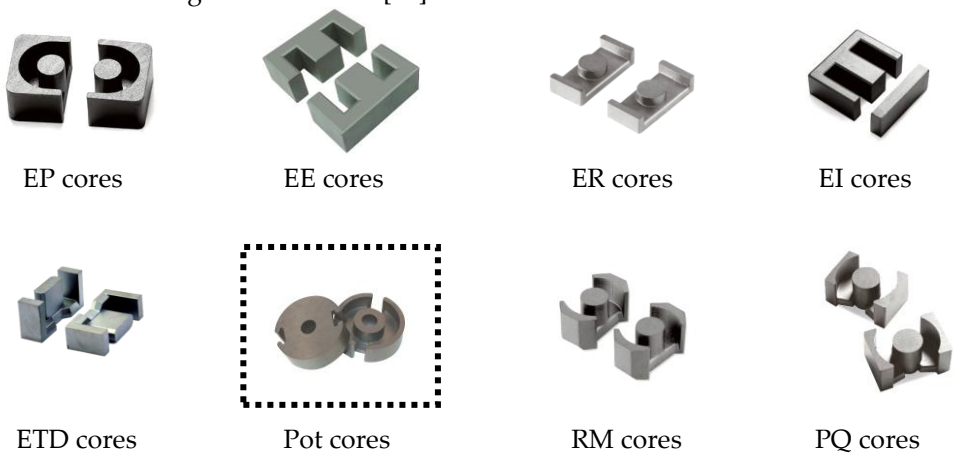

Figure 54. Various core geometries available for power transfer applications

Since, the windings are totally enclosed inside these pot cores, these are considered as excellent self shielded core geometries, which minimize the problems concerning EMI and RFI. In addition to this, these cores are considered as being a good choice and are widely used for low power levels up to 125W and especially for DC/DC converter applications [94], [50]. One of the major disadvantages of these cores in the case of a bobbin wound transformer is the presence of a narrow slot in the ferrite through which the coils exit. Based on this, these were considered as a not good choice, especially for high voltage applications, where there would be a problem of arcing between the two terminals. However, in the case of windings laid on a PCB, this problem can be eliminated by distributing the starting and ending points of the winding for the transformer on two different layers of PCB. Because of these advantages, even though the core cost is high compared to other core geometries, the pot core has been considered for designing the high frequency transformer. After selecting the core shape, the core size was determined by using the window area product method. The required window area product [94] obtained by using the following equation was 0.0256 cm^4.

$$W_a A_c = \frac{P_o D_{cma}}{K_t B_{\max} f} \tag{54}$$

where,

P_o output power in watts

D_{cma}	Current density in circular mils/amp
K_t	topology constant
B_{max}	maximum flux density in mT
f	operating frequency in MHz

Here, the output power is considered as being 45W, the current density is 750 circular mils/amp, the topology constant is 0.0014 for a half bridge converter, and the operating frequency is 3MHz.

The maximum operating flux density is considered as 16mT in order to limit the core losses. Since pot core of 1408 size has a window area product of 0.02cm⁴, the next core size i.e., pot 1811 was considered which has a window area product of 0.07cm⁴.

8.1.3 Calculation of primary and secondary number of turns

After the selection of the core material, shape and size, the required number of primary and secondary turns [73] for the given specifications were calculated by using the following equations.

$$N_{pri} = \frac{V_{in}^{\max} \cdot 10^9}{4 f B^{\max} A_c} \tag{55}$$

$$N_{\sec} = \frac{1.1(V_{out} + V_f) N_{pri}}{V_{in}^{\min} \cdot D_{\max}} \tag{56}$$

where,

V_f	Forward voltage drop of the secondary diodes
A_c	Area of cross section of the core
V_{out}	Output voltage of converter
D_{max}	Maximum duty cycle

By using the above equations, the calculated no. of primary and secondary windings of the transformer for the given specifications are 8 and 2 respectively. The primary/secondary turns of the half bridge center tapped planar transformer were distributed on a six layered PCB and the cross sectional view of the structure is shown in fig. 55.

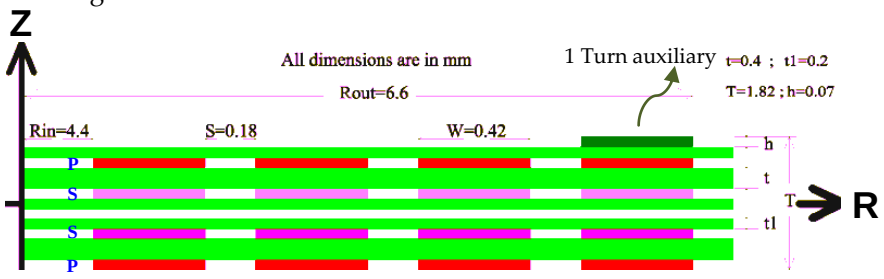

Figure 55. Cross sectional view of planar power transformer in R-Z Plane

Regarding the other geometrical parameters, such as winding width 'W' and separation 'S' between the tracks, the design guidelines mentioned in chapter 6 were considered. According to [75], if the trace width is at least ten times the skin depth corresponding to operating frequency, the quality factor of the winding can be increased. At the minimum operating frequency of 3MHz, the calculated skin depth is 38μm. Therefore, the winding width is considered as being 11 times the skin depth [75] i.e., 0.42mm and also by considering the current carrying capability of the conductor. Regarding the separation between the tracks, it is to be maintained as minimal as possible as discussed earlier within the manufacturing capability and therefore, it is considered as 0.18mm. The 3D view of the designed transformer is illustrated in fig.56. Here, the distance between the various layers of the PCB i.e., auxiliary-primary$_1$-secondary$_1$-midpoint-secondary$_2$-primary$_2$ is 0.2-0.4-0.2-0.2-0.4 mm, resulting in the total thickness of PCB as 1.82mm with a 70μm copper thickness on all layers of the PCB.

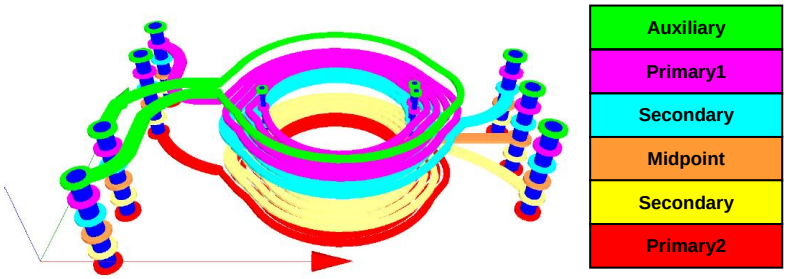

Figure 56. 3D view of the designed high frequency center tapped power transformer

8.1.4 Winding strategy in MHz frequency region

The conventional printed planar transformers employ a solid winding strategy in order to carry large amount of currents in the secondary windings of step-down transformers. However, since the operating frequency of the transformers is increased from several hundred kHz to MHz, it is required to evaluate the winding strategy in order to obtain the optimal performance of the transformer. Therefore, in this regard, this conventional winding strategy was compared to the parallel winding strategy, by considering two parallel winding strands in a conductor instead of a single solid winding. For this purpose, two transformers were designed with the same geometrical parameters, the exception being the width of the windings as shown in fig. 57. The relationship between the widths of both the transformers is given by the following equation by maintaining the same inner/outermost radius (R_{in}/R_{out}).

$$w_p = \frac{w_s}{2} - S \tag{57}$$

where,

w_p Width of the single conductor in parallel strands of the transformer

w_s	Width of the single solid winding
s	Separation between two tracks

(a) (b)

Figure 57. (a) Conventional (solid) and (b) parallel winding strategy of transformer

The measurements were carried out for both the transformers, as a function of frequency and load power, and are illustrated in figs.58 (a) and (b) respectively. In fig. 58 (b), the frequency of operation is considered to be 3MHz and for the entire load power, the sinusoidal excitation voltage is maintained at a constant. From these figures, it can be observed that the energy efficiency, in the case of the transformer with a parallel winding strategy, is higher as compared to that with the solid winding strategy by about 1 - 2% since the rate of rise of the eddy current phenomenon increases rapidly in the MHz frequency region as compared to lower operating frequencies. This results in the higher skin and proximity effects in these windings and, as a consequence, the conduction losses increase in the solid winding strategy. Therefore, in the designed transformers, the parallel winding strategy has been considered instead of the conventional solid winding strategy.

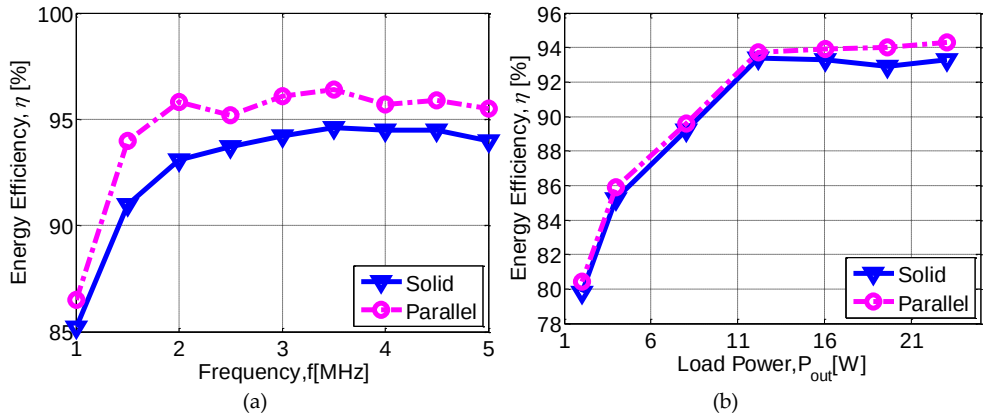

(a) (b)

Figure 58. Efficiency of transformer as a function of (a) frequency and (b) load power

8.2 ELECTRICAL PARAMETERS OF THE PLANAR TRANSFORMER

With the design guidelines mentioned in the previous section, a planar power transformer with a pot core has been designed and evaluated for the considered specifications of the converter. In order to obtain the stringent height, a single pot

core half and a circular flat ferrite plate of the same material are considered. The top and bottom view of the designed transformer is shown in fig.59. It is generally the case that the pot cores are available with an air gap at the center post in order to carry the DC bias current without saturating the core material. The air gaps are of various sizes, however, in this case, an air gap '*G*' of 0.4mm is considered. For the selected pot core, the effective magnetic length 'l_e' is 25.8mm.

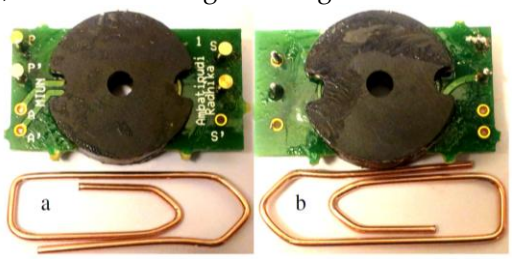

Figure 59. (a) Top and (b) bottom view of POT+I core transformer

With the introduction of the air gap, the permeability of the core material changes, known as the effective permeability from its initial permeability 'μ_i' and can be calculated as follows. Here, the calculated effective permeability of the core is around 36.

$$\mu_e = \frac{\mu_i}{\left(1 + \frac{G \cdot \mu_i}{l_e}\right)} \tag{58}$$

From the obtained effective permeability of the material, the primary/secondary self inductance of the transformers can be calculated from the following equation and are obtained as 4.74/0.3μH respectively.

$$L = \frac{\mu_e N^2 A_c}{l_e} \tag{59}$$

8.2.1 Saturation test of the transformer

In order to determine the saturation of the core, the test was carried out with the assistance of the following experimental setup depicted in fig.60, where a large value of inductance is connected in series with the primary winding of the transformer. By varying the current through the primary winding of the transformer, the self inductance of the secondary winding is measured using a high precision RLC meter as shown in fig.60. The self inductance of the secondary winding as a function of the primary excitation current is illustrated in fig.61.

From fig.61, it can be observed that the saturation of the core occurs after 10A, where the self inductance of the secondary winding of the transformer starts to decrease rapidly.

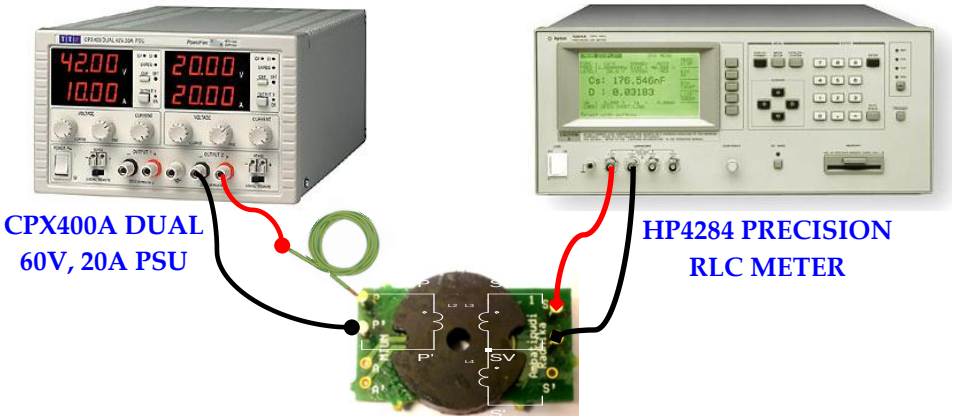

Figure 60. Experimental setup for saturation test of transformer

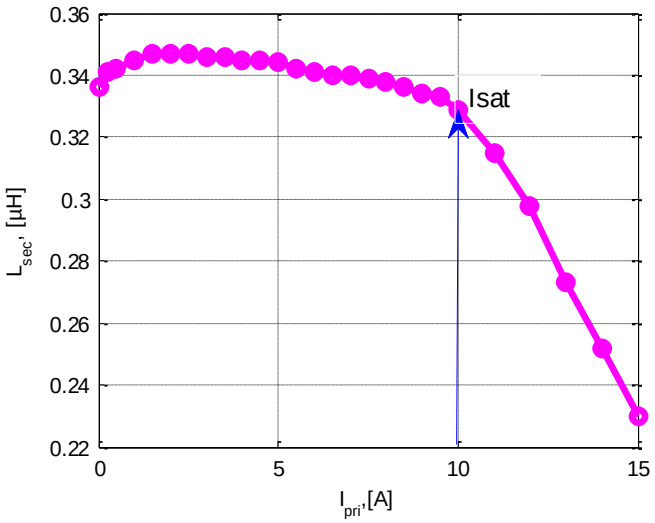

Figure 61. Determination of saturation current 'I_{sat}' of transformer

8.2.2 High frequency model and AC resistance of transformer

The high frequency model of the designed transformer is depicted in fig. 62 (a). The measured primary/secondary DC resistances of the transformer windings are 0.27/0.07Ω respectively. The measured AC resistance of the transformer, as a function of frequency obtained by using sine phase impedance analyzer, is illustrated in fig.62 (b). The other electrical parameters of the transformer were also measured by using a sine phase impedance analyzer at 3MHz and are listed in table.9. The calculated coupling coefficient and the turn's ratio of the transformer obtained from the measured parameters are 0.97 and 3.96 respectively.

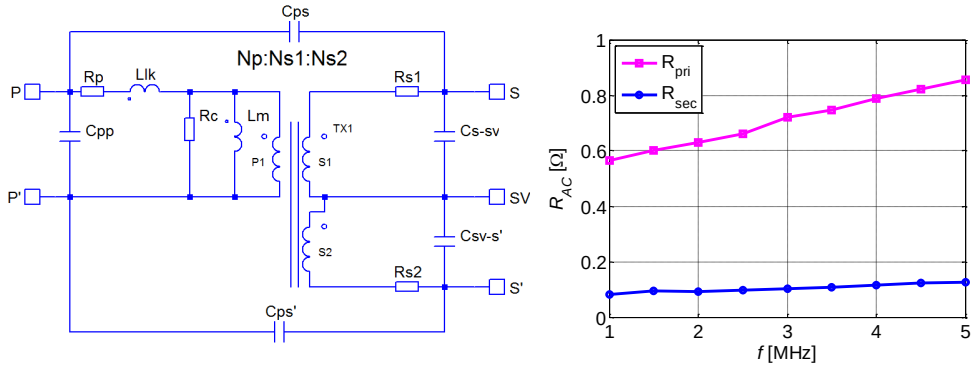

Figure 62. (a) High frequency model and (b) measured AC resistance of the planar transformer

Table 9. Measured electrical parameters at 3MHz

R_P[Ω]	R_S [Ω]	L_P[μH]	L_{lk}[μH]	L_{s1}[μH]	C_{PP}[pF]	C_{ssv}[pF]	C_{ps}[pF]
0.72	0.15	4.88	0.29	0.31	2.08	2.23	22.2

8.2.3 Energy efficiency of transformer

The designed power transformer has been characterized for different load conditions by using the procedure mentioned in chapter 2. It has been evaluated using sinusoidal excitation in the frequency range of 1 – 5 MHz and the corresponding transformer efficiency for different load resistances is depicted in fig.63.

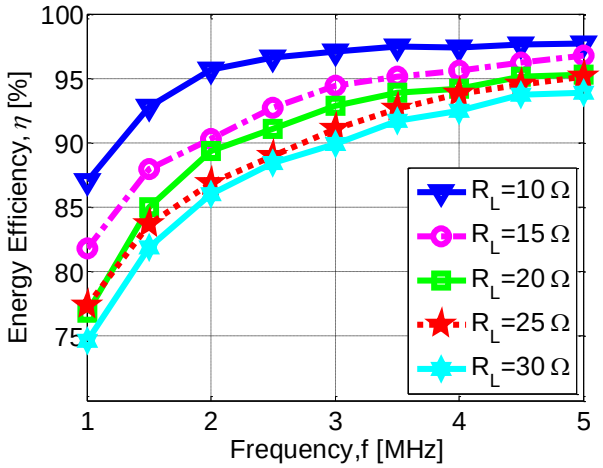

Figure 63. Measured transformer efficiency vs frequency

From this figure, it can be observed that the operating frequency region of the transformer is in the range of 3 – 5 MHz, since the energy efficiency is above 90% for the load range of 10 - 30Ω. At the minimum operating frequency of 3MHz, the efficiency of the hybrid planar power transformer is found to be 97% for a load

resistance of 10Ω. Under these conditions, the primary/secondary voltages across and the RMS currents flowing through the transformer are 42.6/9.63V_{rms} and 0.561/0.928A respectively, with an angle between the voltage and current of the primary winding of 67.3°. This result in the power input fed to the primary winding of the transformer being 9.29W.

From this figure, it can be observed that the transformer is energy efficient in the wide operating frequency region because of a low inter-winding capacitance which is beneficial for obtaining the tightly regulated converter using different modulation techniques, unlike the case of the traditional planar transformers where the large inter-winding capacitance is an obstacle as discussed in introduction. At the minimum operating frequency of 3MHz, the transformer has been characterized from the minimum load power of 2W to 50W with the assistance of an impedance matching network as shown in fig. 64. Here, since the input impedance of the transformer is high, an impedance matching network consisting of '*L*' and '*C*' components is placed across the device under test (DUT) ie., transformer as shown in fig.64, in order to make the impedance offered by load as 50Ω. By doing so, maximum power can be transferred to the load from the source i.e., from power amplifier to the transformer. The calculated values of '*L*' and '*C*' obtained from the measured input impedance and phase angle between the primary voltage and currents are 4.54μH and 1.10nF. The corresponding energy efficiency as a function of load power is illustrated in fig. 65 (a). The reported power density of the transformer at the maximum tested load power is 47W/cm^3.

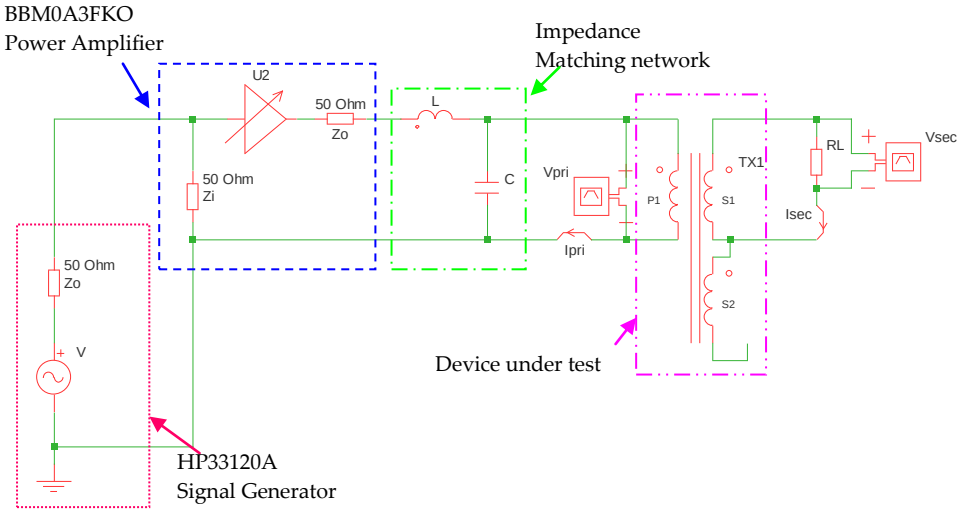

Figure 64. Experimental setup using impedance matching network for power tests of transformer

8.2.4 Thermal profile of transformer and converter efficiency

The thermal profile of the designed transformer at the power level of 50W and an operating frequency of 3MHz is shown in fig.65 (b). The figure shows the transformer under test, together with the capacitor used in the impedance matching network for obtaining the required power from the RF power amplifier at the operating frequency of 3MHz. The spot temperature of the transformer is 86.4°C at an ambient temperature of 25°C with the power loss of about 3.2W, resulting in the energy efficiency of transformer being 94.2%. Here, the capacitor used for the impedance matching network has a spot temperature of 94.6°C as shown in fig.65 (b).

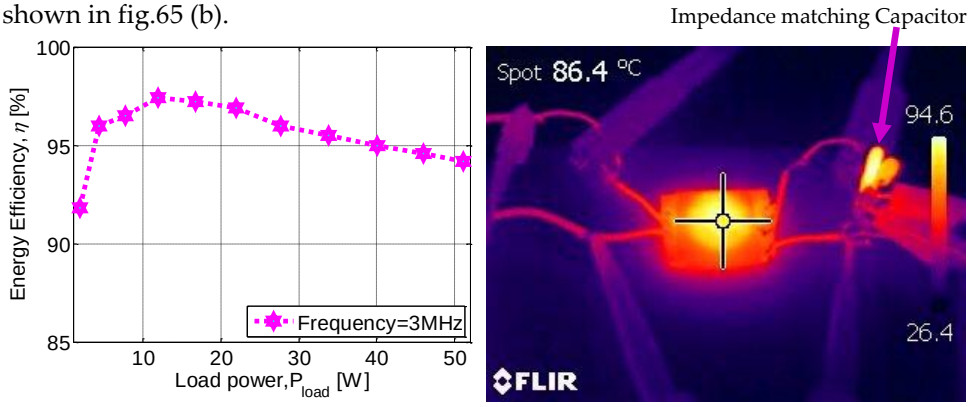

(a) (b)

Figure 65. Transformer (a) energy efficiency and (b) thermal profile at 3MHz

At this particular frequency of operation, the primary/secondary currents flowing through the transformer are 1.31/2.17A respectively. The measured primary/secondary resistances of the transformer windings are 0.72/0.15Ω respectively. Therefore, the copper losses of the desinged transformer at this operating frequency are 1.94W. By knowing the excitation voltage across the primary winding, area of cross section of the core, number of turns of the primary winding and the frequency of operation, the working flux density of the transformer is determined. After obtaining the work flux density, with the assistance of the specific power loss density shown in fig.52, the core losses of the transformer under the specified conditions are obtained and are approximately1.26W.

The designed transformer has been also placed in a multiresonant half bridge converter (MRC) [97] and evaluated at the low line input voltage of $85V_{ac}$ which is equivalent to $120V_{dc}$. The corresponding energy efficiency of the converter, as a function of load power operating at 3.19MHz, is depicted in fig.66. The energy efficiency of the converter circuit with the designed transformer for full load conidtion is 90.5% which is according to the targetted energy efficiency of the converter.

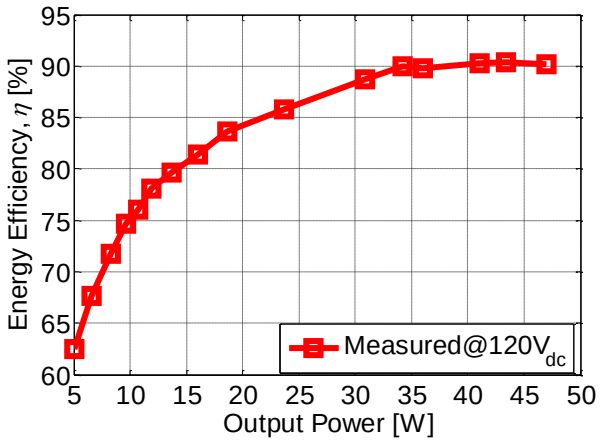

Figure 66. Energy efficiency of MRC at low line input voltage of $120V_{dc}$ [97]

8.3 EFFECT OF AIR GAP ON THE TRANSFORMER PERFORMANCE

In the case of resonant converter topologies such as LCC, LLC etc., the leakage inductance of the transformer plays a prominent role in determining the soft switching behaviour i.e., zero voltage switching (ZVS) of the converter. In general, the resonant and switching frequencies of these converter circuits depends on the resonant inductor, which constitutes the leakage inductance of the transformer and the output capacitances of the MOSFETs [11]. The utilization of the external resonant inductor can be eliminated in order to obtain a highly energy efficient, high power density converter by introducing an optimal air gap in the planar transformer. In this regard, the desired leakage inductance of the transformer can be obtained either by introducing a sufficient air gap at the center post or by distributing the air gap across the core halves with the assistance of plastic shims [94]. However, by following the latter method, the A_L value, which determines the self inductance of the transformer, is varied w.r.t both the temperature and time [94], [98]. In addition to this, the shielding effectiveness of the pot core is degraded by shimming the outer leg of the core. Therefore, by adding the air gap at the center post of the core material, stability exists in terms of inductance and the temperature, particularly in the case of low permeability materials [98]. Here, the effective permeability of the core is reduced due to the introduction of the air gap, which makes it insensitive to the core material permeability [99].

Hence, in this regard, this section deals with the performance of the transformer with the low permeability NiZn-4F1 material for various air gap sizes from 0 – 2mm introduced at the center post of the transformer. The cores with different air gaps at the center post of the pot core halves are depicted in fig.67.

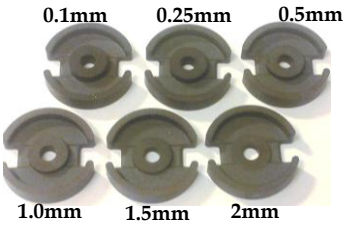

Figure 67. Pot core halves with different air gaps

8.3.1 Self/leakage inductances of transformer with different air gaps

By using the aforementioned core geometries for the different air gaps, the effective permeability and the self inductances of the transformer have been calculated by using equations (58) and (59). The calculated and measured primary self inductance of the transformer is shown in fig. 68(a). Here, the inductances were measured with the assistance of a network analyzer by transforming the '*S*' parameters to '*Z*' parameters as mentioned in chapter 7. From fig. 68(a), it can be observed that the self inductance of the transformer varies as the air gap of the core increases. In addition to this, it can be observed that the calculated and measured inductances are in good agreement with each other. The primary self inductance of the transformer is varied from 16µH to 2µH as the air gap varies from 0 – 2mm at the center post. Fig. 68 (b) depicts the percentage of leakage inductance of the transformer w.r.t self inductance for different air gaps of the core. From this figure, it can be observed that the percentage leakage inductance of the transformer w.r.t to the self inductance varies from 3 to 14% for the air gaps ranging from 0 – 2mm respectively.

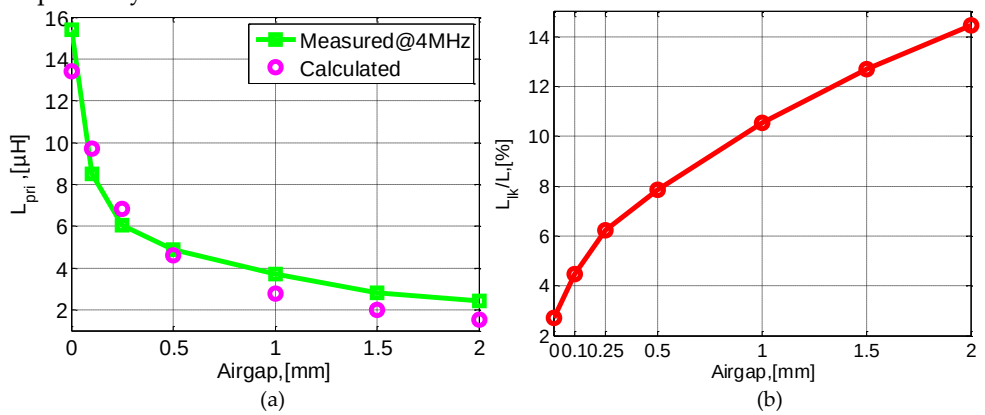

Figure 68. (a) Self inductance and (b) Percentage of leakage inductance w.r.t self inductance for different air gaps

8.3.2 Coupling coefficient of transformer with different air gaps

The calculated coupling coefficient obtained from the measured electrical parameters of the transformer with different air gaps, is illustrated in fig. 69 (a).
From this figure, it can be observed that the coupling coefficient varies from 0.98 to 0.85 as the air gap varies from 0 – 2mm respectively. The coupling coefficient of the transformer depends on the winding strategy and the permeability of the core material [100]. In practice, the coupling coefficient of the practical transformer is less than 1 and also due to the low permeability of the core material, the coupling coefficient of the transformer is 0.98 at a 0mm air gap. The power transferring capability of the transformer for different air gaps and at various operating frequencies is illustrated in fig. 69 (b).
The corresponding energy efficiency of the transformer for various air gaps is illustrated in fig.70. From this figure, it can be observed that the energy efficiency of the transformer with a 0mm air gap is higher when compared to other cases, as is expected. In the frequency range of 1 – 3MHz, the efficiency is low due to the characteristics of the NiZn-4F1 core material, as discussed earlier. For the entire frequency range, the losses in the transformer increase with the introduction of air gaps as the winding losses increase due to fringing effects [101], [102].

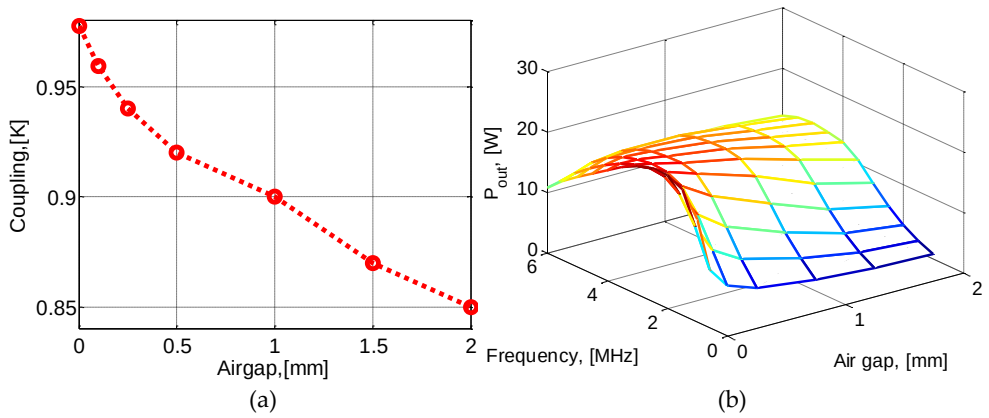

Figure 69. (a) Coupling coefficient and (b) power transferring capability of transformer for different air gaps

In order to make a fair comparison in the energy efficiency of the transformer with different air gaps, the energy efficiency is also measured at a constant load power of 15W and is depicted in fig.71 (a). From this figure, it can be observed that the maximum energy efficiency of the transformer is obtained for an air gap of 0mm whereas, it was reduced to 87% for an air gap of 2mm. However, when the air gap is varied from 0 to 0.25mm, the energy efficiency of the transformer is slightly

affected. Therefore, in order to avoid saturation in the low permeability core material, an air gap of up to 0.25mm can be introduced.

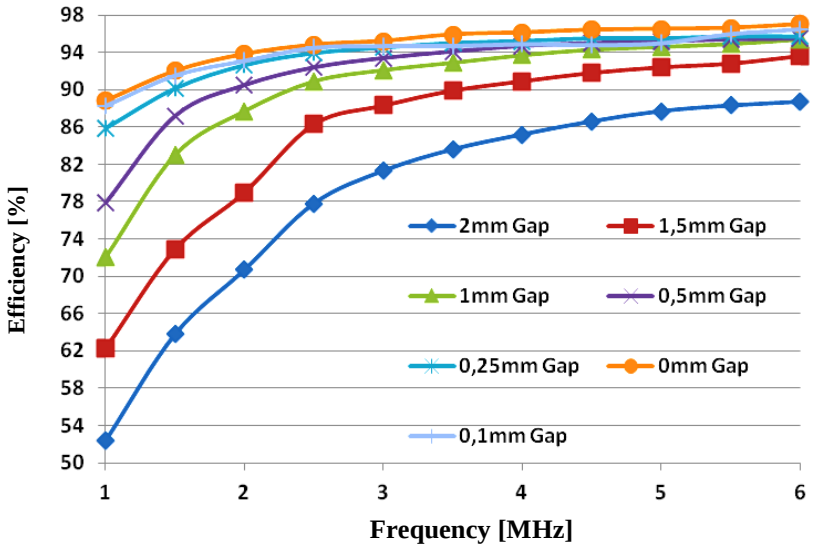

Figure 70. Energy efficiency of transformer as a function of frequency for different air gaps

The high frequency model of the transformer with different air gaps is placed in the multiresonant converter circuit and simulated for a load power of 15W [103]. The corresponding energy efficiency of the converter is illustrated in fig. 71 (b). Under these conditions, the switching frequency of the converter is varied from 2 – 3.75 MHz when the air gap is varied from 0 – 2mm respectively.

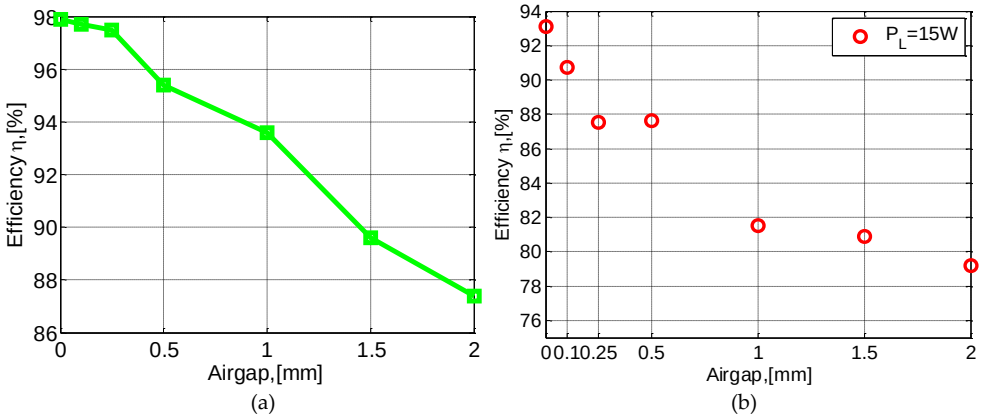

Figure 71. (a) Measured efficiency of transformer and (b) simulated energy efficiency of converter for different air gaps at P_L=15W

9 CUSTOM DESIGN POT CORE CENTER TAPPED TRANSFORMER

In the earlier chapter, the design and analysis of the pot core planar power transformer in the MHz frequency region have been discussed. The power density of the designed transformer, with standard pot cores half and a flat ferrite plate is 47W/cm^3. In order to further increase the power density of the transformer and the operating frequency region, a custom made pot core has been designed and evaluated. In this section, the design details of the core and the performance of the designed transformer will be discussed.

9.1 CORE AND WINDING GEOMETRY

In this section, the custom made core geometry and the winding strategy employed will be discussed.

9.1.1 Custom made core geometry

As discussed in the earlier chapter, the pot core possess good shielding characteristics compared to other available structures. Therefore, the pot core is considered for designing the high frequency transformer. Here, a solid center post is considered [94] since it generates less core loss and hence the temperature of the core can be reduced. By considering a round centre post, the winding losses of the transformer can be reduced by 11% when compared to a square centre post [94]. However, here, the semi-round center post is considered in order to have the provision for the vias on both sides of the transformer primary and secondary windings. This causes the windings to be more uniform (completely circular in shapes without any bend as in the previous transformer) on all sides of the core. The custom made pot core design is shown in fig. 72.

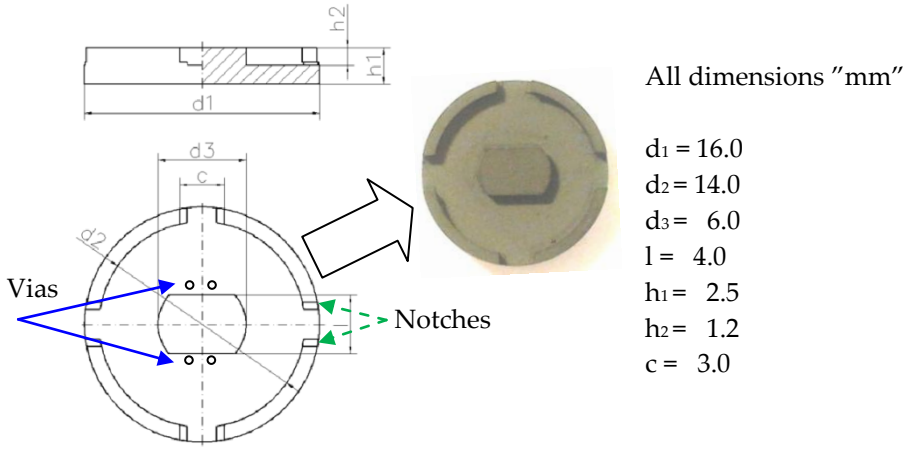

Figure 72. Dimensions of custom made pot core

In this core, it can be observed that 4 slots are provided unlike the previous case where there are only 2 slots. This is in order to provide a better thermal dissipation when compared to the option with only 2 slots. In addition to this, by having 4 slots, the windings can be tapped at different slots when there is a requirement for ½ or ¼ turns which is highly beneficial for auxiliary winding. The diameter and the height of the designed core half are 16 and 2.5mm respectively. The effective length and area of cross section (l_e/A_e) of the core are 15.3mm and 30.3mm^2 respectively resulting in the core volume (V_e) of 464mm^3. In the designed core, the notches were provided on four sides as shown in fig.72 in order to offer a better alignment of the core halves on both sides of PCB.

9.1.2 Winding configuration and transformer prototype

The winding configuration is the same as that described in an earlier chapter and a corresponding 3D view of the transformer is illustrated in fig.73 (a). The windings are circular spiral in shape without any bends, unlike the previous one, due to the change in the shape of the core center post. The inner/outermost radii of the designed transformer are 3.7/6mm respectively. The prototype of the designed transformer is depicted in fig.73 (b).

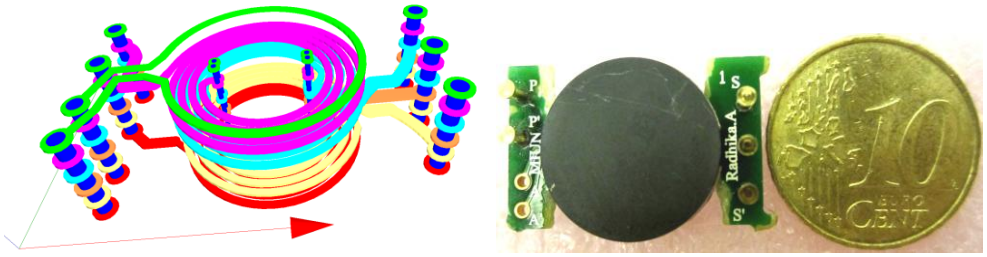

Figure 73. (a) 3D view and (b) prototype of custom made high performance transformer

9.2 ELECTRICAL PARAMETERS OF TRANSFORMER

The measured primary/secondary DC resistances of the transformer are 0.23/0.08Ω respectively and the measured AC resistance, which is increasing in nature, is shown in fig.74. The electrical parameters of the designed transformer, obtained from the sine phase impedance analyzer at 5MHz, are given in table. 10.

Table 10. Measured electrical parameters at 5MHz

R_p[Ω]	R_s [Ω]	L_p[μH]	L_{lk}[μH]	L_{s1}[μH]	C_{ps}[pF]
0.76	0.1	6.79	0.21	0.42	18.5

The calculated coupling coefficient, obtained from measured parameters in this case, is 0.98.

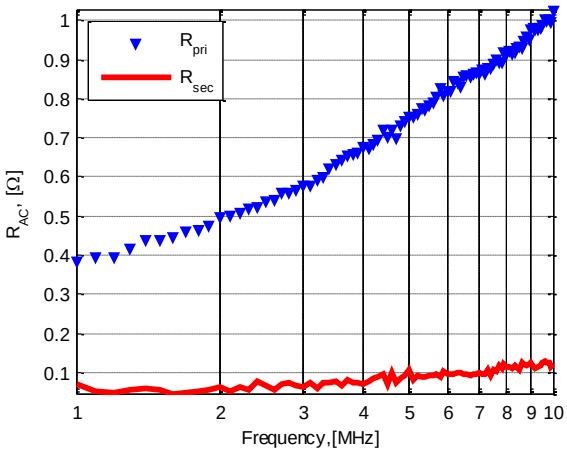

Figure 74. Measured primary/secondary AC resistance of high performance transformer

9.2.1 Efficiency as a function of frequency and load power

The energy efficiency of the transformer is measured by employing the procedure mentioned in chapter 2 and it is illustrated as a function of frequency in fig.75 (a). Here, the load power is maintained at a constant value of 10W for the entire frequency range. From this figure, it can be observed that the energy efficiency is comparatively low in the lower operating frequency region due to the 4F1 material characteristics. Under these conditions, the temperature of the transformer was also measured and is also illustrated in fig. 75(a). From this fig., it can also be observed that the high temperatures of the transformer are recorded for the lower operating frequency region due to the increased core losses.

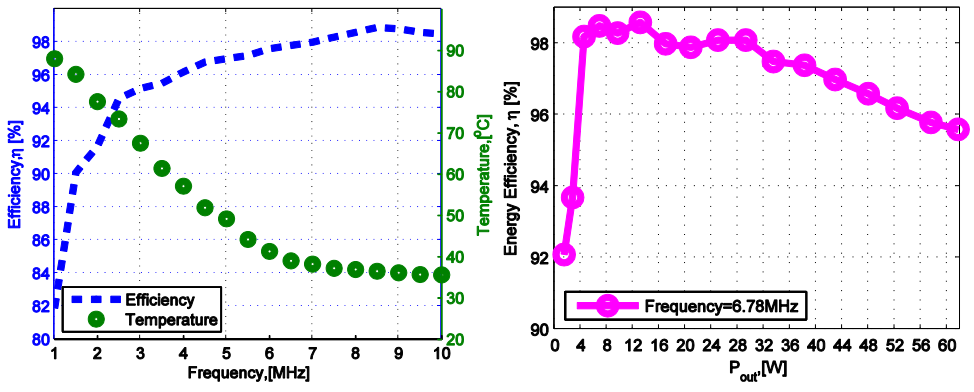

(a) (b)

Figure 75. Measured transformer efficiency as a function of (a) frequency and (b) load power

Here, it can be observed that the energy efficiency of the transformer is high in the frequency range of 5 – 10 MHz. Therefore, the power tests were carried out for the

designed power transformer at a frequency of 6.78MHz and the measured efficiency as a function of load power is illustrated in fig. 75(b).

The peak energy efficiency of the transformer is reported to be 98.5% at the power level of 12W. With the maximum tested power level of 62W at 6.78MHz, the power density of the transformer is obtained as 67.1W/cm^3. Under these conditions, the energy efficiency of the transformer is around 95.8% and is shown in fig. 75(b).

9.2.2 Thermal profile of transformer

When the transformer primary is excited, using a sinusoidal voltage of 106V_{rms}, the secondary voltage/current of the transformer is obtained as 24.8 V_{rms} and 2.33A respectively. Under these conditions, the input/output powers of the transformer are 60.4/58W respectively. The corresponding thermal profile of the transformer is shown in fig.76.

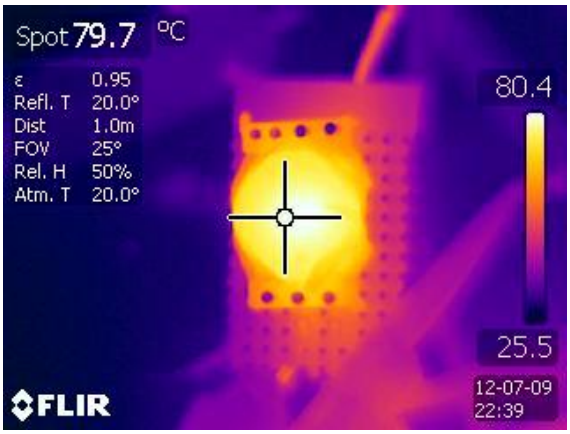

Figure 76. Thermal profile of high performance transformer at 58W and 6.78MHz

Here, the ambient temperature of the transformer is 25^{o}C, resulting in the temperature gradient being 54.7^{o}C. The copper losses of the transformer under these conditions, obtained by knowing the AC resistance of the transformer, are 1.01W. The remaining losses of 1.39W were contributed by the core losses of the transformer. Under, these conditions the peak energy efficiency of the transformer is reported as 96%. Since the optimal performance of the transformer is obtained at a high frequency of 6.78MHz, the transformer can be utilized together with the existing high performance GaN HEMTs for building the low profile energy efficient DC-DC converters. Therefore, the designed transformer was also placed in class E resonant converter and the simulations were carried out at 5MHz. For the output power level of 18W, the simulated energy efficiency of the converter is reported to be 88%. By replacing the secondary side rectifier with the high performance GaN HEMT, the isolated class E resonant converter can be operated

at 6.78MHz which can be useful for many applications. In addition to this, the designed transformer can also be utilized for wireless energy transfer applications as an impedance matching transformer.

10 SUMMARY OF PUBLICATIONS AND AUTHORS CONTRIBUTION

10.1 SUMMARY OF PUBLICATIONS

Paper I: This paper deals with the design and analysis of two layered and three layered coreless PCB step-down power transformers operating in the MHz frequency region. The designed transformers were characterized and compared for the given power transfer application. From this work, the conclusion to be drawn is that, for the same power transfer application, a three layered coreless PCB transformer performance is better in comparison to that of the two layered transformer because of the increased coupling coefficient and the reduced AC resistance, despite the increased inter-winding capacitance. Due to these reasons, the energy efficiency of the three layered transformer was improved by 3% when compared to two layered transformer.

Paper II: In this paper, the design and performance analysis of the two different transformers of the same series (same width, track separation and copper height with different no. of turns) were presented. The modelling procedure, in order to obtain the actual parameters of the transformers, was described. The designed transformers have been tested for the output power levels up to 30W and the energy efficiency of these transformers is found to be within the range of 90 - 97%. From the results presented in this paper, it can be observed that the coreless PCB step down 2:1 transformers, which are highly energy efficient in nature in the MHz frequency region, can replace the existing core based transformer in order to achieve the stringent height, low profile converters. Here, the application potentials of the designed transformers are also discussed.

Paper III: The radiated emissions of two layered and multilayered transformers were estimated and compared in this paper. The calculations were made according to antenna theory at a load power of 20W, for both sinusoidal and square wave excitations. It can be concluded from the results that the multilayered coreless PCB transformers have a low radiated EMI compared to the two layered transformer for the given power due to the reduction in the area of the transformer in the former case. In addition, for the sinusoidal excitation, the radiated power obtained is low compared to that of the square wave excitation. From the results obtained it can also be concluded that these coreless PCB transformers are best suited to resonant converter topologies in terms of EMI emissions.

Paper IV: In this paper, the guidelines for designing the coreless PCB step down transformer for the given power transfer application and the signal transformer for driving the high side MOSFET in double ended converter topologies is proposed. Based upon the proposed design guidelines, a multilayered half bridge center tapped transformer of 4:1:1 step down transformer was designed. Its parameters

were extracted, and performance analyses, such as input impedance, energy efficiency as a function of frequency and load power were presented. The power transformer was characterized up to a power level of 50W with the energy efficiency range of 87 – 96% at an operating frequency of 2.6MHz. The achieved power density of the transformer for the maximum tested load power is 107W/cm^3. Both the designed signal and power transformers were evaluated in the series resonant converter in the switching frequency range of 2.4 – 2.75MHz. The converter was simulated and tested up to a power level of 34.5W with the maximum converter energy efficiency at these operating frequencies being 86.5%. From the results shown in this paper, it can be concluded that it is feasible to obtain energy efficient power converters using coreless PCB transformer technology for low power applications.

Paper V: In this paper, the effect of a dielectric material on the performance of a printed circuit board transformer in the MHz frequency region was analyzed and presented. In this regard, two transformers on different dielectric materials were designed and analyzed. The finite element analysis (FEA) was conducted for both transformers using Ansoft simulation software in terms of magnetic field intensity and current density distribution. The parameters of the designed transformers were extracted using a network analyzer. The transformer performance was also analyzed by conducting power tests using an RF power amplifier. Finally, the results of the paper show that the energy efficiency of the transformer with a high frequency dielectric material i.e., Rogers 4450B is higher compared to the transformer with a traditional FR-4 material. The high frequency dielectric material possess a low dielectric constant due to which, the overall performance of the transformers was improved. The indirect effect of the dielectric fields on the current density distribution and magnetic field intensity were observed. Therefore, it can concluded that with the assistance of a high frequency dielectric laminate, the energy efficiency of the next generation power transformers (both coreless and core based transformers) suitable for SMPS applications can be enhanced at higher operating frequencies.

Paper VI: In this paper, a novel high frequency core based power transformer operating in the MHz frequency region was designed and analyzed. A hybrid core structure consisting of standard pot core half of 18x11 and a flat ferrite plate was considered in order to have excellent shielding characteristics in the MHz frequency of operation. The designed center tapped 4:1:1 power transformer has been characterized at a frequency of 3MHz up to a power level of 50W with the achieved transformer power density being 47W/cm^3. The peak energy efficiency of the transformer is reported to be 98% in the frequency range of 1 – 5 MHz. The designed power transformer has been evaluated in a multiresonant half bridge converter using wide band gap material devices i.e., EPC corporations GaN

HEMTs. The converter has been evaluated in the switching frequency range of 3 – 4.5MHz up to a power level of 40W. Here, the converter is maintained to be operated in ZVS condition in order to achieve high energy efficiency for the converter. The maximum energy efficiency of the converter is reported to be 92% in the switching frequency range of 3 – 4.5MHz and the converter has been regulated to the output voltage of 15V for a DC input voltage of 90V. From the results of the paper, it can be concluded that high frequency highly energy efficient isolated converters can be realized with the assistance of the novel planar power transformer and the state-of-the-art GaN technology. For this contribution, this paper has been selected in relation to one of the three young engineer awards sponsored by ECPE, Mitsubishi Electric and Infineon technologies in PCIM conference held in Nuremberg, Germany, 2012.

Paper VII: It is required to have sufficient air gap in the transformer in order to achieve the ZVS of the transistors in the converter as well as to avoid the saturation of the core. Therefore, this paper discusses the effect of the air gap with regards to the low permeability material on the performance of a hybrid core planar power transformer designed for high frequency SMPS. The air gap effects in terms of the coupling coefficient, AC resistance and performance of the transformer were presented. From the obtained results, the optimal air gap required is proposed in terms of the energy efficiency of the transformers and converter as well as the saturation of the core.

Paper VIII: This paper provides the design guidelines of the novel hybrid core planar power transformer for a given power converter application. It also suggests the optimal core material required for the desired operating frequency region of the transformer and thereby the converter. The simulation and experiments were conducted on the multiresonant half bridge converter for laptop adapter application by considering the low line input voltage and the obtained results were presented. In addition to this, for the given application, the comparison has been made on both diode rectification and synchronous rectification in terms of energy efficiency, power density in the MHz frequency region and the optimum rectification method is proposed. The pulse skip modulation technique for improving the light load energy efficiency is explained analytically and the simulation results for the considered converter specifications are presented.

Paper IX: In this paper a record power density transformer using a custom made core design has been presented. The designed transformer has been characterized in the frequency region of 1 – 10MHz. It has been characterized up to the power level of 62W at an operating frequency of 6.78 MHz. The power density of the designed high performance transformer is reported to be ~67.1W/cm^3 at the maximum tested power level of 62W and the maximum energy efficiency is

reported to be 98.5%. Its performance is evaluated by considering class E resonant converter topology. The simulation results show that for the output power level of 18W, the simulated energy efficiency of the converter at the switching frequency of 5MHz using GaN HEMTs is reported to be 88.5%. The paper emphasises the feasibility in relation to the development of the next generation high power density, low profile, highly energy efficient isolated converters.

10.2 AUTHORS CONTRIBUTIONS

The contributions of authors for the following nine papers in this thesis are summarized in table 11. In this table M and C represent the main author and co-author respectively.

Table 11. Author's Contribution

Paper	*RA*	*HK*	*SH*	*KB*	**Contributions**
I	M	C	-	C	**RA:** Estimation of inductive, resistive and capacitive parameters using MATLAB code, design and modelling of transformers, power tests of transformers, experiments and results **HK:** Modelling, analysis and discussion on application potentials, review of paper **KB:** Review of paper and Supervision
II	M	C	-	C	**RA:** Design and modelling of transformers, characterization of transformers and experimental analysis **HK:** Idea of comparing two different layer transformers, Suggestions, characterization of transformer using power amplifier and analysis, review of paper **KB:** Review of paper and Supervision
III	M	C	-	C	**RA:** Design of transformers, Implementation of MATLAB code for EMI calculations and analyzing the theoretical and experimental results **HK:** Implementation of idea using different transformers, discussions and suggestion of topology for the designed transformers based on the results obtained, review of paper **KB:** Idea, review of paper and supervision
IV	C	M	-	C	**RA:** Proposal of design guidelines for both the power and signal transformers, analysis of the designed transformers, parameter extraction and experimental analysis of transformer in converter circuit, review of paper **HK:** Implementation of series resonant converter topology, theoretical, simulation and experimental analysis of the designed converter and loss estimation **KB:** Review of paper and supervision

V	M	C	-	C	**RA:** Design of transformers by considering two different dielectric materials, testing and analysis of the result. **HK:** Discussions, analysis and review of paper **KB:** Review of paper and supervision
VI	C	M	C	C	**RA:** Design of novel planar transformer and secondary inductor, parameter extraction, power tests of designed power transformer and review of paper **HK:** Design and analysis of multiresonant converter, implementation and optimization of code using dsPIC microcontroller for optimized dead time between gate drive signals of main GaN HEMTs and synchronous devices (GaN HEMTs) to obtain high energy efficiency, experimental evaluation of the designed multiresonant converter **SH:** PCB Design and selection of high speed digital optocoupler **KB:** Supervision and review of paper
VII	M	C	-	C	**RA:** Design of planar transformer and analyzing the effect of air gaps on the performance of transformer in terms of energy efficiency. Also analyzing its performance in half bridge resonant converter topology **HK:** Analysis of the effect of air gap on the performance of converter, simulation of the converter, review of paper **KB:** Supervision and review of paper
VIII	C	M	-	C	**RA:** Proposal of the design guidelines for the power transformer for a given power transfer application, Selection of core material for the given switching frequency of power converter, review of paper **HK:** Simulation, theoretical and experimental analysis of multiresonant converter, comparison between synchronous and diode rectification and discussion of results **KB:** Supervision and review of paper
IX	M	C	-	C	**RA:** Design and characterization of high performance transformer **HK:** Simulation and theoretical analysis of class E resonant converter and discussion of results, implementation of PSM technique and discussion of results, review of paper **KB:** Supervision and review of paper
	1. Radhika Ambatipudi (RA) 2. Hari Babu Kotte (HK) 3. Kent Bertilsson (KB) 4. Stefan Haller (SH)				

11 SUMMARY OF THESIS, CONCLUSIONS AND FUTURE WORK

Initially, the design and analysis of two layered and three layered coreless PCB step-down transformers operating in the MHz frequency region for a given power transfer application have been discussed. The conclusion to be drawn from the work presented in this chapter is that for the same power transfer application, a three layered transformer is better in comparison to that of the two layered transformer because of the increased coupling coefficient and the reduced AC resistance. The energy efficiency of the three layered transformer was improved by 3% and the area of the transformer was reduced by 32% as compared to that of the two layered transformer.

A set of 4 different transformers have been designed for determining the optimized transformer in terms of coupling coefficient and AC resistance for a given power transfer application. A detailed modelling procedure was proposed in order to determine the actual electrical parameters of the coreless PCB step down transformers. Since, these transformers possess high energy efficiencies; they have been compared with the existing core based counterparts for the same power transfer application. From the comparison between these designed transformers and the existing core based transformers, it can be concluded that a vast volume reduction can be obtained for the given power transfer application.

From the estimated radiated EMI emissions in case of two layered and three layered transformers, it can be concluded that the multilayered coreless PCB transformers have a low radiated EMI compared to the two layered transformer for the given power transfer application due to a reduction in the area of the transformer. In addition to this, for the sinusoidal excitation, the radiated power obtained is low compared to that of the square wave excitation. This shows that these coreless PCB transformers are best suited for resonant converter topologies where the power is processed in a sinusoidal manner in terms of EMI emissions.

The design procedure for the signal and power transformer using 'coreless PCB transformer technology' have been proposed and evaluated the designed transformers successfully in double ended converter topologies. The design guidelines proposed for these transformers can be useful to the practising designers/engineers in order to build the low profile converters.

The investigations were carried out on different dielectric materials influence on the performance of the planar transformers operating in MHz. From the results obtained, it can be concluded that the energy efficiency of the transformer with high frequency dielectric laminate is better when compared to that of the traditional FR-4 laminate.

In the latter part of the thesis, the design guidelines of the high frequency (1 – 10MHz) core based transformers using the existing core materials have been proposed and the designed transformers have been evaluated. The winding strategy suitable for transformers operating in MHz frequency region was proposed. The performance characteristics of the low permeability material pot core transformer w.r.t different air gaps was evaluated and the optimum air gap required for the given power transfer application was suggested. Further in order to increase the power density of the transformer, the custom made pot core transformer was designed and its design details are covered in the thesis.

11.1 CONCLUSION

The first part of the work presented in the thesis has dealt with the design, development and characterization of multilayered coreless PCB power/signal transformers, suitable for ultra low profile SMPS with high power density and high energy efficiency. For the very stringent height applications, the designed multilayered coreless PCB transformers can be utilized.

In the second part of the thesis, the work was focussed on the design and development of miniaturized novel core based transformers operating in the 1 - 10 MHz frequency region with record power densities of 67.1W/cm^3 and high energy efficiency, which are useful for both DC/DC and AC/DC converter applications.

11.2 FUTURE WORK

The coreless PCB step down power transformers discussed in the thesis possess high power density and high energy efficiency. However, in order to commercialize these transformers for some of the consumer applications in future, it is necessary to measure the EMI emissions from these transformers. When these transformers are utilized in the converter circuits, if the emissions are not within the FCC and CISPR limits, it is required to shield them using the low loss (flexible and thin sheets) ferrite polymer composite sheets or EMI absorbers of optimal thickness in order to suppress the emissions.

In this thesis, the winding strategies in terms of conventional solid winding and parallel winding were studied in MHz frequency region. However, in future, the work can be further extended to realize the circular spiral litz winding structure in order to further minimize the AC resistance of the winding and thereby the energy efficiency of transformers and converters can be improved.

12 REFERENCES

[1] Lee, C.K.; Su, Y.P.; Hui, S.Y.R., "Printed Spiral Winding Inductor with Wide Frequency Bandwidth," *Power Electronics, IEEE Transactions on*, vol.26, no.10, pp.2936, 2945, Oct. 2011.

[2] Erkmen, B.; Demirel, I., "A Very Low Profile Dual Output LLC Resonant Converter for LCD/LED TV Applications," *Power Electronics, IEEE Transactions on*, vol.PP, no.99, pp.1, 1, 0.

[3] Oeder, C., "Analysis and design of a low-profile LLC converter," *Industrial Electronics (ISIE), 2010 IEEE International Symposium on*, vol., no., pp.3859, 3864, 4-7 July 2010.

[4] Wong, Fu Keung, "High Frequency transformers for switch mode power supplies'', PhD thesis, Griffith University, 2004.

[5] Glaser, J.S.; Rivas, J.M.; , "A 500 W push-pull dc-dc power converter with a 30 MHz switching frequency," *Applied Power Electronics Conference and Exposition (APEC), 2010 Twenty-Fifth Annual IEEE* , vol., no., pp.654–661, 21–25 Feb. 2010.

[6] Quinn, C.; Rinne, K.; O'Donnell, T.; Duffy, M.; Mathuna, C.O.;, "A review of planar magnetic techniques and technologies," *Applied Power Electronics Conference and Exposition, 2001. APEC 2001. Sixteenth Annual IEEE*, vol.2, no., pp.1175-1183 vol.2, 2001.

[7] Katayama, Y.; Sugahara, S.; Nakazawa, H.; Edo, M.; "High-power-density MHz-switching monolithic DC-DC converter with thin-film inductor," *Power Electronics Specialists Conference 2000. PESC 00. 2000 IEEE 31st Annual*, vol.3, no., pp.1485–1490.

[8] Perreault, D.J.; Jingying Hu; Rivas, J.M.; Yehui Han; Leitermann, O.; Pilawa-Podgurski, R.C.N.; Sagneri, A.; Sullivan, C.R., "Opportunities and Challenges in Very High Frequency Power Conversion," *Applied Power Electronics Conference and Exposition, 2009. APEC 2009. Twenty-Fourth Annual IEEE*, vol., no., pp.1, 14, 15-19 Feb. 2009.

[9] Shu Ji; Reusch, D.; Lee, F.C., "High-Frequency High Power Density 3-D Integrated Gallium-Nitride-Based Point of Load Module Design," *Power Electronics, IEEE Transactions on*, vol.28, no.9, pp.4216, 4226, Sept. 2013.

[10] W. G. Hurley, W. H. Wölfle, "Transformers and Inductors for Power Electronics: Theory, Design and Applications", John Wiley & Sons, 2013.

[11] Bo Yang, "Topology investigation of front end DC/DC converter for distributed power system", PhD thesis, 2003 Virginia Polytechnic Institute and State University, USA.

[12] Colonel William, T. Mc Lyman, "Transformer and Inductor design Handbook''; Marcel Dekker, Inc., 3rd edition, 2004, ISBN: 0-8247-5393-3.

[13] Lim, M.H.; Van Wyk, J.D.; Lee, F.C.; Ngo, K. D T, "A Class of Ceramic-Based Chip Inductors for Hybrid Integration in Power Supplies," *Power Electronics, IEEE Transactions on* , vol.23, no.3, pp.1556,1564, May 2008.

[14] Shenai, K.; Shah, K.; Huili Xing, "Performance evaluation of silicon and gallium nitride power FETs for DC/DC power converter applications," *Aerospace and Electronics Conference (NAECON), Proceedings of the IEEE 2010 National* , vol., no., pp.317,321, 14-16 July 2010.

[15] Ashot Melkonyan,"High Efficiency Power Supply using new SiC devices", PhD dissertation, 2007, University of Kassel.

[16] Omura, I.; Saito, W.; Domon, T.; Tsuda, K., "Gallium Nitride power HEMT for high switching frequency power electronics," *Physics of Semiconductor Devices, 2007. IWPSD 2007. International Workshop on*, vol., no., pp.781, 786, 16-20 Dec. 2007.

[17] Nihal Kularatna, "Power Electronics Design Handbook, Low-Power Components and Applications", 1998, ISBN-10:0750670738, Butterworth-Heinemann Publications, pp.116.

[18] Xose M.Lopez-Fernandez, H.Bulent Ertan, Janusz Turowski, "Transformers: Analysis, Design and Measurement", CRC Press, 2013, ISBN: 978-1-4665-0824-8.

[19] S. Hayano, Y.Nakajima, H. Saotome, and Y. Saito, "A New Type High Frequency Transformer", *IEEE Transactions on Magnetics, vol. 27, no. 6,November 1991, pp.5205–5207.*

[20] I. Marinova, Y.Midorrikawa, S.Hayano, and Y. Saito, "Thin Film Transformer and Its Analysis by Integral Equation Method'', IEEE Transactions on Magnetics, vol.31, no.4, July 1995, pp.2432-2437.

[21] Hui, S.Y.R.; Chung, H.; Tang, S. C., "Coreless PCB-based transformers for power MOSFET/IGBT gate drive circuits," *Power Electronics Specialists Conference, 1997. PESC '97 Record., 28th Annual IEEE*, vol.2, no., pp.1171, 1176 vol.2, 22-27 Jun 1997.

[22] Hui, S.Y.R.; Chung, H.; Tang, S. C., "Coreless Printed Circuit Board (PCB) Transformers – Fundamental Characteristics and Application Potential", *IEEE Circuits and Systems Society Newsletter, vol.11, no.3.,third quarter, 2000, ISSN:1049-3654,pp.3-15.*

[23] Tang, S. C.; Hui, S.Y.R.; Chung, H.S.-H., "Coreless planar printed-circuit-board (PCB) transformers-a fundamental concept for signal and energy transfer," *Power Electronics, IEEE Transactions on, vol.15, no.5, pp.931, 941, Sep 2000.*

[24] Hui, S.Y.R.; Tang, S. C.; Chung, H.S.-H., "Some electromagnetic aspects of coreless PCB transformers," *Power Electronics, IEEE Transactions on, vol.15, no.4, pp.805, 810, Jul 2000.*

[25] Tang, S. C.; Hui, S.Y.R.; Chung, H., "Coreless printed circuit board (PCB) transformers with high power density and high efficiency," *Electronics Letters, vol.36, no.11, pp.943, 944, 25 May 2000.*

[26] Dallago, E.; Passoni, M.; Venchi, G., "Design and optimization of a high insulation voltage DC/DC power supply with coreless PCB transformer," *Industrial Technology, 2004. IEEE ICIT '04. 2004 IEEE International Conference on*, vol.2, no., pp.596, 601 Vol. 2, 8-10 Dec. 2004.

[27] Bouabana, A.; Sourkounis, C., "Design and analysis of a coreless flyback converter with a planar printed-circuit-board transformer," *Optimization of Electrical and Electronic Equipment (OPTIM), 2010 12th International Conference on*, vol., no., pp.557, 563, 20-22 May 2010.

[28] Bouabana, A.; Sourkounis, C.; Mallach, M., "Implementation of different layouts of a coreless planar transformer for a flyback converter," *IECON 2012 - 38th Annual Conference on IEEE Industrial Electronics Society*, vol., no., pp.483, 487, 25-28 Oct. 2012.

[29] Meyer, P.; Germano, P.; Perriard, Y., "FEM modeling of skin and proximity effects for coreless transformers," *Electrical Machines and Systems (ICEMS), 2012 15th International Conference on*, vol., no., pp.1, 6, 21-24 Oct. 2012.

[30] *4F1 from Ferroxcube*, 2008, pp. 251-253. http://www.elnamagnetics.com/wp-content/uploads/library/Ferroxcube-Materials/4F1_Material_Specification.pdf, last accessed, 27th August 2013.

[31] Wang, Yin; Kim, Woochan; Zhang, Zhemin; Calata, Jesus; Ngo, Khai D.T, "Experience with 1 to 3 megahertz power conversion using eGaN FETs," *Applied Power Electronics Conference and Exposition (APEC), 2013 Twenty-Eighth Annual IEEE* , vol., no., pp.532,539, 17-21 March 2013.

[32] Tang, S. C.; Hui, S.Y.R.; Chung, H.S.-H., "A low-profile wide-band three-port isolation amplifier with coreless printed-circuit-board (PCB) transformers," *Industrial Electronics, IEEE Transactions on , vol.48, no.6, pp.1180,1187, Dec 2001*

[33] Tang, S. C.; Hui, S.Y.; Henry Shu-Hung Chung, "A low-profile low-power converter with coreless PCB isolation transformer," *Power Electronics, IEEE Transactions on, vol.16, no.3, pp.311, 315, May 2001.*

[34] Tang, S. C.; Hui, S.Y.R.; Chung, H.S.-H., "A low-profile power converter using printed-circuit board (PCB) power transformer with ferrite polymer composite," *Power Electronics, IEEE Transactions on , vol.16, no.4, pp.493,498, Jul 2001.*

[35] C.F.Coombs, "Printed Circuits handbooks" 5th Edition, McGraw-Hill, August 27, 2001.

[36] U.S. Patenet 5,990,776, "Low Noise Full Integrated Multilayers Magnetic for Power Converters", I. Jitaru, November 23, 1999.

[37] S.Y.R Hui, S.C. Tang, and H.Chung, "Characterization of Coreless Printed Circuit Board (PCB) Transformers", *IEEE Transactions on Power Electronics, Vol. 15, No. 6, November 2000.*

[38] Kawabe, K.; Koyama, H.; Shirae, K., "Planar inductor," *Magnetics, IEEE Transactions on* , vol.20, no.5, pp.1804,1806, Sep 1984.

[39] Jonsenser Zhao, "A new calculation for designing multilayer planar spiral inductors", July 29, 2010, http://www.edn.com/design/components-and-packaging/4363548/A-new-calculation-for-designing-multilayer-planar-spiral-inductors, last accessed: 30th August 2013.

[40] Sunderarajan S. Mohan, "The Design, Modeling and optimization of On-Chip Inductor and Transformer Circuits", *PhD. Dissertation, Stanford University, USA, 1999.*

[41] Al M. Niknejad, "Analysis, Simualtion, and Applications of Passive Devices on Conductive Substrates", *PhD. Dissertation, University of California, Berkeley, 2000.*

[42] W.G. Hurley and M.C. Duffy, 'Calculation of self and mutual impedances in planar magnetic structures', *IEEE Transactions on Magnetics, Vol.33, No. 3, May 1997,pp.2282- 2290.*

[43] Hurley, W.G.; Duffy, M.C.; O'Reilly, S.; O'Mathuna, S.C., "Impedance formulas for planar magnetic structures with spiral windings," Industrial Electronics, *IEEE Transactions on, vol.46, no.2, pp.271, 278, Apr 1999.*

[44] Su, Y.P.; Xun Liu; Hui, S.Y.R., "Extended Theory on the Inductance Calculation ofPlanar Spiral Windings Including the Effectof Double-Layer Electromagnetic Shield," *Power Electronics, IEEE Transactions on, vol.23, no.4, pp.2052, 2061, July 2008.*

[45] Fernandez, C.; Prieto, R.; Garcia, O.; Herranz, P.; Cobos, J.A.; Uceda, J., "Modelling core-less high frequency transformers using finite element analysis," *Power Electronics Specialists Conference, 2002. pesc 02. 2002 IEEE 33rd Annual, vol.3, no., pp.1260, 1265 vol.3, 2002.*

[46] Chan, P. C F; Lee, C.K.; Hui, S.Y.R., "Stray capacitance calculation of coreless planar transformers including fringing effects," *Electronics Letters* , vol.43, no.23, pp.,, Nov. 8 2.

[47] Heng-Ming Hsu, "Effective series-resistance model of spiral inductors", *Microwave and Optical technology letters, vol.46, No.2, July 20, 2005. pp. 107-109*.

[48] Ferreira, J.A., "Improved analytical modeling of conductive losses in magnetic components," *Power Electronics, IEEE Transactions on, vol.9, no.1, pp.127, 131, Jan 1994.*

[49] Ouyang, Ziwei; Thomsen, O.C.; Andersen, M. A E, "Optimal Design and Tradeoff Analysis of Planar Transformer in High-Power DC–DC Converters," *Industrial Electronics, IEEE Transactions on, vol.59, no.7, pp.2800, 2810, July 2012.*

[50] Marian K. Kazimierczuk, "High-Frequency Magnetic Components", 2nd Edition, Wiley publications, 2011, ISBN-13:978-0470714539.

[51] Alex Van den Bossche and Vencislav Cekov Valchev, "Inductors and Transformers for Power Electronics"1st Edition, CRC Press, March24, 2005.

[52] Tektronix, 'AC Current Probes' CT1.CT2.CT6 Datasheet, June 2009.
[53] Tektronix, 'Passive 1x/10x Voltage Probe', P2220. P2221 Datasheet, June 2009.
[54] www.coilcraft.com
[55] T.C.Lun, "Designing for Board Level Electromagnetic Compatibility", Freescale Semiconductor, Application note: AN2321, 2005.
[56] C.A.Balanis, "Antenna Theory, Analysis and Design", New York, John Wiley & Sons.
[57] K.F.Lee, "Principles of Antenna Theory", John Wiley & Sons Limited, 1984.
[58] Vasic, F. Costa, E. Sarraute, Comparing piezoelectric and coreless electromagnetic transformer approaches in IGBT driver, The European Physical Journal - Applied Physics (EPJAP), *Eur. Phys. J. Appl. Phys. 34, 237-242, June 2006.*
[59] High-Speed Half-Bridge MOSFET Drivers datasheet from Maxim Integrated, http://www.maxim-ic.com/pst/run.mvp?q=MAX15018, last accessed: 31st August 2013.
[60] Hui, S.Y.R.; Chung, H.S.-H.; Tang, S. C., "Coreless printed circuit board (PCB) transformers for power MOSFET/IGBT gate drive circuits," *Power Electronics, IEEE Transactions on*, vol.14, no.3, pp.422, 430, May 1999.
[61] Dai, N.; Lofti, A. W.; Skutt, G.; Tabisz, W.; Lee, F.C., "A comparative study of high-frequency, low-profile planar transformer technologies," *Applied Power Electronics Conference and Exposition, 1994. APEC '94. Conference Proceedings 1994., Ninth Annual*, vol., no., pp.226, 232 vol.1, 13-17 Feb 1994.
[62] Bourgeois, J.M., "PCB based transformer for power MOSFET drive," *Applied Power Electronics Conference and Exposition, 1994. APEC '94. Conference Proceedings 1994., Ninth Annual*, vol., no., pp.238, 244 vol.1, 13-17 Feb 1994.
[63] Yamaguchi, K.; Ohnuma, Shigehiro; Imagawa, Takao; Toriu, J.; Matsuki, H.; Murakami, K., "Characteristics of a thin film microtransformer with circular spiral coils," *Magnetics, IEEE Transactions on* , vol.29, no.5, pp.2232,2237, Sep 1993.
[64] Jesus Doval-Gandoy, Moises Pereira Martinez, "Isolated MOSFET driver has wide duty-cycle range", Spain, http://m.eet.com/media/1137551/42904di.pdf, last accessed: 31st August 2013.
[65] Hui, S.Y.; Tang, S. C.; Chung, H.S.-H., "Optimal operation of coreless PCB transformer-isolated gate drive circuits with wide switching frequency range," *Power Electronics, IEEE Transactions on* , vol.14, no.3, pp.506,514, May 1999.
[66] Tang, S. C.; Hui, S.Y.; Chung, H.S.-H., "Coreless printed circuit board (PCB) transformers with multiple secondary windings for complementary gate drive circuits," *Power Electronics, IEEE Transactions on* , vol.14, no.3, pp.431,437, May 1999.

[67] Majid, A.; Kotte, H.B.; Saleem, J.; Ambatipudi, R.; Haller, S.; Bertilsson, K., "High frequency half-bridge converter using multilayered coreless Printed Circuit Board step-down power transformer," *Power Electronics and ECCE Asia (ICPE & ECCE), 2011 IEEE 8th International Conference on* , vol., no., pp.1177,1181, May 30 2011-June 3 2011.

[68] Kotte, H.B.; Ambatipudi, R.; Bertilsson, K., "High-Speed (MHz) Series Resonant Converter (SRC) Using Multilayered Coreless Printed Circuit Board (PCB) Step-Down Power Transformer," *Power Electronics, IEEE Transactions on*, vol.28, no.3, pp.1253, 1264, March 2013.

[69] A. K. Hari, "Voltage-mode push-pull converters deserve a second look", *Power Electron.Technol.*, pp.14-19, March 2009.

[70] Bob Bell (2006), "Half-bridge topology finds high-density power converter apps", USA, http://www.eetimes.com/document.asp?doc_id=1273093, last accessed: 31st August 2013.

[71] Nihal Kularatna, "Power Electronics Design Handbook, Low-Power Components and Applications", pp. 69-70, Newnes publications, 1998, ISBN: 0-7506-7073-8.

[72] SwitchMode™ power supplies, reference manual and design guide, pp.9, July 2002. Available: http://www.onsemi.com/pub_link/Collateral/SMPSRM-D.PDF, last accessed: 31st August 2013.

[73] Marty Brown, "Power supply cookbook", Second edition, pp: 29, Newnes publications, 2001, ISBN: 0-7506-7329-X

[74] Matsuura, K.; Yanagi, H.; Tomioka, S.; Ninomiya, T., "Power-density development of a 5MHz-switching DC-DC converter," *Applied Power Electronics Conference and Exposition (APEC), 2012 Twenty-Seventh Annual IEEE*, vol., no., pp.2326, 2332, 5-9 Feb. 2012.

[75] Yipeng Su; Xun Liu; Chi Kwan Lee; Hui, S. Y., "On the relationship of quality factor and hollow winding structure of coreless printed spiral winding (CPSW) inductor," *Power Electronics, IEEE Transactions on* , vol.27, no.6, pp.3050,3056, June 2012.

[76] Dai, N.; Lee, F.C., "High-frequency eddy-current effects in low-profile transformer windings," *Power Electronics Specialists Conference, 1997. PESC '97 Record., 28th Annual IEEE*, vol.1, no., pp.641, 647 vol.1, 22-27 Jun 1997.

[77] Kotte, H.B.; Ambatipudi, R.; Bertilsson, K., "High-Speed (MHz) Series Resonant Converter (SRC) Using Multilayered Coreless Printed Circuit Board (PCB) Step-Down Power Transformer," *Power Electronics, IEEE Transactions on, vol.28, no.3, pp.1253, 1264, March 2013.*

[78] Colotti, J., "Analog, RF & EMC considerations in printed wiring board design," *Long Island Systems, Applications and Technology, 2005. IEEE Conference*, vol., no., pp.16, 30, 6 May, 2005.

[79] John,C.(2010), Rogers Corporation, FR-4 Versus High Frequency Laminates, http://mwexpert.typepad.com/rog_blog/2010/08/fr4-versus-highfrequency-laminates.html, last accessed on 1st September 2013.

[80] RO4400™ Datasheet,http://www.rogerscorp.com/documents/1850/acm/RO4400-Series-Prepreg-Data-Sheet-RO4450B-and-RO4450F-Prepregs.pdf,Rogers Corporation, last accessed on 1st September 2013.

[81] Pozar, D.M. (2005), Microwave Engineering, 3rd Edition New York: Wiley, pp.536-553.

[82] Biernacki, J.; Czarkowski, D., "High frequency transformer modeling," Circuits and Systems, 2001. ISCAS 2001. The 2001 IEEE International Symposium on , vol.3, no., pp.676,679 vol. 2, 6-9 May 2001.

[83] Damnjanovic, M.; Zivanov, L.; Radosavljevic, G.; Maric, A.; Menicanin, A., "Parameter extraction of ferrite transformers using S-parameters," *Power Electronics and Motion Control Conference (EPE/PEMC), 2010 14th International* , vol., no., pp.T8-31,T8-36, 6-8 Sept. 2010

[84] Kehrer, D.; Simburger, W.; Wohlmuth, H. -D; Scholtz, A.L., "Modeling of monolithic lumped planar transformers up to 20 GHz," Custom Integrated Circuits, 2001, IEEE Conference on. , vol., no., pp.401, 404, 2001.

[85] Radhika Ambatipudi, Hari Babu Kotte and Kent Bertilsson, " Effect of Dielectric Material on the Performance of Planar Power Transformers in MHz Frequency Region", Proceedings of *INDUCTICA 2012 Coil Winding, Insulation and Electrical Manufacturing International Conference and Exhibition (CWIEME), Berlin, Germany 26 – 28, June 2012*

[86] Meyer, C.D.; Bedair, S.S.; Morgan, B.C.; Arnold, D.P., "High-Inductance-Density, Air-Core, Power Inductors, and Transformers Designed for Operation at 100–500 MHz," *Magnetics, IEEE Transactions on*, vol.46, no.6, pp.2236, 2239, June 2010.

[87] Barnes.H, Moreira.J, McCarthy.T, Burns.W, Gutierrez.C, Resso.M (2008), ATE Interconnect Performance to 43Gbps Using Advanced PCB Materials, 1-24, DesignCon 2008.

[88] John Coonrod, Understanding When to Use FR-4 or High Frequency Laminates,pp.26-30. http://www.rogerscorp.com/documents/2122/acm/articles/Understanding-When-To-Use-FR-4-Or-High-Frequency-Laminates.pdf, last accessed on 1st September 2013.

[89] Datasheet, Ferroxcube 4F1 Material Specification, 01 September 2008, Available: http://www.ferroxcube.com/prod/assets/4f1.pdf, last accessed, 1st September 2013.

[90] Soft Ferrites, Ferrite material survey, 01 September 2008, Available: http://www.ferroxcube.com/prod/assets/sfmatgra_frnt.pdf, last accessed, 1st September 2013.

[91] Ferrite cores,http://www.kolektor.com/resources/files/doc/Pregled_izdelkov-feritna_jedra.pdf, last accessed, 1st September 2013.

[92] Lim, M. H F; Van Wyk, J.D., "Applying the Steinmetz Model to Small Cores in LTCC Ferrite for Integration Applications," *Applied Power Electronics Conference and Exposition, 2009, APEC 2009. Twenty-Fourth Annual IEEE*, vol., no., pp.1027, 1033, 15-19 Feb. 2009.

[93] Michele Hui Fern Lim, "Low temperature co-fired ceramics technology for power magnetics integration", PhD thesis, November 2008, Virginia Tech, Blacksburg, Virginia.

[94] Abraham I Pressman, "Switching Power Supply Design", Second edition, Tata Mc Graw Hill, 1998, pp.273.

[95] Ferrite Cores 2013 catalog from Magnetics Inc. pp.3. Available: http://www.mag-inc.com/products/ferrite-cores/ferrite-shapes/learn-more-shapes, last accessed, 1st September 2013.

[96] "Magnetic cores for switching power supplies" by Magnetics Inc., 2001.

[97] Hari Babu Kotte, Radhika Ambatipudi and Kent Bertilsson, "Design and Analysis of 45W Multi Resonant Half Bridge Converter in Mihs Frequency Region using GaN HEMTs", *Submitted for publication in Journal of Power Electronics (JPE), South Korea.*

[98] "A critical comparison of ferrites with other magnetic materials" by Magnetic Inc., 2000, last accessed: 1st September 2013.

[99] Lotfi, A.W.; Wilkowski, Matthew A., "Issues and advances in high-frequency magnetics for switching power supplies," *Proceedings of the IEEE*, vol.89, no.6, pp.833, 845, Jun 2001.

[100] Howard, T.O.; Carpenter, K.H., "A numerical study of the coupling coefficients for pot core transformers," *Magnetics, IEEE Transactions on*, vol.31, no.3, pp.2249, 2253, May 1995.

[101] T.McLyman, "Fringing flux and its side effects", http://www.kgmagnetics.org/APNOTES-06/An-115.pdf,

[102] Jean Picard, "Under the hood of flyback SMPS designs", 2010, http://focus.ti.com/asia/download/Topic_1_Picard_42pages.pdf, TI Power Supply Design Seminar, last accessed: 1st September 2013.

[103] Radhika Ambatipudi, Hari Babu Kotte and Kent Bertilsson, "Effect of Air Gap on the Performance of Hybrid Planar Power Transformer in High Frequency (MHz) Switch Mode Power Supplies (SMPS)", *Proceedings of INDUCTICA 2012, Coil Winding, Insulation and Electrical Manufacturing International Conference and Exhibition (CWIEME), Berlin, Germany 26 – 28, June 2012.*